In Vitro Model of Injury/Cytokine-Induced Cartilage Catabolism Modulated by Dynamic Compression, Growth Factors, and Glucocorticoids

by

Yang Li

B.S. Chemical Engineering
Georgia Institute of Technology, 2008

Submitted to the Department of Biological Engineering in Partial Fulfillment of the Requirements for the Degree of

DOCTOR OF PHILOSOPHY IN BIOLOGICAL ENGINEERING

at the

MASSACHUSETTS INSTITUTE OF TECHNOLOGY

June 2013

Signature of Author _____
Department of Biological Engineering
May 24, 2013

Certified by _____
Alan J. Grodzinsky
Professor of Biological, Electrical, and Mechanical Engineering
Thesis Supervisor

Accepted by _____
Forest White
Associate Professor of Biological Engineering
Chair, Graduate Program Committee

Thesis Committee

Dr. Alan J. Grodzinsky
Thesis Advisor
Professor of Biological, Electrical, and Mechanical Engineering
Massachusetts Institute of Technology

Dr. Scott R. Manalis
Thesis Committee Chair
Professor of Biological and Mechanical Engineering
Massachusetts Institute of Technology

Dr. Guoan Li
Professor, Department of Orthopaedic Surgery
Massachusetts General Hospital

In Vitro Model of Injury/Cytokine-Induced Cartilage Catabolism Modulated by Dynamic Compression, Growth Factors, and Glucocorticoids

by

Yang Li

Submitted to the Department of Biological Engineering on May 24, 2013 in Partial Fulfillment of the Requirements for the Degree of Doctor of Philosophy in Biological Engineering at the Massachusetts Institute of Technology

Abstract

The degradation of articular cartilage is the hallmark in the pathogenesis of osteoarthritis (OA). It still remains largely unknown which precise mechanisms initiate cartilage degradation. However, risks factors include traumatic joint injury that results in immediate upregulation of inflammatory cytokines within the joint, as well as direct mechanical damage to the cartilage, factors known to contribute to the onset of OA and its progression.

The first aim of this thesis focused on elucidating the importance of post-injury mechanical loading of cartilage. An *in vitro* model was used to simulate aspects of joint injury: mechanically damaged cartilage was co-cultured in the presence of inflammatory cytokines (TNF-α and IL-6). Intermittent dynamic compression was then applied to simulate different strain levels known to exist *in vivo* after joint injury. Strain-dependent modulation of aggrecan biosynthesis and degradation, aggrecanase cleavage of aggrecan, chondrocyte gene expression profiles and changes in cell viability (apoptosis) were observed. Results imply that appropriate biomechanical stimuli can be beneficial during rehabilitation for post traumatic OA (PTOA) treatment.

In the second aim, a combination therapy of insulin-like growth factor-1 (IGF-1) and the glucocorticoid dexamethasone (Dex) was tested as a potential therapeutic for PTOA. The effects of this combination were examined at the transcriptional and protein levels in the presence of IL-1α. Our results showed that the combination of IGF-1 and Dex significantly improved aggrecan biosynthesis, blocked aggrecan and collagen proteolysis and loss, and rescued cell viability. These dramatic results could not be achieved by using either IGF-1 or Dex alone, thus providing strong support for the concept and use of a combination therapy for PTOA treatment.

Dex is used to relieve inflammation and pain for short term OA treatment; however, it has not been studied as a potential disease-modifying drug for OA. In the last aim, the pro-survival role of Dex was investigated at the signaling, gene expression, and protein levels. Results suggest that Dex inhibits caspase-dependent apoptosis pathways, possibly through suppression of the phosphorylation of JNK and NF-κB/iκB signaling pathways. Taken together, these studies support the use of glucocorticoid treatment for inflammation-related cartilage cell death such as that found in PTOA.

Thesis Supervisor: Alan J. Grodzinsky.
Title: Professor of Biological, Electrical, and Mechanical Engineering

Acknowledgement

My interest for science was developed as early as in the middle school when I was taking my first Chemistry course back in China. I was particularly fascinated by the chemical reactions involving color changes in the solution, and I even started my mini lab at home by bringing back the residue chemicals from school. Of course this was a bad practice but back then I haven't taken a safety class yet, and the teacher gave them to me after I asked so I didn't think this was wrong, I guess she trusted me very much. Luckily I didn't blow up my house, but my interest to become a scientist was seeded. At that time, I thought I was going to become a Chemist since I loved Chemistry so much that I even memorized the entire periodic table. I would like to thank my Chemistry teacher who was very encouraging and helped me to answer many naïve questions and opened up my mind to the world of science.

I moved to the United Stated during high school with my parents. Though life has changed dramatically, I was lucky that I didn't lose myself during that transition. For that, I would like to really thank my high school friends Libo Deng, Chuan Tian, and Wenjie Wang, for giving me the strength to move forward with my life.

As for the science, I entered into the Chemical and Biomolecular Engineering program at Georgia Tech, which I guess was still somewhat influenced by my interest for chemistry. Prof. Yulin Deng led me to the first research lab in chemical engineering while Prof. Athanassios Sambanis cultivated me interest into the biomedical engineering, both helped me to apply to MIT. I would like to particularly thank Dr. Indra Mukherjee, who was a graduate student in Prof. Sambanis's lab, for his specific guidance in research and a great friend in lab. I would also like to thank Prof. Kevin Healy and Prof. Krishanu Saha at UC Berkeley, where I did my summer research internship.

My experience in Prof. Alan Grodzinsky's lab at MIT has been fascinating and will be unforgettable. Al was always encouraging for me to pursue new ideas, and helped me to get onto the right route with specific guidance. At the same time, I had a lot of freedom to think independently and became a real researcher who has learned how to manage different projects and push them towards the right direction. I would like to thank the entire Grodzinsky's lab members for the helpful discussions, especially Yang Wang who collaborated with me and helped me to get experiments done on time. In addition, Paul Kopesky was extremely supportive to my research and it was great fun to work with him. I would like also to thank my committee Prof. Scott Manalis and Prof. Guan Li for their great guidance.

I wouldn't become the same person I am now if without the support of my family. My parents have gone through a really difficult life journey to raise me and support me, and they are the most precious treasure I have in my life. I would really want to thank my uncle Ping Liang and my aunt Songfang Yang for helping me tremendously in life. My wife Siyu Peng was always there for me and I'm grateful to have her companionship and love.

Lastly, my work was funded by NIH, the NIH biomechanics training grant, grant from Merrimack Pharmaceuticals, and Presidential and Chyn Duog Shiah Memorial Fellowships from MIT.

CHAPTER 1

INTRODUCTION

Contents

1.1 CARTILAGE BIOLOGY AND DISEASE

Articular cartilage functions as a critical load-absorbing material and provides the lubricating surface between two contacting joints. The load-bearing property of cartilage comes from its poroelastic structure that composed of abundance extracellular matrix (ECM) proteins, together account for ~15-40% by wet weight and the rest is water (60-85%) (1). Aggrecan, one of the most important structural ECM proteins, is a large proteoglycan with a core protein backbone attached with abundant sulfated glycosaminoglycan (sGAG) side chains of chondroitin sulfate (CS) and keratan sulfate (KS). The highly negatively charged sGAG chains of aggrecan provide the compressive stiffness under tissue deformation. The tensile strength of cartilage is mainly a result of the collagen network, which is formed by the predominant type II collagen along with type IX and XI collagens incorporated into the heteropolymers. Other matrix proteins such as COMP, biglycan, matrillin, fibromodulin, and fibronetin also play important roles in cartilage matrix assembly and function. Chondrocyte is the only cell type found in cartilage and is responsible for the regulation of cartilage matrix protein synthesis and degradation under the homeostatic condition.

Osteoarthritis (OA) is the most prevalent musculoskeletal disease, with more than 27 million Americans affected (2). Traditionally, OA was believed to be a disease of "wear-and-tear", which is the consequence of sole mechanical factors with articular cartilage as the diseased tissue. However, it is now well-accepted that OA is a complex disease involving the entire joint, including the cartilage, meniscus, subchondral bone, ligament and joint capsule. Multiple risk factors for OA have been identified such as age, gender, obesity, genetic factors, and mechanical injury. Among them, injury occurred

from abnormal loading can predispose the injured joints to the development of early OA at a much younger age. The resulting post-injury OA (PTOA) represents a significant portion of the disease population with major economic burden to the society, and is therefore in urgent need for effective treatments.

1.2 IN VITRO INJURY MODELS

In vivo, articular cartilage is subjected to a complex combination of shear, compressive, and tensile stress under normal loading conditions such as walking, running, and climbing. There have been *in vivo* studies trying to examine cartilage biomechanics under varies loading regime using 3-dimensional imaging techniques such as magnetic resonance imaging (3, 4). For example, Van de velde (5) reported the use of dual fluoroscopic and magnetic resonance imaging technique to quantify tibiofemoral joint kinematics, i.e. contact deformation, of both normal and ACL-deficient human patients. Their results showed that ACL-deficiency altered both cartilage contact location and contact deformation compared to the healthy contralateral knee. Other studies have characterized the change in cartilage composition, mechanical properties, and metabolism upon varies loading conditions (6, 7). These *in vivo* studies provided valuable information on cartilage responds to physiological loads; however, these mechanical stimuli are often too complex to study *in vivo*. In addition, the need to quantify the response of chondrocyte-mediated biosynthesis, degradation, and repair of cartilage matrix to varying mechanical stimuli in a more systematic and controlled manner, as well as to understand the specific mechanotransduction pathways leading to these events, requires the

examination of individual biomechanical stimulation with defined parameters in an *in vitro* setting.

1.3 MATRIX BIOSYNTHESIS

During the past decades, numerous studies have focused on the effects of mechanical loading on cell-mediated ECM biosynthesis and degradation using varies *in vitro* model systems. These include explants studies with human, bovine, canine, and other animal tissue samples, both immature and mature (8-10), as well as 3-dimensional tissue-engineered cartilage with chondrocytes cultured in agarose (11, 12), alginate (13) gels, and other systems (14, 15). In addition, chondrocyte cultured as monolayer is also used to decouple cell responses to direct mechanical stimulation from the complex cell-matrix interactions under loading (10, 16). Each model system covers certain aspects of the complex involvement of mechanical stimulation in cartilage with inherent advantages and disadvantages, and therefore, caution should be taken when interpreting the physiological relevance of each system and comparing the results between different systems.

It is now well-accepted that the biomechanical effects on cartilage matrix synthesis depends not only on the model system in which they are studied, but also on the nature of the applied mechanical stimulation, whether it is static or dynamic compression, shear, or tensile, as well as the loading parameters used such as frequency, strain/stress, and time (17-19). Likewise, the precise biomechanical, physiochemical, or electrical transduction mechanism by which chondrocyte responds to physical stimuli depends on the form and kinetics of the loading. Static compression can cause equilibrium cell

deformation (20) and physiochemical changes such as water loss, change in local ion concentration and pH (21), as well as concomitant increase in osmotic pressure (8). In contrast, dynamic loading can additionally produce interstitial fluid flow and the resulting fluid pressurization and streaming currents (22, 23).

1.4 STATIC COMPRESSION

Static compression has been consistently shown to reduce biosynthesis of PGs and other matrix components with increasing compressive stress or strain, and this inhibition is at least partially reversible upon removal of the applied load, although variations exist on the magnitude of response to a particular stress/strain (8, 9, 18, 21, 24, 25). In addition, it has been shown that static compression can alter specific post-translational modifications of aggrecan (26, 27). To elucidate the specific transduction mechanism induced by static loading, Gray et al. (21) found that depressed sulfate and proline biosynthesis in bovine explants depend on the interstitial pH, but not the local concentration of certain ions such as sulfate and potassium. This pH effect on chondrocyte biosynthesis was confirmed by using human chondrocyte cultured in monolayer (28). Other studies have suggested that hydrostatic pressure can have stimulatory or suppressive effect on cartilage matrix biosynthesis, and the direction depends on the magnitude of pressure, as well as the method being applied (10, 29, 30). Of note, response variations to the same loading treatment could be seen within a given study and between different studies, and this is at least partly due to topographical and animal-to-animal variations, young versus adult animals, and cell and matrix heterogeneity within the tissue (8, 10). Additionally, compression-induced alteration in

cell conformation (20), nucleus volume and height (31, 32), and intracellular organelles morphology (33) have been documented and proposed as possible mechanotransduction mechanisms. It is still unclear, however, whether these changes are consequences of chondrocyte's adaptation to mechanical environment or causal events that lead to the resulting cellular responses such as change in matrix biosynthesis. One important mechanism that attracted much attention is through mechanically-induced interactions between extracellular matrix and cytoskeleton via integrin binding (34, 35), leading to downstream intracellular signaling.

1.5 DYNAMIC COMPRESSION

In contrast to the overall inhibitory effect of static compression on cartilage matrix biosynthesis, compression applied in dynamic or cyclic manner often has anabolic effects on matrix production, although the response depends on the compression frequency and amplitude (17, 18, 24, 36). Sah et al. (17) reported a threshold frequency of ~0.001 Hz under which biosynthesis was not affected by unconfined compression on bovine cartilage explants with low strain amplitude (~1-5%). In contrast, higher frequency regime (0.01-1 Hz) significantly stimulated both sulfate and proline synthesis at the same strain amplitude. It was proposed that the very low frequency (<0.001 Hz) dynamic compression acts equivalently as static compression (18) in that fluid exudation can occur in concomitant with changes in physicochemical parameters, while higher frequency dynamic compression induces fluid flow, hydrostatic pressure gradients, and streaming potential and current (23). Therefore, finding correlations between these physical stimuli and spatial variation in biosynthesis could provide clues as to which

mechanisms are critical for cell-mediated response in matrix metabolism. This has motivated a series of studies that examined tissue- and cell-level matrix synthesis and distribution using quantitative autoradiography for static, dynamic, and shear compression (32, 37-39). On the other hand, finite element method has been implemented in varies forms of poroelastic models to couple mechanical, chemical and electrical constitute laws and apply them in characterizing load-induced biophysical and physiochemical phenomena within a defined tissue geometry (37, 40-43), and results were compared with the biosynthesis distribution data.

As an example, Buschmann et al. (37) quantified the radial distribution of newly synthesized aggrecan within 3-mm diameter bovine cartilage explant, under unconfined uniaxial dynamic compression at different frequencies. The results indicated that at lower frequency (0.01 Hz), aggrecan biosynthesis was uniformly stimulated throughout the tissue compared to the static-offset control, with no radial or axial dependence. When compression frequency increased to 0.1 Hz, however, significant stimulation was found at the peripheral radial positions while central regions showed no or little increase in biosynthesis. Combining these data with the previous study that reported a lack of response at very low frequency of 0.001 Hz (18), clear patterns of frequency- and spatial-dependent biosynthesis were established. By using a fibril-reinforced poroelastic model developed by Soulhat (43), the biosynthesis results can be closely matched with model-predicted interstitial fluid velocity profiles, but not with fluid pressure and radial strain. Quinn et al. (38) further elaborated this approach to examine spatial distribution of biosynthesis at the cell level with a length scale of 1 μm. Most newly synthesized PGs were deposited at the pericellular region and the radial and directional dependence of

biosynthesis in this region were affected by the type, magnitude, and frequency of loading.

1.6 INJURIOUS LOADING

Joint injury such as ACL tear has been suggested to be a major risk factor for OA development later in life. The initial joint trauma can be a single disruption of the ligament, or accompanies by damages to the articular cartilage, meniscus, synovium, and subchondral bone. Trauma-induced joint instability alters contact mechanics between articular surfaces and induces inflammatory response within the joint (44-46). Biochemical changes associated with inflammation are now well-documented by evaluating the synovial fluid content post-injury, which contains increased levels of inflammatory cytokines such as TNF-α, IL-1, and IL-6, elevated concentrations of MMPs, as well as degradation products of matrix proteins (47-50). This inflammatory response, which can sustain for years after the initial injury, is believed to work in conjunction with abnormal mechanical loading to accelerate cartilage degeneration that eventually leads to OA. Indeed, studies comparing OA patients with or without prior joint injury provided strong evidence that ACL tear can significantly increase the risk for early OA (51-53). Currently, no surgical interventions, i.e. ACL reconstruction, have been shown to be capable of preventing OA progression (47, 52, 54). Hence, the development of effective treatment to posttraumatic OA requires significant understanding of its pathological events, including the onset, progression, and late-stage of the disease, as well as the mechanistic pathways within each stage.

Over the last two decades, extensive efforts have been invested in characterizing the effects of joint injury with *in vitro* explants and *in vivo* animal models. Using methods such as ACL transection, morphologic and biochemical changes have been monitored over long-term course in experimental OA (55-57). On the other hand, explants studies circumvent the complex mechanical environment inherent *in vivo* and are used to explore the specific mechanism of mechanical stimuli and the subsequent effects. A series of studies simulating controlled impact load have determined the threshold peak stress, strain, or strain rate that constitute an *in vitro* injury model (58-61). Specifically, Chen et al. (58) reported a minimum of 2.5 MPa peak stress applied with 30 MPa/s stress rate was sufficient to induce immediate loss of matrix molecules and increase tissue water content. As a comparison, Loening et al. (62) showed that peak stress of 4.5 MPa with 1 mm/s strain rate resulted in significant increase in cell apoptosis while compromised tissue mechanical properties appeared beyond 7 MPa. These differences in threshold values were attributed to the distinct loading protocols as well as the types of tissue used.

Following the initial impact load, an immediate increase in PGs loss was accompanied by rise in tissue water content (61, 63). Significant decrease in unconfined compression equilibrium modulus was also measured while confined compression equilibrium modulus was not affected to the same extent (62, 64). These data suggested that mechanical disruption of the collagen fibrils occurred, which compromised collagen network's ability to counteract the PG-induced swelling pressure. Indeed, immunohistochemical staining showed more denatured collagen in injured cartilage, although collagenase-cleaved collagen fragments could also be detected, suggesting the presence of cell-mediated matrix degradation (58, 65). Additionally, studies on the

kinetics of proteoglycan release following injury revealed an sharp increase in sGAG loss, which was not due to increase in newly synthesized matrix nor to aggrecanase or MMP activity, consistent with mechanical damage (66). Consequently, the mechanically damaged network is likely to have an increased effective pore size that contributes to the elevated matrix loss, as supported by an increased amount of intact aggrecan detected in the culture medium (62).

Matrix biosynthesis was also affected by injury (59, 60, 63), either by reducing viable cell number or modulating metabolic activity of live cells. Kurz et al. (60) showed reduction in biosynthesis on a per viable cell basis, while others reported opposite effect (58, 63). This inconsistency is likely caused by the different injury protocols (cyclic versus one-time) and cell viability evaluation methods used in these studies. Quinn et al. (64) also examined the effect of injurious compression on matrix turnover at cell-level using quantitative autoradiography. Marked increase in cell death was noticed as these cells failed to metabolize pericellular matrix compared to the control, and the remaining viable cells exhibited a more rapid matrix turnover rate, reflecting upregulation of cell-mediated enzymatic activity. In addition, Kurz et al. (60) assessed the biosynthetic activity of injured bovine cartilage explants respond to moderate dynamic compression, which has been demonstrated to promote matrix synthesis in normal cartilage (17). The lack of response of injured cartilage to dynamic stimulation implicated impaired chondrocyte function and capacity to repair.

1.7 CHONDROCYTE VIABILITY AND APOPTOSIS

D'Lima (67) used both bovine and human cartilage explants and showed significantly increased apoptosis induced by injury, and depends on the loading stress. Compression-induced apoptosis seems to be linked to reactive oxygen species, and one study showed oxidant preconditioning at low concentration may improve the resistance of chondrocyte to injurious mechanical stress (68). Chen et al. (65) investigated chondrocyte cell death in bovine explants under confined dynamic compression and cell death is load stress-dependent and mainly localized in the superficial zone.

The exact pathways for apoptosis induction is unknown but many hypothesis were proposed, such as binding of CD95, nitric oxide involvement, and loss of survival signals induced by extracellular matrix loss. Apoptosis involves with reactive oxygen species and Healy et al. (69) examined the involvement of COX-2 and antioxidant proteins in shear-induced apoptosis of human chondrocytes. Results showed high shear stress-induced COX-2 can inhibit phosphatidylinositol 3-kinase (PI3-K) activity, which leads to antioxidant response element (ARE) and NF-E2 related factor 2 (Nrf2)-mediated suppression of phase 2 and antioxidant proteins expression. This decrease in antioxidant capacity disrupts the inhibition on caspase-9 activation and induces mitochondrial depolarization, leading to apoptosis. The same response was not observed with low shear stress, however, indicating the importance of the magnitude of mechanical stimulation.

1.8 DEXAMETHASONE

Dexamethasone (Dex) is a potent synthetic glucocorticoid (GC) that has been widely used intra-articularly to relieve inflammation for the treatment of OA and other types of arthritis (70). Long-term use of Dex has been considered as a potential treatment for chronic OA (71) but negative side-effects such as osteoporosis have been noticed, which may be resulted from high dose usage (72) or ineffective local delivery method (73). In vitro, Dex has been shown to significantly block cytokine-induced cartilage degradation and alleviate suppressed matrix biosynthesis via glucocorticoid receptor (GR)-dependent pathways (74). Once diffused into the the cytoplasm, Dex binds to the intracellular GRs and they together serve as nuclear transcriptional factors.

1.9 THESIS OUTLINE

The objective of this thesis was to explore the role of biomechanical stimulation on the cartilage biosynthesis and degradation in an inflammatory environment, and to study the drug potential of IGF-1 and Dex combination in counteracting the damaging effects of pro-inflammatory cytokines.

In Chapter 2, the effects of dynamic strain were examined on TNF-α and IL-6/sIL-6R-treated cartilage with/without mechanical injury. Matrix biosynthesis, aggrecan degradation, chondrocyte apoptosis, as well as gene expression profiles were studied.

In Chapter 3, the combination therapy with IGF-1 and Dex was compared with other growth factor-based therapies using an IL-1α-based in vitro cartilage degradation

model, and the beneficial roles of the IGF-1 and Dex were examined at gene, protein, and cell level

In Chapter 4, the anti-apoptotic effects of Dex were explored using IL-1α as the apoptosis-inducing model.

Finally, in Chapter 5, major findings are presented and conclusions are discussed.

1.10 REFERENCES

1. Mankin HJ, Thrasher AZ. Water content and binding in normal and osteoarthritic human cartilage. J Bone Joint Surg Am. 1975;57(1):76-80.
2. Bitton R. The economic burden of osteoarthritis. Am J Manag Care. 2009;15(8 Suppl):S230-5.
3. Herberhold C, Faber S, Stammberger T, Steinlechner M, Putz R, Englmeier KH, et al. In situ measurement of articular cartilage deformation in intact femoropatellar joints under static loading. J Biomech. 1999;32(12):1287-95.
4. Kozanek M, Hosseini A, Liu F, Van de Velde SK, Gill TJ, Rubash HE, et al. Tibiofemoral kinematics and condylar motion during the stance phase of gait. J Biomech. 2009;42(12):1877-84.
5. Van de Velde SK, Gill TJ, Li G. Evaluation of kinematics of anterior cruciate ligament-deficient knees with use of advanced imaging techniques, three-dimensional modeling techniques, and robotics. The Journal of bone and joint surgery American volume. 2009;91 Suppl 1:108-14.
6. Palmoski MJ, Colyer RA, Brandt KD. Joint motion in the absence of normal loading does not maintain normal articular cartilage. Arthritis and rheumatism. 1980;23(3):325-34.
7. Guilak F, Ratcliffe A, Lane N, Rosenwasser MP, Mow VC. Mechanical and biochemical changes in the superficial zone of articular cartilage in canine experimental osteoarthritis. Journal of orthopaedic research : official publication of the Orthopaedic Research Society. 1994;12(4):474-84.
8. Schneiderman R, Keret D, Maroudas A. Effects of mechanical and osmotic pressure on the rate of glycosaminoglycan synthesis in the human adult femoral head cartilage: an in vitro study. Journal of orthopaedic research : official publication of the Orthopaedic Research Society. 1986;4(4):393-408.
9. Burton-Wurster N, Vernier-Singer M, Farquhar T, Lust G. Effect of compressive loading and unloading on the synthesis of total protein, proteoglycan, and fibronectin by canine cartilage explants. Journal of orthopaedic research : official publication of the Orthopaedic Research Society. 1993;11(5):717-29.
10. Hall AC, Urban JP, Gehl KA. The effects of hydrostatic pressure on matrix synthesis in articular cartilage. Journal of orthopaedic research : official publication of the Orthopaedic Research Society. 1991;9(1):1-10.
11. Buschmann MD, Gluzband YA, Grodzinsky AJ, Hunziker EB. Mechanical compression modulates matrix biosynthesis in chondrocyte/agarose culture. Journal of cell science. 1995;108 (Pt 4):1497-508.
12. Lee DA, Noguchi T, Frean SP, Lees P, Bader DL. The influence of mechanical loading on isolated chondrocytes seeded in agarose constructs. Biorheology. 2000;37(1-2):149-61.
13. Ragan PM, Chin VI, Hung HH, Masuda K, Thonar EJ, Arner EC, et al. Chondrocyte extracellular matrix synthesis and turnover are influenced by static compression in a new alginate disk culture system. Archives of biochemistry and biophysics. 2000;383(2):256-64.

14. Kisiday JD, Jin M, DiMicco MA, Kurz B, Grodzinsky AJ. Effects of dynamic compressive loading on chondrocyte biosynthesis in self-assembling peptide scaffolds. J Biomech. 2004;37(5):595-604.
15. Mizuno S, Tateishi T, Ushida T, Glowacki J. Hydrostatic fluid pressure enhances matrix synthesis and accumulation by bovine chondrocytes in three-dimensional culture. Journal of cellular physiology. 2002;193(3):319-27.
16. Smith RL, Rusk SF, Ellison BE, Wessells P, Tsuchiya K, Carter DR, et al. In vitro stimulation of articular chondrocyte mRNA and extracellular matrix synthesis by hydrostatic pressure. Journal of orthopaedic research : official publication of the Orthopaedic Research Society. 1996;14(1):53-60.
17. Sah RL, Kim YJ, Doong JY, Grodzinsky AJ, Plaas AH, Sandy JD. Biosynthetic response of cartilage explants to dynamic compression. Journal of orthopaedic research : official publication of the Orthopaedic Research Society. 1989;7(5):619-36.
18. Kim YJ, Sah RL, Grodzinsky AJ, Plaas AH, Sandy JD. Mechanical regulation of cartilage biosynthetic behavior: physical stimuli. Archives of biochemistry and biophysics. 1994;311(1):1-12.
19. Sauerland K, Raiss RX, Steinmeyer J. Proteoglycan metabolism and viability of articular cartilage explants as modulated by the frequency of intermittent loading. Osteoarthritis and cartilage / OARS, Osteoarthritis Research Society. 2003;11(5):343-50.
20. Freeman PM, Natarajan RN, Kimura JH, Andriacchi TP. Chondrocyte cells respond mechanically to compressive loads. Journal of orthopaedic research : official publication of the Orthopaedic Research Society. 1994;12(3):311-20.
21. Gray ML, Pizzanelli AM, Grodzinsky AJ, Lee RC. Mechanical and physiochemical determinants of the chondrocyte biosynthetic response. Journal of orthopaedic research : official publication of the Orthopaedic Research Society. 1988;6(6):777-92.
22. Lee RC, Frank EH, Grodzinsky AJ, Roylance DK. Oscillatory compressional behavior of articular cartilage and its associated electromechanical properties. Journal of biomechanical engineering. 1981;103(4):280-92.
23. Frank EH, Grodzinsky AJ. Cartilage electromechanics--I. Electrokinetic transduction and the effects of electrolyte pH and ionic strength. J Biomech. 1987;20(6):615-27.
24. Palmoski MJ, Brandt KD. Effects of static and cyclic compressive loading on articular cartilage plugs in vitro. Arthritis and rheumatism. 1984;27(6):675-81.
25. Guilak F, Meyer BC, Ratcliffe A, Mow VC. The effects of matrix compression on proteoglycan metabolism in articular cartilage explants. Osteoarthritis and cartilage / OARS, Osteoarthritis Research Society. 1994;2(2):91-101.
26. Lammi MJ, Inkinen R, Parkkinen JJ, Hakkinen T, Jortikka M, Nelimarkka LO, et al. Expression of reduced amounts of structurally altered aggrecan in articular cartilage chondrocytes exposed to high hydrostatic pressure. The Biochemical journal. 1994;304 (Pt 3):723-30.
27. Kim YJ, Grodzinsky AJ, Plaas AH. Compression of cartilage results in differential effects on biosynthetic pathways for aggrecan, link protein, and hyaluronan. Archives of biochemistry and biophysics. 1996;328(2):331-40.

28. Schwartz ER, Kirkpatrick PR, Thompson RC. The effect of environmental pH on glycosaminoglycan metabolism by normal human chondrocytes. The Journal of laboratory and clinical medicine. 1976;87(2):198-205.
29. Lippiello L, Kaye C, Neumata T, Mankin HJ. In vitro metabolic response of articular cartilage segments to low levels of hydrostatic pressure. Connect Tissue Res. 1985;13(2):99-107.
30. Jones IL, Klämfeldt A, Sandström T. The effect of continuous mechanical pressure upon the turnover of articular cartilage proteoglycans in vitro. Clin Orthop Relat Res. 1982(165):283-9.
31. Guilak F. Compression-induced changes in the shape and volume of the chondrocyte nucleus. J Biomech. 1995;28(12):1529-41.
32. Buschmann MD, Hunziker EB, Kim YJ, Grodzinsky AJ. Altered aggrecan synthesis correlates with cell and nucleus structure in statically compressed cartilage. Journal of cell science. 1996;109 (Pt 2):499-508.
33. Szafranski JD, Grodzinsky AJ, Burger E, Gaschen V, Hung HH, Hunziker EB. Chondrocyte mechanotransduction: effects of compression on deformation of intracellular organelles and relevance to cellular biosynthesis. Osteoarthritis and cartilage / OARS, Osteoarthritis Research Society. 2004;12(12):937-46.
34. Loeser RF. Integrin-mediated attachment of articular chondrocytes to extracellular matrix proteins. Arthritis and rheumatism. 1993;36(8):1103-10.
35. Ingber D. Integrins as mechanochemical transducers. Curr Opin Cell Biol. 1991;3(5):841-8.
36. Ackermann B, Steinmeyer J. Collagen biosynthesis of mechanically loaded articular cartilage explants. Osteoarthritis and cartilage / OARS, Osteoarthritis Research Society. 2005;13(10):906-14.
37. Buschmann MD, Kim YJ, Wong M, Frank E, Hunziker EB, Grodzinsky AJ. Stimulation of aggrecan synthesis in cartilage explants by cyclic loading is localized to regions of high interstitial fluid flow. Archives of biochemistry and biophysics. 1999;366(1):1-7.
38. Quinn TM, Grodzinsky AJ, Buschmann MD, Kim YJ, Hunziker EB. Mechanical compression alters proteoglycan deposition and matrix deformation around individual cells in cartilage explants. Journal of cell science. 1998;111 (Pt 5):573-83.
39. Jin M, Frank EH, Quinn TM, Hunziker EB, Grodzinsky AJ. Tissue shear deformation stimulates proteoglycan and protein biosynthesis in bovine cartilage explants. Archives of biochemistry and biophysics. 2001;395(1):41-8.
40. Kim YJ, Bonassar LJ, Grodzinsky AJ. The role of cartilage streaming potential, fluid flow and pressure in the stimulation of chondrocyte biosynthesis during dynamic compression. J Biomech. 1995;28(9):1055-66.
41. Levenston ME, Frank EH, Grodzinsky AJ. Variationally derived 3-field finite element formulations for quasistatic poroelastic analysis of hydrated biological tissues. Computer Methods in Applied Mechanics and Engineering. 1998;156(1-4):231-46.
42. Levenston ME, Eisenberg SR, Grodzinsky AJ. A variational formulation for coupled physicochemical flows during finite deformations of charged porous media. International Journal of Solids and Structures. 1998;35(34-35):4999-5019.

43. Soulhat J, Buschmann MD, Shirazi-Adl A. A fibril-network-reinforced biphasic model of cartilage in unconfined compression. Journal of biomechanical engineering. 1999;121(3):340-7.
44. Andriacchi TP, Mundermann A, Smith RL, Alexander EJ, Dyrby CO, Koo S. A framework for the in vivo pathomechanics of osteoarthritis at the knee. Annals of biomedical engineering. 2004;32(3):447-57.
45. Andriacchi TP, Dyrby CO. Interactions between kinematics and loading during walking for the normal and ACL deficient knee. J Biomech. 2005;38(2):293-8.
46. Van de Velde SK, Bingham JT, Hosseini A, Kozanek M, DeFrate LE, Gill TJ, et al. Increased tibiofemoral cartilage contact deformation in patients with anterior cruciate ligament deficiency. Arthritis and rheumatism. 2009;60(12):3693-702.
47. Beynnon BD, Uh BS, Johnson RJ, Abate JA, Nichols CE, Fleming BC, et al. Rehabilitation after anterior cruciate ligament reconstruction: a prospective, randomized, double-blind comparison of programs administered over 2 different time intervals. The American journal of sports medicine. 2005;33(3):347-59.
48. Higuchi H, Shirakura K, Kimura M, Terauchi M, Shinozaki T, Watanabe H, et al. Changes in biochemical parameters after anterior cruciate ligament injury. International orthopaedics. 2006;30(1):43-7.
49. Elsaid KA, Fleming BC, Oksendahl HL, Machan JT, Fadale PD, Hulstyn MJ, et al. Decreased lubricin concentrations and markers of joint inflammation in the synovial fluid of patients with anterior cruciate ligament injury. Arthritis and rheumatism. 2008;58(6):1707-15.
50. Catterall JB, Stabler TV, Flannery CR, Kraus VB. Changes in serum and synovial fluid biomarkers after acute injury (NCT00332254). Arthritis research & therapy. 2010;12(6):R229.
51. Hill CL, Seo GS, Gale D, Totterman S, Gale ME, Felson DT. Cruciate ligament integrity in osteoarthritis of the knee. Arthritis and rheumatism. 2005;52(3):794-9.
52. von Porat A, Roos EM, Roos H. High prevalence of osteoarthritis 14 years after an anterior cruciate ligament tear in male soccer players: a study of radiographic and patient relevant outcomes. Ann Rheum Dis. 2004;63(3):269-73.
53. Lohmander LS, Ostenberg A, Englund M, Roos H. High prevalence of knee osteoarthritis, pain, and functional limitations in female soccer players twelve years after anterior cruciate ligament injury. Arthritis and rheumatism. 2004;50(10):3145-52.
54. Asano H, Muneta T, Ikeda H, Yagishita K, Kurihara Y, Sekiya I. Arthroscopic evaluation of the articular cartilage after anterior cruciate ligament reconstruction: a short-term prospective study of 105 patients. Arthroscopy : the journal of arthroscopic & related surgery : official publication of the Arthroscopy Association of North America and the International Arthroscopy Association. 2004;20(5):474-81.
55. Alhadlaq HA, Xia Y, Moody JB, Matyas JR. Detecting structural changes in early experimental osteoarthritis of tibial cartilage by microscopic magnetic resonance imaging and polarised light microscopy. Ann Rheum Dis. 2004;63(6):709-17.
56. Matyas JR, Atley L, Ionescu M, Eyre DR, Poole AR. Analysis of cartilage biomarkers in the early phases of canine experimental osteoarthritis. Arthritis and rheumatism. 2004;50(2):543-52.
57. Lorenz H, Wenz W, Ivancic M, Steck E, Richter W. Early and stable upregulation of collagen type II, collagen type I and YKL40 expression levels in cartilage during early

experimental osteoarthritis occurs independent of joint location and histological grading. Arthritis research & therapy. 2005;7(1):R156-65.
58. Chen CT, Burton-Wurster N, Lust G, Bank RA, Tekoppele JM. Compositional and metabolic changes in damaged cartilage are peak-stress, stress-rate, and loading-duration dependent. Journal of orthopaedic research : official publication of the Orthopaedic Research Society. 1999;17(6):870-9.
59. Torzilli PA, Grigiene R, Borrelli J, Jr., Helfet DL. Effect of impact load on articular cartilage: cell metabolism and viability, and matrix water content. Journal of biomechanical engineering. 1999;121(5):433-41.
60. Kurz B, Jin M, Patwari P, Cheng DM, Lark MW, Grodzinsky AJ. Biosynthetic response and mechanical properties of articular cartilage after injurious compression. Journal of orthopaedic research : official publication of the Orthopaedic Research Society. 2001;19(6):1140-6.
61. Ewers BJ, Dvoracek-Driksna D, Orth MW, Haut RC. The extent of matrix damage and chondrocyte death in mechanically traumatized articular cartilage explants depends on rate of loading. Journal of orthopaedic research : official publication of the Orthopaedic Research Society. 2001;19(5):779-84.
62. Loening AM, James IE, Levenston ME, Badger AM, Frank EH, Kurz B, et al. Injurious mechanical compression of bovine articular cartilage induces chondrocyte apoptosis. Archives of biochemistry and biophysics. 2000;381(2):205-12.
63. Jeffrey JE, Thomson LA, Aspden RM. Matrix loss and synthesis following a single impact load on articular cartilage in vitro. Biochimica et biophysica acta. 1997;1334(2-3):223-32.
64. Quinn TM, Grodzinsky AJ, Hunziker EB, Sandy JD. Effects of injurious compression on matrix turnover around individual cells in calf articular cartilage explants. Journal of orthopaedic research : official publication of the Orthopaedic Research Society. 1998;16(4):490-9.
65. Chen CT, Bhargava M, Lin PM, Torzilli PA. Time, stress, and location dependent chondrocyte death and collagen damage in cyclically loaded articular cartilage. J Orthop Res. 2003;21(5):888-98.
66. DiMicco MA, Patwari P, Siparsky PN, Kumar S, Pratta MA, Lark MW, et al. Mechanisms and kinetics of glycosaminoglycan release following in vitro cartilage injury. Arthritis and rheumatism. 2004;50(3):840-8.
67. D'Lima DD, Hashimoto S, Chen PC, Lotz MK, Colwell CW. Prevention of chondrocyte apoptosis. J Bone Joint Surg Am. 2001;83-A Suppl 2(Pt 1):25-6.
68. Ramakrishnan P, Hecht BA, Pedersen DR, Lavery MR, Maynard J, Buckwalter JA, et al. Oxidant conditioning protects cartilage from mechanically induced damage. J Orthop Res. 2010;28(7):914-20.
69. Healy ZR, Lee NH, Gao X, Goldring MB, Talalay P, Kensler TW, et al. Divergent responses of chondrocytes and endothelial cells to shear stress: cross-talk among COX-2, the phase 2 response, and apoptosis. Proc Natl Acad Sci U S A. 2005;102(39):14010-5.
70. Mina R, Melson P, Powell S, Rao M, Hinze C, Passo M, et al. Effectiveness of dexamethasone iontophoresis for temporomandibular joint involvement in juvenile idiopathic arthritis. Arthritis Care Res (Hoboken). 2011;63(11):1511-6.

71. Stein A, Yassouridis A, Szopko C, Helmke K, Stein C. Intraarticular morphine versus dexamethasone in chronic arthritis. Pain. 1999;83(3):525-32.
72. Ishida Y, Heersche JN. Glucocorticoid-induced osteoporosis: both in vivo and in vitro concentrations of glucocorticoids higher than physiological levels attenuate osteoblast differentiation. J Bone Miner Res. 1998;13(12):1822-6.
73. Gerwin N, Hops C, Lucke A. Intraarticular drug delivery in osteoarthritis. Adv Drug Deliv Rev. 2006;58(2):226-42.
74. Lu YCS, Evans CH, Grodzinsky AJ. Effects of short-term glucocorticoid treatment on changes in cartilage matrix degradation and chondrocyte gene expression induced by mechanical injury and inflammatory cytokines. Arthritis Research & Therapy. 2011;13(5).

CHAPTER 2

Moderate Dynamic Compression Inhibits Pro-Catabolic Response of Cartilage to Mechanical Injury, TNF-α and IL-6, but Accentuates Degradation Above a Strain Threshold

Contents

ABSTRACT

Objective: Traumatic joint injury can initiate early cartilage degeneration in the presence of elevated inflammatory cytokines (e.g., TNF-α and IL-6). The positive/negative effects of post-injury dynamic loading on cartilage degradation and repair in vivo is not well-understood. This study examined the effects of dynamic strain on bovine and human cartilage in vitro challenged with TNF-α + IL-6 and its soluble receptor (sIL-6R) with/without initial mechanical injury.

Methods: Groups of mechanically injured or non-injured explants were cultured in TNF-α + IL-6/sIL-6R for 8 days. Intermittent dynamic compression was applied concurrently at 10%, 20%, or 30% strain amplitude. Outcome measures included sGAG loss (DMMB), aggrecan biosynthesis (^{35}S-incorporation), aggrecanase activity (Western blot), chondrocyte viability (fluorescence staining) and apoptosis (nuclear blebbing via light microscopy), and gene expression (qPCR).

Results: In bovine explants, injury-plus-cytokine treatment markedly increased sGAG loss and aggrecanase activity, and induced chondrocyte apoptosis. These effects were abolished by moderate 10% and 20% strains. However, 30% strain-amplitude greatly increased apoptosis and had no inhibitory effect on aggrecanase activity. TNF+IL-6/sIL-6R downregulated matrix gene expression and upregulated expression of inflammatory genes, effects that were rescued by moderate dynamic strains but not by 30% strain. In human ankle and knee cartilage explants, only 10% strain-amplitude inhibited cytokine-induced increases in sGAG loss, aggrecanase activity, and cell death.

Conclusions: Moderate dynamic compression inhibits the pro-catabolic response of cartilage to mechanical injury and cytokine challenge, but there is a threshold strain-amplitude above which loading becomes detrimental to cartilage. Our findings support the concept of appropriate loading for post-injury rehabilitation.

2.1 INTRODUCTION

Joint injuries such as the anterior cruciate ligament (ACL) tear are a major risk factor for osteoarthritis (OA) later in life. The initial joint trauma can be a single disruption of the ligament, or accompanied by damage to cartilage, meniscus, synovium, and subchondral bone. Post-injury evaluation of the synovial fluid from ACL-deficient patients has revealed inflammation-associated biochemical changes including increased levels of pro-inflammatory cytokines (e.g., TNF-α, IL-1, and IL-6) as well as matrix protein degradation products generated by matrix metalloproteinases (MMPs) and ADAMTS aggrecanases (A Disintegrin And Metalloproteinase with Thrombospondin Motifs)[1-4]. This inflammatory response, which can be prolonged after the initial injury, is believed to act in conjunction with abnormal mechanical loading to accelerate cartilage degeneration that eventually leads to OA. Indeed, studies comparing OA patients with or without prior joint injury provided strong evidence that ACL tears can significantly increase the risk for early OA[5-7].

In vivo, articular cartilage is subjected to a complex combination of shear, compressive, and tensile stress under normal loading conditions. After joint injury, in addition to the inflammatory response, trauma-induced joint instability also alters the contact mechanics between articular surfaces[8]. In particular, Van de Velde[9,10] used

dual fluoroscopic and MR imaging techniques to quantify tibiofemoral joint kinematics in both normal and ACL-deficient human patients. Their results showed that cartilage contact deformation increased significantly to ~20-30% in the ACL-deficient knee from ~15-20% in the contralateral healthy knee during lunge motion with 0-30° flexion[10]; while surgical reconstruction restored some of the in vivo contact biomechanics, the increased cartilage deformation was not ameliorated[11]. These studies raise the question of whether post-injury joint loading can cause additional damage to cartilage, and whether there exists a range of motion within which rehabilitative loading can be beneficial in maintaining cartilage structure and function.

Over the last two decades, *in vitro* injury models have been developed to facilitate understanding of cartilage mechanical injury on the onset and progression of OA[12-14]. Consistently, injurious loading has been shown to result in loss of proteoglycans[15], tissue swelling[14], collagen network damage[12], and reduced tissue stiffness[13]. In addition, significantly increased chondrocyte apoptosis was observed[16,17], especially in the superficial zone[18], and the degree of cell damage was age-dependent[19]. Matrix biosynthesis by remaining live cells was also suppressed by injury[13]. Furthermore, injury potentiates proteoglycan catabolism induced by exogenous cytokines TNF-α and IL-6[20], which were introduced to simulate the inflammatory environment seen *in vivo* after joint injury. These studies have furthered our understanding of the immediate effects of mechanical injury; however, the interplay between cytokines and post-injury mechanical signals is less understood.

Dynamic compression can induce anabolic responses in normal cartilage which promote matrix biosynthesis with a strong dependence on compression frequency and

amplitude[21-23]. The spatial profiles of cell-mediated matrix biosynthesis have been correlated with compression-induced interstitial fluid flow[24-26], and the mechano-transduction pathways involve MAPK activation, intracellular calcium and cyclic AMP[27,28]. Additionally, dynamic compression can mitigate the catabolic responses of chondrocytes to cytokines in tissue-engineered cultures[29]. However, little is known about the effects of follow-on dynamic compression after injury/cytokine-challenge in intact cartilage.

In the present study, we implemented a previously-characterized *in vitro* injury model involving cytokines TNF-α and IL-6/sIL-6R with or without initial mechanical injury, and investigated the effects of intermittent unconfined dynamic compression (10%-30% strain amplitude) on both immature bovine and mature human cartilage. We hypothesized that (1) dynamic compression maintains anabolic effects in an inflammatory environment by rescuing matrix biosynthesis suppressed by cytokines[30]; (2) dynamic compression has an additional anti-catabolic role in reducing cytokine-mediated cartilage degradation; (3) there is a range of strain amplitudes within which dynamic compression is beneficial, and (4) dynamic compression will have differential effects on young bovine vs. adult human cartilage due to their known differences in biomechanical properties[31,32].

2.2 MATERIALS AND METHODS

Bovine articular cartilage harvest and culture. Articular cartilage disks were harvested from the femoropatellar grooves of 1-2-week-old calves, obtained on the day of

slaughter (Research '87, Boylston, MA). A total of 17 joints from 13 different animals and 2 humans were used. Full-thickness cartilage cylinders were cored using a 3-mm dermal punch, and the top 1-mm disk containing intact superficial zone was harvested with a blade. Disks were incubated in serum-free medium (low-glucose Dulbecco's Modified Eagle's Medium [DMEM; 1g/L]) supplemented with 1% insulin–transferrin–selenium (ITS, 10 g/ml, 5.5 g/ml, and 5 g/ml, respectively, Sigma, St. Louis, MO), 10 m*M* HEPES buffer, 0.1 m*M* nonessential amino acids, 0.4 m*M* proline, 20 g/ml ascorbic acid, 100 units/ml penicillin G, 100 g/ml streptomycin, and 0.25 g/ml amphotericin B for 2-3 days (5% CO_2; 37°C). Disks for each test were match for anatomic location on the joint surface, and the thickness variation for those receiving dynamic compression was limited to <5%.

Adult human cartilage. Cartilage from adult human knee and ankle joints was obtained postmortem from the Gift of Hope Organ and Tissue Donor Network (Itasca, IL). All procedures were approved by the Rush University Medical Center Institutional Review Board (ORA Number: 08082803-IRB01-AM01) and the Committee on the Use of Humans as Experimental Subjects at MIT. Cartilage explants with intact superficial zone were harvested from the talar domes of both ankle joints of a 71-old-male (joint surfaces scored as modified Collins grade 0 [33]) and the tibial plateau from one knee joint of a 52-old-male (Collins grade 1), using the same procedure as for bovine joints. Ankle disks were cored full thickness (~1.0 mm); for tibial plateau disks, only un-fibrillated cartilage with full thickness greater than 1.0 mm was used and sliced to 1-mm disks. Explants were equilibrated for 2-3 days in high-glucose DMEM (4.5 g/L)

containing the same supplements as the bovine culture medium with the addition of 1 m*M* pyruvate.

Injurious compression and exogenous cytokines. After equilibration, groups of cartilage disks were injuriously compressed in a custom-designed, incubator-housed loading apparatus (Figure 1A)[34]. As described previously[35], each bovine disk was placed in a polysulfone chamber and subjected to radially unconfined compression to 50% final strain at a strain rate of 100%/s, followed by immediate release at the same rate (Figure 1B). After injury, disks were immediately placed in treatment medium in the presence or absence of rhTNF-α (25 ng/ml), rhIL-6 (50 ng/ml), and sIL-6R (250 ng/ml) (R&D Systems, Minneapolis, MN). Previous studies showed that this combination of cytokines caused significantly greater sulfated glycosaminoglycan (sGAG) loss than either cytokine alone[20,36].

Dynamic compression. On Day 0 (Figure 1B), one disk was placed (with superficial surface facing upward) in each well of a 12-well polysulfone loading chamber, with 0.3 ml treatment medium. The chamber was then inserted into the loading apparatus (Figure 1A). Disks were statically compressed to 10% strain to ensure contact, and unconfined dynamic compression was then superimposed using a displacement-controlled haversine waveform (0.5 Hz, 40% duty cycle) continuously for 1 hour, followed by 5 hours rest with the applied static and dynamic load removed. This [1-hour load]—[5-hour-rest] cycle was repeated 4 times per day (Figure 1B). Dynamic compression at three different strain amplitudes (10%, 20%, and 30%) was applied to 3 different groups of 12 explants simultaneously using three identical loading instruments. Medium was changed every 2 days for bovine, and every 3 days for human explants.

sGAG biosynthesis and biochemical analysis. Two days prior to termination, culture medium was supplemented with 5 μCi/ml [^{35}S]-sulfate (Perkin-Elmer, Norwalk, CT). Upon termination, disks were washed, weighed, and digested with proteinase K (Roche, Indianapolis, MN). The amount of radiolabel was measured using a liquid scintillation counter[21]. The sGAG content in the medium and digested explants was quantified using the dimethylmethylene blue assay[37]. Radiolabel concentration was normalized to DNA (measured via Hoechst 33258 dye-binding)[38] for bovine explants, and to wet weight for human explants.

Histologic analysis. After 4 days of treatments, disks (N = 4 from each group) were fixed in 4% paraformaldehyde overnight at 4°C. Next day, disks were cut in half and one of the halves was embedded in paraffin. Serial cross-sections (3 mm-long × 1 mm-wide × 5 μm-thick) were microtomed, immobilized on glass slides, and stained with Mayer's hematoxylin. To quantify cell apoptosis, 1-2 slices from each cross-section were evaluated by light microscopy with a 40x objective. To exclude artifacts of cutting-induced cell death at specimen edges, only cells 100 μm inward from the cut-edges were examined (the superficial-most cells were examined). Nine optical fields (each 0.2 mm × 0.2 mm) were examined for each slice, distributed evenly between left, central, and right positions of the superficial, middle, and deep zones of the tissue. Chondrocytes with condensed and blebbed nuclei were counted as apoptotic cells based on previously published methods and analyses[19], and the rest were counted as normal cells (30-70 total cells/field).

Cell viability. To further study the effect of dynamic compression on chondrocyte viability, tested bovine and human disks were cut into 100-200 μm-thick slices (3 mm-

long × 1 mm-wide cross-sections from superficial surface to 1-mm deep). Fluorescein diacetate (FDA; 4 μg/ml in PBS) was used to stain viable cells green while propidium iodide (PI; 40 μg/ml in PBS) (both from Sigma) stained non-viable cells red. Two slices from each explant were stained for 2-3 minutes in the dark and then washed with PBS. Two separate images were taken for each slice using a Nikon fluorescence microscope with a 4x objective. Cell viability quantification was performed by using the imaging software FIJI (ImageJ). The numbers of viable and non-viable cells were counted via the Image-based Tool for Counting Nuclei (ITCN version 1.6) plug-in.

Gene expression analyses. Bovine cartilage explants from 4 different animals (6 disks per condition per animal) were treated for 48 hours and stored in -80°C after flash-freezing. On the extraction day, the 6 disks from each condition were pooled, pulverized, and lysed in TRIzol reagent (Invitrogen, Carlsbad, CA) with a homogenizer. The extract was then separated using phase-gel tubes (Eppendorf, Hamburg, Germany), and the supernatant was purified following the Qiagen RNeasy mini kit protocol (Qiagen, Chatsworth, CA). Reverse transcription was performed with equal amounts of RNA from each condition using the AmpliTaq-Gold Reverse Transcription kit (Applied Biosystems, Foster City, CA). Primer pairs used were previously reported [27,39] except for the newly designed primer: NF-κB (p65 unit; forward 5'-CGGGTGAATCGGAACTCTGG-3', reverse 5'-TCGATGTCCTCTTTCTGCACC-3'). Real-time qPCR was performed via 384-well plate format using the Applied Biosystems 7700HT instrument with SYBR Green Master Mix (Applied Biosystems) and analyzed as described in detail previously[27]. Gene expression levels were normalized to the housekeeping gene 18S.

Aggrecan degradation by western analysis. Explants were diced and extracted in 4M Guanidine for 48 hours at 4°C. The extracted aggrecan was precipitated overnight at -20°C in 100% ethanol with 5 mM sodium acetate, and then deglycosylated using chondroitinase ABC, keratanase II, and endo-β-galactosidases (all from Seikagaku America, Rockville, MD). Equal amounts of sGAG were loaded on a 4-12% Bis-Tris gradient gel (Invitrogen), and proteins were separated by electrophoresis. Western blot analysis was performed using the monoclonal antibody anti-NITEGE (kindly provided by Dr. Carl Flannery), which is specific to aggrecanase-generated NITEGE neoepitope (Glu^{373}-Ala^{374})[40].

Statistical analysis. To analyze the effects of dynamic compression on sGAG loss and biosynthesis in bovine explants, a linear mixed effects model was used with animal as a random factor, followed by Tukey's post hoc comparison. Bovine chondrocyte apoptosis data from histological images were analyzed using three-way analysis of variance (ANOVA), followed by Tukey's post hoc comparison. Bovine chondrocyte gene expression was log-transformed and analyzed by the linear mixed effect model with animal as a random factor, followed by Bonferroni's test for pair-wise comparisons. Human explant studies were all evaluated using two-way ANOVA with Tukey's post hoc comparison. Statistical analysis was performed using Systat 12 software (Richmond, CA).

2.3 RESULTS

Effects of dynamic compression on sGAG loss, sGAG biosynthesis, and aggrecanase activity in injury/cytokine-treated bovine explants. The initial injurious compression produced peak stresses of 18.5 ± 0.2 MPa (mean ± SEM, n = 96 disks from 4 different animals). Without dynamic compression, the combined injury plus 8-day-cytokine treatment induced 51.4 ± 4.5% sGAG loss (Figure 2A) which was significantly greater than the 7.8 ± 0.1% sGAG loss from untreated controls ($p < 0.0001$), consistent with previous findings[20]. However, the addition of moderate dynamic compression at 10% and 20% strain amplitude reduced this 51.4 ± 4.5% sGAG loss to 39.4 ± 2.8% ($p = 0.007$) and 35.1 ± 3.0% ($p < 0.0001$), respectively (Figure 2A). The largest inhibitory effect of dynamic compression was at 30% strain amplitude (22.9 ± 1.3%), which was a significant decrease even from the 20% strain amplitude ($p = 0.003$).

^{35}S-sulfate incorporation during the last 2 days of culture was used to assess sGAG biosynthesis. Compared to controls (114.0 ± 4.1 pmoles/hour/μg DNA), injury-plus-cytokine treatment significantly reduced biosynthesis ($p < 0.0001$, Figure 2B). Addition of 10% and 20% dynamic compressive strains did not alter this result ($p = 0.946$ and $p = 0.434$, respectively); however, 30% dynamic strain caused a further decrease in biosynthesis rate compared to 20% strain amplitude ($p = 0.015$).

Aggrecan core protein neoepitope NITEGE^{373}-A^{374} generated by aggrecanases (ADAMTS-4/5) was assessed on Days 2, 4, and 8 after treatments. No detectable NITEGE fragments were found in any conditions on Day 2 or Day 4 (data not shown), consistent with a previous study[41]. However, by Day 8, NITEGE-positive fragments were detected following injury-plus-cytokine treatment. The abundance of NITEGE neoepitopes was markedly reduced by 10% dynamic strain amplitude, essentially

abolished by 20%, but unaffected by 30% (Figure 2C). This experiment was repeated using two additional animals with similar results (data not shown).

Effects of dynamic compression on cytokine-induced apoptosis in bovine cartilage. Chondrocyte apoptosis was assessed 4 days after treatments. Compared to normal cells (Figure 3A), apoptotic chondrocytes exhibited condensed cytoplasm and chromatin, as well as nuclear blebbing (Figure 3B). Treatment with cytokines alone significantly increased cell apoptosis compared to untreated controls ($p = 0.011$, Figure 3C), consistent with the consensus that TNF-α signals through apoptotic pathways[42]. Interestingly, 20% dynamic strain reduced apoptosis to levels not different than controls ($p = 0.879$). But at 30% strain amplitude, apoptosis dramatically increased ($p < 0.0001$ compared to cytokines-alone), reaching levels not different from treatment by injurious compression plus cytokines ($p = 0.232$), which is significant from cytokines-alone treatment ($p = 0.002$).

Chondrocyte viability in bovine cartilage. Cell viability in the explants after 2, 4, and 8 days treatments was further assessed via live-dead fluorescence. Representative images (Figure 4) showed minimal cell death in control samples over 8 days. In contrast, injury-plus-cytokines caused marked cell death throughout tissue cross-sections, especially in the superficial zone (cell death in the radial periphery was caused by cutting-induced damage). Qualitatively, dynamic compression at 10% or 20% strain amplitude had little or no additional effect, consistent with the absence of additional apoptosis (Figure 3C). However, 30% dynamic strain resulted in marked loss of cell viability by Day 4, and more so by Day 8.

Bovine chondrocyte gene expression. Aggrecan gene expression was markedly suppressed by cytokines-alone ($p < 0.0001$, Figure 5), consistent with previous findings[36]. Dynamic compression partially rescued this decrease regardless of the strain amplitude ($p < 0.0001$ for all 3 strains). Collagen II expression showed a similar overall response, except that 30% dynamic strain did not rescue the cytokine-induced decrease in collagen II expression ($p = 0.21$). Cytokine treatment markedly upregulated expression of ADAMTS-4 and -5 compared to controls ($p < 0.0001$ for both). While dynamic compression had no effect on ADAMTS-4 expression ($p > 0.1$), 30% dynamic strain amplitude increased ADAMTS-5 expression by more than two fold ($p = 0.012$) compared to cytokine treatment alone. Cytokine treatment increased IL-6 mRNA levels ($p < 0.0001$) but dynamic compression reduced this response to control levels ($p = 0.001$ for 10% and $p < 0.0001$ for both 20% and 30% amplitude). Dynamic strain also significantly countered the increase in NF-κB expression caused by cytokines alone ($p = 0.027$ for 10%, $p = 0.02$ for 20%, and $p = 0.002$ for 30%). While cytokine-plus-dynamic compression at 10% or 20% strain increased COX-2 expression by 3-4 fold compared to cytokines-alone ($p = 0.01$ and $p = 0.002$, respectively), 30% strain caused a further increase to >40 fold compared to cytokines alone ($p < 0.0001$). Cytokines increased iNOS mRNA levels by more than 200 fold ($p < 0.0001$), but 30% strain significantly suppressed this increase in expression ($p = 0.001$).

Effects of dynamic compression on cytokine-treated adult human explants. In an 8-day experiment, human ankle explants were treated similarly to bovine disks but without the initial injurious compression. sGAG release to the medium over 8 days was significantly higher in disks treated with cytokines compared to controls (19.4 ± 3.86%

versus 6.87 ± 0.29%, respectively, $p = 0.003$, Figure 6A). 10% dynamic strain reduced sGAG loss to levels not different than controls ($p = 0.659$). sGAG loss increased further with increasing strain amplitude and was highest at 30% strain (21.95 ± 2.26%), which was not different from cytokine-alone treatment ($p = 0.926$). Biosynthesis rates were decreased by cytokine-treatment (7.70 ± 1.97 pmoles/hour/mg wet weight) compared to control levels (20.37 ± 0.94 to, $p < 0.0001$), and not further affected by dynamic compression (Figure 6B). 2-way ANOVA revealed no differences among all four cytokine ± dynamic compression treatment groups ($p > 0.5$).

Unlike bovine explants, adult human ankle control cartilage showed detectable NITEGE neoepitopes, suggesting the presence of aggrecanase activity even without treatment (Figure 6C). The abundance of NITEGE fragments increased moderately upon cytokine treatment, in the presence and absence of 10% and particularly 20% dynamic strain, but the effect of loading was less at 30% strain. An additional 12-day study was performed using cartilage disks from the tibial plateau of a 52-year-old male donor (Collins grade 1). The pattern of NITEGE abundance (Figure 6D) was similar to that of Figure 6C, though the decrease at 10% dynamic strain, increase at 20% and then decrease at 30% was even more apparent.

Influence of dynamic compression on human ankle chondrocyte viability. Live-dead fluorescence staining showed that the majority of cells in the middle and deep zones of control disks were viable (Figure 7A), though a thin layer of red-stained cells was observed in the superficial zone (possibly the result of previous *in vivo* loading and aging[43]). In contrast, significant cell death throughout the entire thickness of disks was observed for specimens challenged with cytokines plus 30% dynamic compression

(Figure 7B). Imaging analysis (ImageJ software) showed that cytokine treatment alone significantly increased cell death compared to untreated controls ($p = 0.004$, Figure 7C), and 10% dynamic compression abolished this increase to a level not different than controls ($p = 0.522$). 30% strain amplitude significantly increased cell death compared to 10% strain ($p = 0.006$)

2.4 DISCUSSION

Using in vitro models of joint injury, we demonstrated that moderate, intermittent dynamic compression (i.e., 10%-20% strain amplitude with immature bovine and 10% with adult human cartilage) has significant anti-catabolic effects on cartilage homeostasis. Moderate dynamic compression of bovine cartilage rescued cell apoptosis caused by cytokine challenge and upregulated cytokine-suppressed matrix gene expression. In contrast, high compression amplitude (30%) caused severe loss of cell viability and increased matrix degradation in both bovine and human cartilage, and decreased matrix gene expression and biosynthesis in bovine tissue. Consistent with these results, Torzilli[44] reported that load-controlled confined cyclic compression (0.5 Hz) with 0.5 MPa (but not 0.2) peak stress counteracted IL-1α-induced sGAG loss in mature bovine explants. While their loading configuration was different than that of Fig. 1B, their reported inhibitory effect of cyclic loading on sGAG loss is consistent with that demonstrated here for moderate dynamic compression in immature bovine, which sustained a comparable peak stress of 0.55 ± 0.10 MPa at 10% strain amplitude (mean ± SEM, 4 animals).

Interestingly, high (30%) dynamic strain resulted in the greatest inhibition of sGAG loss compared to moderate strains in immature cartilage (Figure 2A). However, high dynamic strain caused significant apoptosis (Figure 3C, as high as injurious compression), and loss of cell viability (Figure 4). Such nonviable cells cannot respond to catabolic cytokines and upregulate aggrecanases that cause sGAG loss. Consistent with this interpretation, 30% dynamic strain also suppressed chondrocyte biosynthesis (Figure 2B). In contrast, 20% strain inhibited apoptosis (Figure 3C), further suggesting that moderate dynamic compression may transduce anti-apoptotic signals, though the mechano-transduction pathways remain to be elucidated. In addition, the increased abundance in NITEGE neoepitope at 30% strain (Figure 2C) indicated elevated aggrecanase activity in the tissue, again contrary to the anti-catabolic effects of moderate dynamic compression. Together, these results lead to our hypothesis that high-magnitude dynamic compression is pro-inflammatory, and the suppression of sGAG loss by 30% strain resulted from load-induced reduction in cell viability, resulting in a slower rate of live-cell-dependent matrix degradation mediated by cytokines.

Adult human cartilage exhibited somewhat different responses to loading. 30% dynamic strain increased sGAG loss compared to 10% strain (Figure 6A), and lower NITEGE abundance was seen at 30% strain compared to 20% (Figure 6C,D). Moderate dynamic at 10% appeared to exert beneficial effects, rather than 20% in immature bovine cartilage. These differences are likely age-related, associated with differences in matrix composition and distribution[45], matrix maturity[19], mechanical properties[31], and cell density[46,47]. The immature bovine tissue is likely more vulnerable, especially the soft superficial zone, which receives the most local strain during compression[32], likely

causing more cell damage at higher strain amplitudes than in human cartilage (Figure 2A vs. 5A). Thus, there appears to be a different threshold in strain amplitude for loss of cell viability and increased matrix degradation in adult human versus immature bovine cartilage and, potentially, a different optimal range of loading amplitude for induction of beneficial effects.

Certain mechanisms by which dynamic compression may regulate cytokine-induced cartilage degradation and biosynthesis were revealed at the gene transcription level. Consistent with previous reports that moderate dynamic compression is an anabolic stimulus for cartilage matrix biosynthesis[21], we observed that 10% and 20% strain amplitude significantly upregulated aggrecan and type II collagen mRNA levels even in the presence of cytokines. This suggests that the anabolic nature of moderate dynamic compression is preserved in an inflammatory environment. Although moderate dynamic compression did not significantly suppress cytokine-induced upregulation of ADAMTS-4 and -5 genes, Western analyses showed strong reduction in aggrecanase activity (Figure 2C). This differences between signals at the gene and protein levels may be due to (1) the time-dependence of gene activation, which we evaluated only at the 48-hour time point, and/or (2) the effects of dynamic compression on post-transcriptional processes such as aggrecanase activation by proprotein convertases[48].

Inflammatory genes cyclo-oxygenase (COX-2) and inducible nitric oxide synthase (iNOS) were activated by cytokines at 48-hour; however, moderate dynamic compression had no inhibitory effects on either gene. Consistent with these results, Chowdhury[29] showed significant inhibition of IL-1β-induced COX-2 and iNOS expression by 15% dynamic compression (1 Hz) at 6 and 12 hours but not 48 hours using

chondrocyte-seeded agarose gels, further emphasizing the time-dependence of gene transcription of mechanical signals. Dynamic compression of bovine explants suppressed cytokine-induced upregulation of IL-6 and NF-κB transcription (Figure 5). Interestingly, Agarwal[49] reported a magnitude-dependent mechanism through which cyclic tensile strain transduced signals via the NF-κB pathway in isolated chondrocytes. Lastly, 30% strain significantly increased ADAMTS-5 and COX-2 expression and had no stimulatory effect on type II collagen expression, further strengthening our hypothesis that high-magnitude dynamic compression is pro-inflammatory.

In the present study, we demonstrated the anti-catabolic effects of moderate dynamic compression on injury/TNF + IL-6/sIL-6R-challenged immature bovine and adult human cartilage. Importantly, we discovered that there exists a threshold strain amplitude above which dynamic compression becomes detrimental to cell viability as well as upregulation of inflammatory genes and aggrecanase activity in the remaining viable cells. Together, these results provide evidence to support the concept that appropriate loading-rehabilitation post-joint injury can be beneficial at the cell level, but above threshold dynamic loading may further contribute to loss of cell and tissue function. Further studies exploring the effects of frequency and loading type (e.g., continuous vs. intermittent) are suggested to optimize the beneficial effects of dynamic loading.

2.5 ACKNOWLEDGEMENTS

This work has been supported by NIH Grants AR060331 and AR045779, and NIH Biomechanics Training Grant Fellowship (YL). The funding sources had no

involvement in the design, collection, analysis and interpretation of data, nor in the writing and submission of this manuscript.

2.6 FIGURES

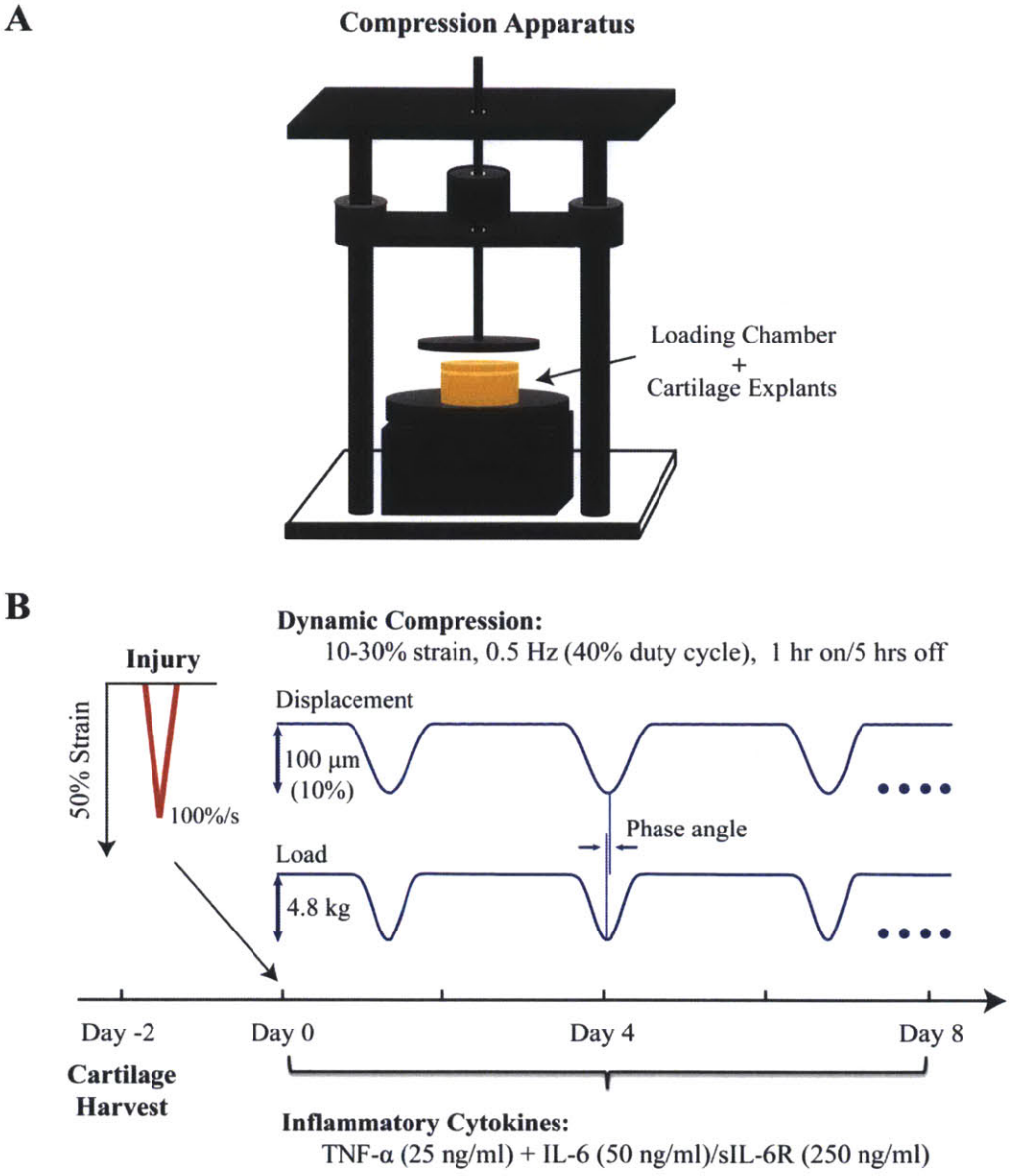

Figure 2.1 **A,** Schematic of custom-designed, incubator-housed loading apparatus [32] used to perform injurious and dynamic compression. **B,** Experimental design: Injurious compression was applied to cartilage explants on Day 0, followed by immediate incubation in TNF-α + IL-6/sIL-6R. Intermittent dynamic compression started on Day 0 (10%, 20% or 30% applied strain amplitude) and continued up through Day 8. Representative waveforms shown for a 10% dynamic strain amplitude applied to a group of 12 disks within the loading chamber, and the corresponding measured total compressive load.

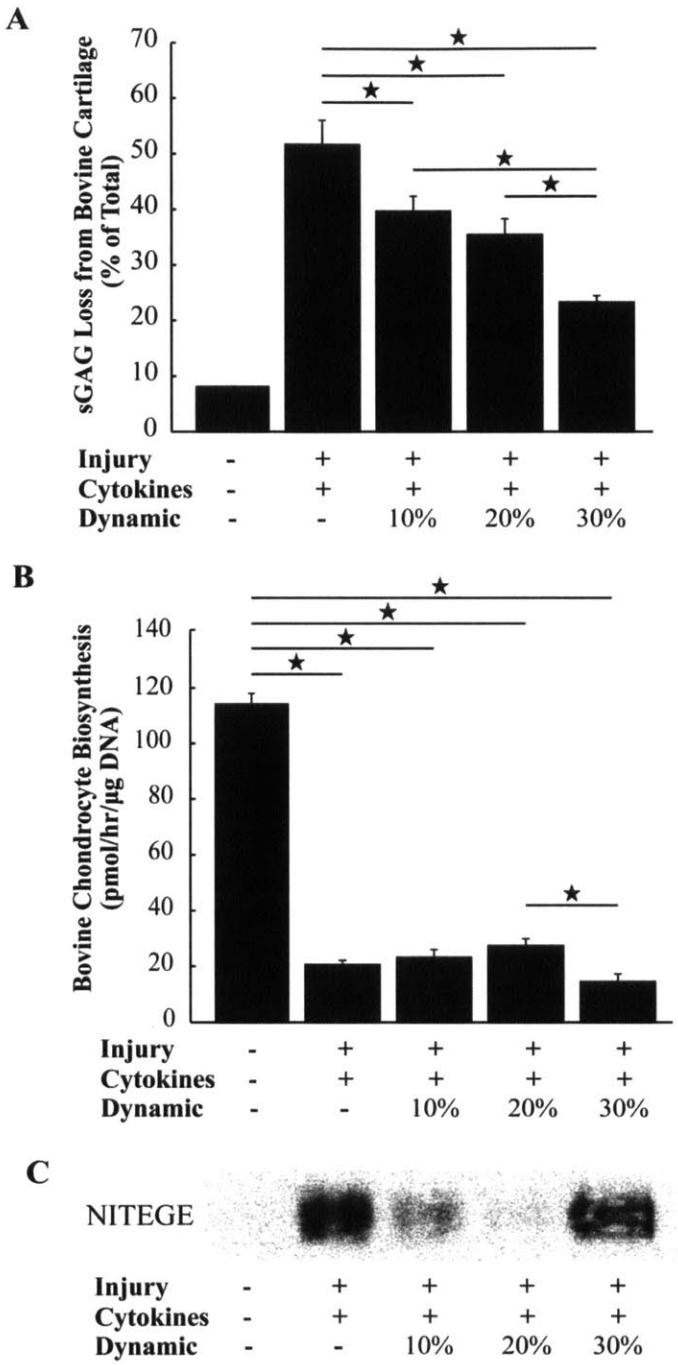

Figure 2.2 **A,** Cumulative sGAG loss from bovine cartilage to the medium in response to 8-day treatments. The total sGAG content in the untreated control group was 439.0 ±12.3 µg sGAG/disk. N = 4 animals (4-6 disks/animal). **B,** Bovine chondrocyte biosynthesis measured during day 6-8 as ^{35}S-sulfate incorporation rate for the same cartilage disks as in **A**. **C,** Western analysis of aggrecan fragments using the antibody to the aggrecanase-generated neoepitope, NITEGE, with aggrecan extracted from the bovine explants 8 days after treatments. Values in A and B are mean ± SEM; * = $P < 0.05$.

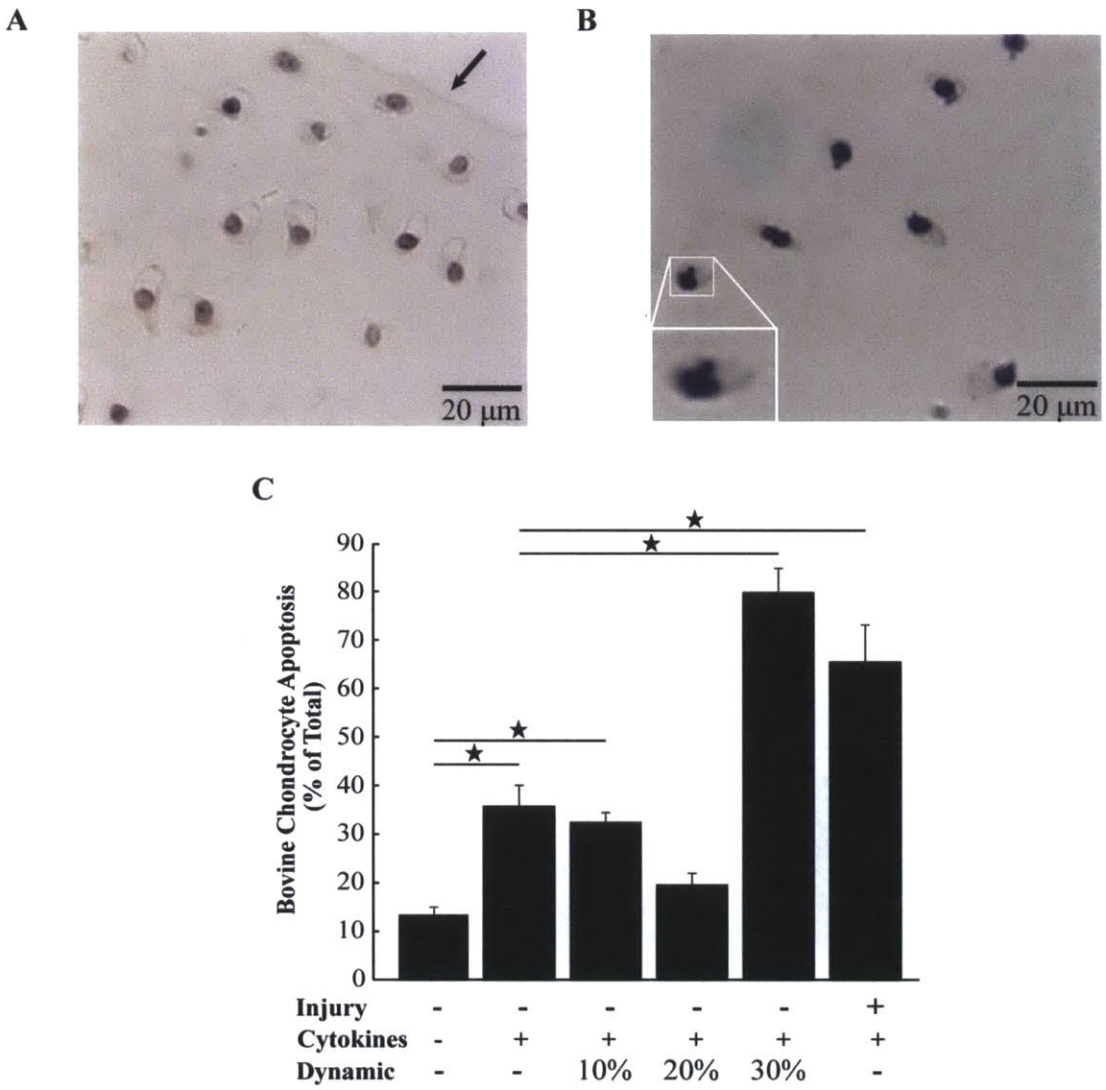

Figure 2.3 Bovine chondrocyte apoptosis within the explants in response to 4-day treatments. **A,** Representative image (40X objective) of histological sections from untreated control disks using hematoxylin staining for the nucleus. The superficial-most surface is visualized in the upper right corner (arrow). **B,** Histological section from explant treated with the combination of cytokines (TNF-α + IL-6/sIL-6R) plus intermittent 30% dynamic strain amplitude. Image (40X objective) was taken from middle zone cartilage: apoptotic cells displayed nuclear blebbing, a morphological marker of apoptosis [17]. Insert: Higher magnification of nuclear blebbing. **C,** Percentage of chondrocytes in histological sections that underwent apoptosis, quantified as the ratio of cells showing nuclear blebbing to total cell count; n = 4 disks per condition (see Methods). Values are mean ± SEM; * = $P < 0.05$.

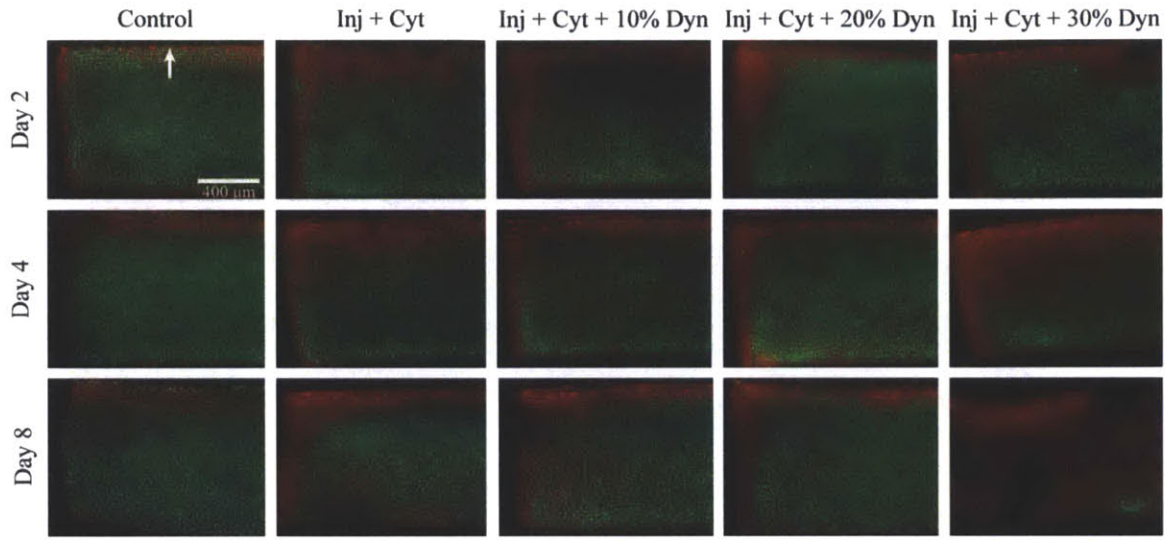

Figure 2.4 Fluorescently stained bovine explants after treatments for 2, 4, and 8 days. A single injurious compression was applied on Day 0, followed by culture in exogenous cytokines. Intermittent dynamic compression (10%, 20%, or 30% strain amplitude) was applied and continued throughout the entire 2-8 day culture period (Figure 1B). Cartilage disks were stained immediately upon termination of culture with fluorescein diacetate (FDA, green) for viable cells and propidium iodide (PI, red) for non-viable cells. Images were taken with a 4X objective. The superficial-most surface is at the top of each image (arrow), while a cut at the middle/deep zone is at the bottom. The left edge of each disk was created when a dermal punch was used to harvest the cartilage disks, each having dimensions 3 mm diameter by 1 mm thick. Inj: injurious compression; Cyt: cytokines TNF-α + IL-6/sIL-6R; Dyn: dynamic compression. Bar = 400 μm.

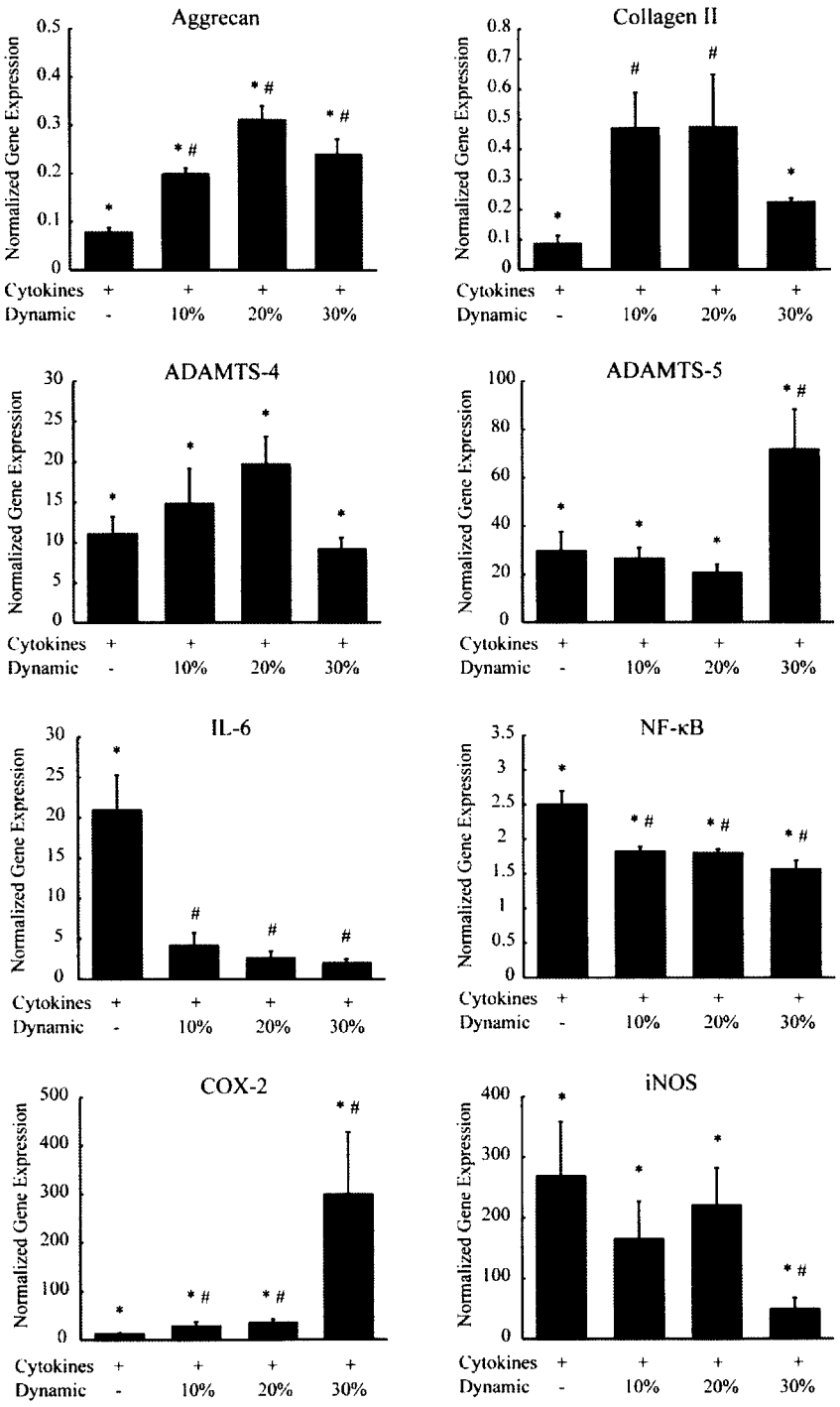

Figure 2.5 The effects of dynamic compression on bovine chondrocyte gene expression after 48 hours of treatment with exogenous cytokines. For each condition, 6 cartilage disks from the same animal were pooled for mRNA extraction; n = 4 animals. Gene expression levels were normalized to that of the 18S gene and then normalized to the no-cytokine, no-compression control condition which had an expression level = 1. Data are presented as mean ± SEM, * = $P < 0.05$ compared with untreated control; # = $P < 0.05$ compared with cytokines-alone treatment.

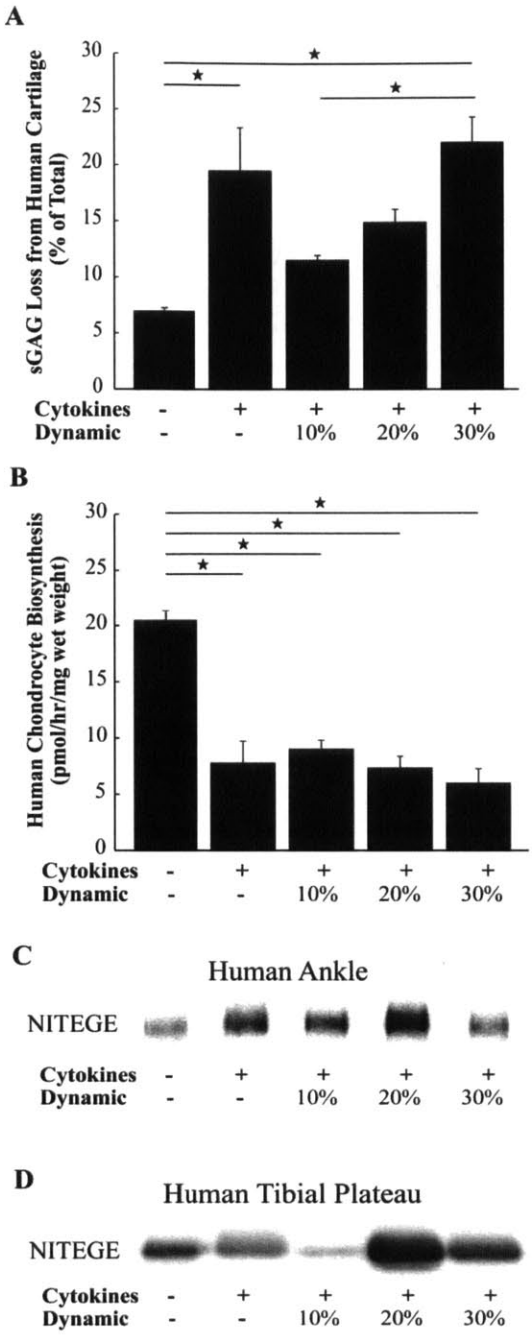

Figure 2.6 **A,** Cumulative sGAG loss from adult human ankle cartilage disks to the medium in response to 8-day treatments. The total sGAG content in the untreated control group was 205.5 ±34.0 µg sGAG/disk, n = 6 disks. **B,** Human chondrocyte biosynthesis measured during day 6-8 as ^{35}S-sulfate incorporation rate for the same cartilage disks as in **A** during days 6-8. **C,** Western analysis of aggrecan fragments using the antibody to the aggrecanase-generated neoepitope, NITEGE, with aggrecan extracted from the human ankle cartilage 8 days after treatments. **D,** Western analysis using aggrecan extracted from human knee cartilage 12 days after treatments. Values in A and B are mean ± SEM, * = $P < 0.05$.

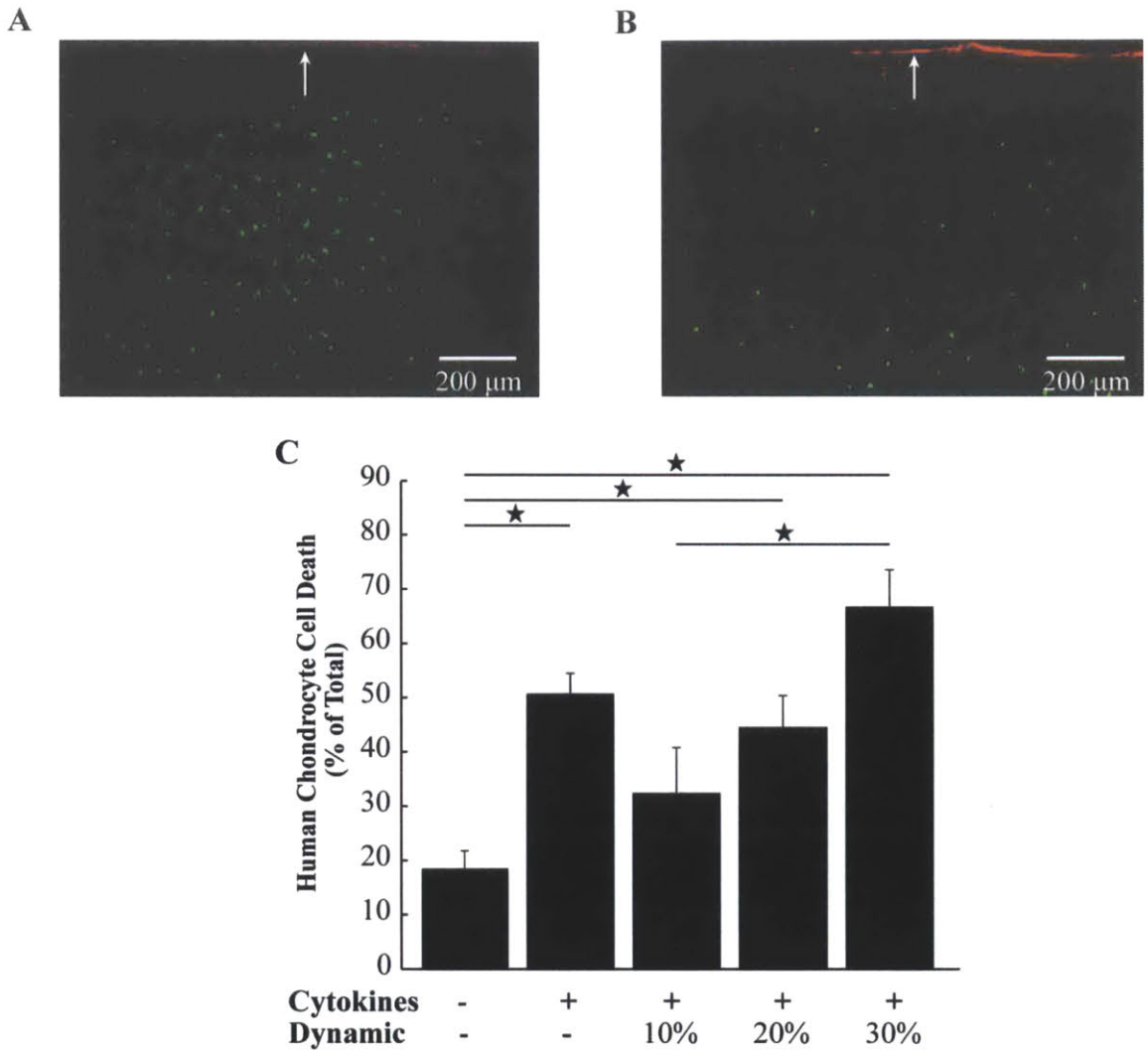

Figure 2.7 Human chondrocyte cell viability in adult human ankle cartilage in response to 8-day treatments. **A,** Representative image (4X objective) from untreated control disks stained with FDA (green, viable cells) and PI (red, non-viable cells). A thin layer of red-stained cells can be seen in the superficial zone at the top (arrow). **B,** Cartilage disks treated with the combination of exogenous cytokines (TNF-α + IL-6/sIL-6R) plus intermittent 30% dynamic compression, with superficial zone at the top of the image (arrow). **C,** Percentage of cell death quantified using the image processing software FIJI (ImageJ). Values are mean ± SEM, * = $P < 0.05$.

2.7 REFERENCES

1. Beynnon BD, Uh BS, Johnson RJ, Abate JA, Nichols CE, Fleming BC, et al. Rehabilitation after anterior cruciate ligament reconstruction: a prospective, randomized, double-blind comparison of programs administered over 2 different time intervals. Am J Sports Med 2005; 33: 347-359.
2. Higuchi H, Shirakura K, Kimura M, Terauchi M, Shinozaki T, Watanabe H, et al. Changes in biochemical parameters after anterior cruciate ligament injury. Int Orthop 2006; 30: 43-47.
3. Elsaid KA, Fleming BC, Oksendahl HL, Machan JT, Fadale PD, Hulstyn MJ, et al. Decreased lubricin concentrations and markers of joint inflammation in the synovial fluid of patients with anterior cruciate ligament injury. Arthritis Rheum 2008; 58: 1707-1715.
4. Catterall JB, Stabler TV, Flannery CR, Kraus VB. Changes in serum and synovial fluid biomarkers after acute injury (NCT00332254). Arthritis Res Ther 2010; 12: R229.
5. Hill CL, Seo GS, Gale D, Totterman S, Gale ME, Felson DT. Cruciate ligament integrity in osteoarthritis of the knee. Arthritis Rheum 2005; 52: 794-799.
6. Lohmander LS, Ostenberg A, Englund M, Roos H. High prevalence of knee osteoarthritis, pain, and functional limitations in female soccer players twelve years after anterior cruciate ligament injury. Arthritis Rheum 2004; 50: 3145-3152.
7. von Porat A, Roos EM, Roos H. High prevalence of osteoarthritis 14 years after an anterior cruciate ligament tear in male soccer players: a study of radiographic and patient relevant outcomes. Ann Rheum Dis 2004; 63: 269-273.
8. Andriacchi TP, Dyrby CO. Interactions between kinematics and loading during walking for the normal and ACL deficient knee. J Biomech 2005; 38: 293-298.
9. Van de Velde SK, Gill TJ, Li G. Evaluation of kinematics of anterior cruciate ligament-deficient knees with use of advanced imaging techniques, three-dimensional modeling techniques, and robotics. J Bone Joint Surg Am 2009; 91 Suppl 1: 108-114.
10. Van de Velde SK, Bingham JT, Hosseini A, Kozanek M, DeFrate LE, Gill TJ, et al. Increased tibiofemoral cartilage contact deformation in patients with anterior cruciate ligament deficiency. Arthritis Rheum 2009; 60: 3693-3702.
11. Hosseini A, Van de Velde S, Gill TJ, Li G. Tibiofemoral cartilage contact biomechanics in patients after reconstruction of a ruptured anterior cruciate ligament. J Orthop Res 2012; 30: 1781-1788.
12. Chen CT, Burton-Wurster N, Lust G, Bank RA, Tekoppele JM. Compositional and metabolic changes in damaged cartilage are peak-stress, stress-rate, and loading-duration dependent. J Orthop Res 1999; 17: 870-879.
13. Kurz B, Jin M, Patwari P, Cheng DM, Lark MW, Grodzinsky AJ. Biosynthetic response and mechanical properties of articular cartilage after injurious compression. J Orthop Res 2001; 19: 1140-1146.
14. Torzilli PA, Grigiene R, Borrelli J, Jr., Helfet DL. Effect of impact load on articular cartilage: cell metabolism and viability, and matrix water content. J Biomech Eng 1999; 121: 433-441.

15. Ewers BJ, Dvoracek-Driksna D, Orth MW, Haut RC. The extent of matrix damage and chondrocyte death in mechanically traumatized articular cartilage explants depends on rate of loading. J Orthop Res 2001; 19: 779-784.
16. Loening AM, James IE, Levenston ME, Badger AM, Frank EH, Kurz B, et al. Injurious mechanical compression of bovine articular cartilage induces chondrocyte apoptosis. Arch Biochem Biophys 2000; 381: 205-212.
17. D'Lima DD, Hashimoto S, Chen PC, Colwell CW, Jr., Lotz MK. Human chondrocyte apoptosis in response to mechanical injury. Osteoarthritis Cartilage 2001; 9: 712-719.
18. Chen CT, Burton-Wurster N, Borden C, Hueffer K, Bloom SE, Lust G. Chondrocyte necrosis and apoptosis in impact damaged articular cartilage. J Orthop Res 2001; 19: 703-711.
19. Kurz B, Lemke A, Kehn M, Domm C, Patwari P, Frank EH, et al. Influence of tissue maturation and antioxidants on the apoptotic response of articular cartilage after injurious compression. Arthritis Rheum 2004; 50: 123-130.
20. Sui Y, Lee JH, DiMicco MA, Vanderploeg EJ, Blake SM, Hung HH, et al. Mechanical injury potentiates proteoglycan catabolism induced by interleukin-6 with soluble interleukin-6 receptor and tumor necrosis factor alpha in immature bovine and adult human articular cartilage. Arthritis Rheum 2009; 60: 2985-2996.
21. Sah RL, Kim YJ, Doong JY, Grodzinsky AJ, Plaas AH, Sandy JD. Biosynthetic response of cartilage explants to dynamic compression. J Orthop Res 1989; 7: 619-636.
22. Ackermann B, Steinmeyer J. Collagen biosynthesis of mechanically loaded articular cartilage explants. Osteoarthritis Cartilage 2005; 13: 906-914.
23. Kim YJ, Sah RL, Grodzinsky AJ, Plaas AH, Sandy JD. Mechanical regulation of cartilage biosynthetic behavior: physical stimuli. Arch Biochem Biophys 1994; 311: 1-12.
24. Quinn TM, Grodzinsky AJ, Buschmann MD, Kim YJ, Hunziker EB. Mechanical compression alters proteoglycan deposition and matrix deformation around individual cells in cartilage explants. J Cell Sci 1998; 111 (Pt 5): 573-583.
25. Buschmann MD, Kim YJ, Wong M, Frank E, Hunziker EB, Grodzinsky AJ. Stimulation of aggrecan synthesis in cartilage explants by cyclic loading is localized to regions of high interstitial fluid flow. Arch Biochem Biophys 1999; 366: 1-7.
26. Soulhat J, Buschmann MD, Shirazi-Adl A. A fibril-network-reinforced biphasic model of cartilage in unconfined compression. J Biomech Eng 1999; 121: 340-347.
27. Fitzgerald JB, Jin M, Dean D, Wood DJ, Zheng MH, Grodzinsky AJ. Mechanical compression of cartilage explants induces multiple time-dependent gene expression patterns and involves intracellular calcium and cyclic AMP. J Biol Chem 2004; 279: 19502-19511.
28. Fitzgerald JB, Jin M, Chai DH, Siparsky P, Fanning P, Grodzinsky AJ. Shear- and compression-induced chondrocyte transcription requires MAPK activation in cartilage explants. J Biol Chem 2008; 283: 6735-6743.
29. Chowdhury TT, Arghandawi S, Brand J, Akanji OO, Bader DL, Salter DM, et al. Dynamic compression counteracts IL-1beta induced inducible nitric oxide

synthase and cyclo-oxygenase-2 expression in chondrocyte/agarose constructs. Arthritis Res Ther 2008; 10: R35.
30. Wilbrink B, Nietfeld JJ, den Otter W, van Roy JL, Bijlsma JW, Huber-Bruning O. Role of TNF alpha, in relation to IL-1 and IL-6 in the proteoglycan turnover of human articular cartilage. Br J Rheumatol 1991; 30: 265-271.
31. Demarteau O, Pillet L, Inaebnit A, Borens O, Quinn TM. Biomechanical characterization and in vitro mechanical injury of elderly human femoral head cartilage: comparison to adult bovine humeral head cartilage. Osteoarthritis Cartilage 2006; 14: 589-596.
32. Rolauffs B, Muehleman C, Li J, Kurz B, Kuettner KE, Frank E, et al. Vulnerability of the superficial zone of immature articular cartilage to compressive injury. Arthritis Rheum 2010; 62: 3016-3027.
33. Muehleman C, Bareither D, Huch K, Cole AA, Kuettner KE. Prevalence of degenerative morphological changes in the joints of the lower extremity. Osteoarthritis Cartilage 1997; 5: 23-37.
34. Frank EH, Jin M, Loening AM, Levenston ME, Grodzinsky AJ. A versatile shear and compression apparatus for mechanical stimulation of tissue culture explants. J Biomech 2000; 33: 1523-1527.
35. Patwari P, Cook MN, DiMicco MA, Blake SM, James IE, Kumar S, et al. Proteoglycan degradation after injurious compression of bovine and human articular cartilage in vitro: interaction with exogenous cytokines. Arthritis Rheum 2003; 48: 1292-1301.
36. Lu YC, Evans CH, Grodzinsky AJ. Effects of short-term glucocorticoid treatment on changes in cartilage matrix degradation and chondrocyte gene expression induced by mechanical injury and inflammatory cytokines. Arthritis Res Ther 2011; 13: R142.
37. Farndale RW, Buttle DJ, Barrett AJ. Improved quantitation and discrimination of sulphated glycosaminoglycans by use of dimethylmethylene blue. Biochim Biophys Acta 1986; 883: 173-177.
38. Kim YJ, Sah RL, Doong JY, Grodzinsky AJ. Fluorometric assay of DNA in cartilage explants using Hoechst 33258. Anal Biochem 1988; 174: 168-176.
39. Wheeler CA, Jafarzadeh SR, Rocke DM, Grodzinsky AJ. IGF-1 does not moderate the time-dependent transcriptional patterns of key homeostatic genes induced by sustained compression of bovine cartilage. Osteoarthritis Cartilage 2009; 17: 944-952.
40. Sandy JD, Neame PJ, Boynton RE, Flannery CR. Catabolism of aggrecan in cartilage explants. Identification of a major cleavage site within the interglobular domain. J Biol Chem 1991; 266: 8683-8685.
41. Patwari P, Gao G, Lee JH, Grodzinsky AJ, Sandy JD. Analysis of ADAMTS4 and MT4-MMP indicates that both are involved in aggrecanolysis in interleukin-1-treated bovine cartilage. Osteoarthritis Cartilage 2005; 13: 269-277.
42. Carames B, Lopez-Armada MJ, Cillero-Pastor B, Lires-Dean M, Vaamonde C, Galdo F, et al. Differential effects of tumor necrosis factor-alpha and interleukin-1beta on cell death in human articular chondrocytes. Osteoarthritis Cartilage 2008; 16: 715-722.

43. Hashimoto S, Ochs RL, Komiya S, Lotz M. Linkage of chondrocyte apoptosis and cartilage degradation in human osteoarthritis. Arthritis Rheum 1998; 41: 1632-1638.
44. Torzilli PA, Bhargava M, Park S, Chen CT. Mechanical load inhibits IL-1 induced matrix degradation in articular cartilage. Osteoarthritis Cartilage 2010; 18: 97-105.
45. Stockwell RA, Scott JE. Distribution of acid glycosaminoglycans in human articular cartilage. Nature 1967; 215: 1376-1378.
46. Jadin KD, Wong BL, Bae WC, Li KW, Williamson AK, Schumacher BL, et al. Depth-varying density and organization of chondrocytes in immature and mature bovine articular cartilage assessed by 3d imaging and analysis. J Histochem Cytochem 2005; 53: 1109-1119.
47. Gilmore RS, Palfrey AJ. Chondrocyte distribution in the articular cartilage of human femoral condyles. J Anat 1988; 157: 23-31.
48. Tortorella MD, Arner EC, Hills R, Gormley J, Fok K, Pegg L, et al. ADAMTS-4 (aggrecanase-1): N-terminal activation mechanisms. Arch Biochem Biophys 2005; 444: 34-44.
49. Agarwal S, Deschner J, Long P, Verma A, Hofman C, Evans CH, et al. Role of NF-kappaB transcription factors in antiinflammatory and proinflammatory actions of mechanical signals. Arthritis Rheum 2004; 50: 3541-3548.

2.8 SUPPLEMENTAL DATA

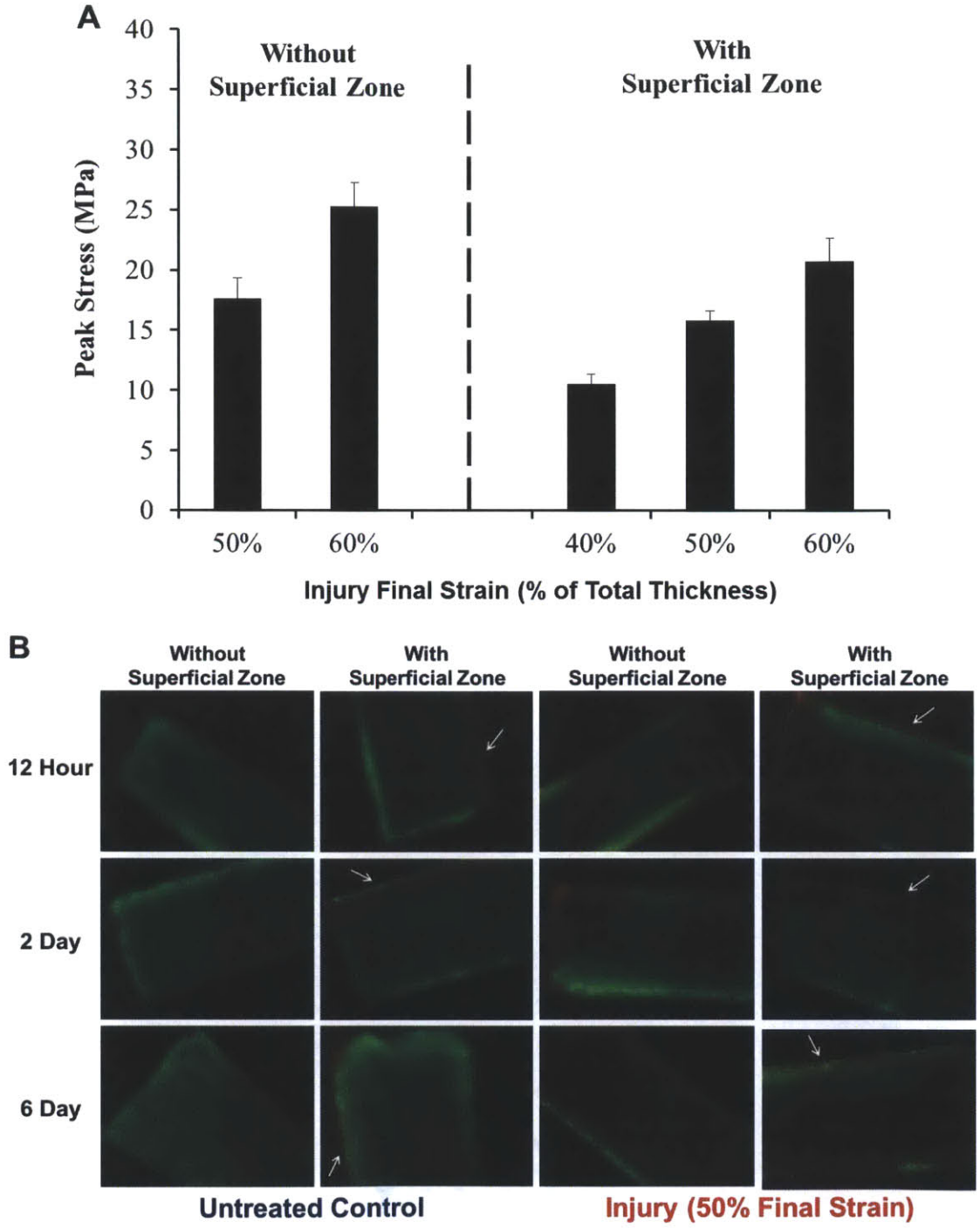

Figure 2S.1 **A,** Peak stress of injury applied on bovine cartilage with or without the superficial zone. Injurious compression was applied at 100%/s to the indicated final strain. Values are mean ± SEM, N = 5 disks. **B,** Fluorescently stained bovine explants after treatments for 12 hour, 2, and 6 days. White arrow indicates the superficial surface.

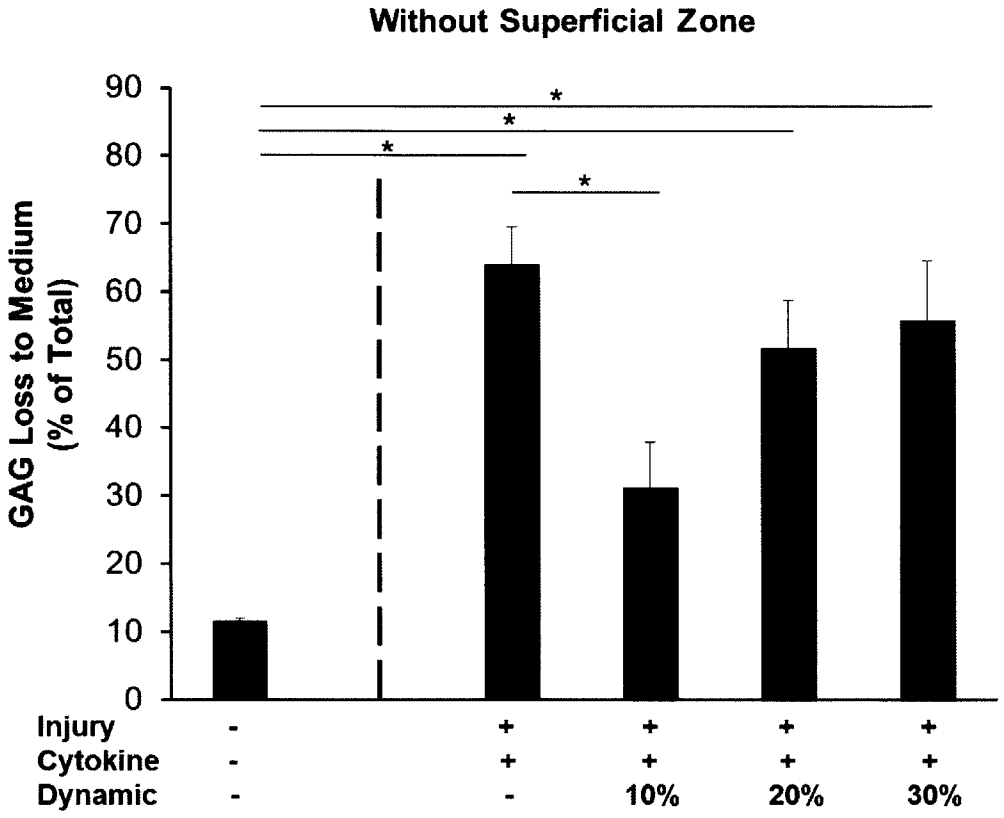

Figure 2S.2 Percent sGAG loss to the medium of bovine cartilage explants without the superficial zone in respond to 8-day treatments. Cytokines: TNF-α (10 ng/ml), IL-6 (20 ng/ml), sIL-6R (100 ng/ml). Values are mean ± SEM, N = 6 disks; * = $P < 0.05$.

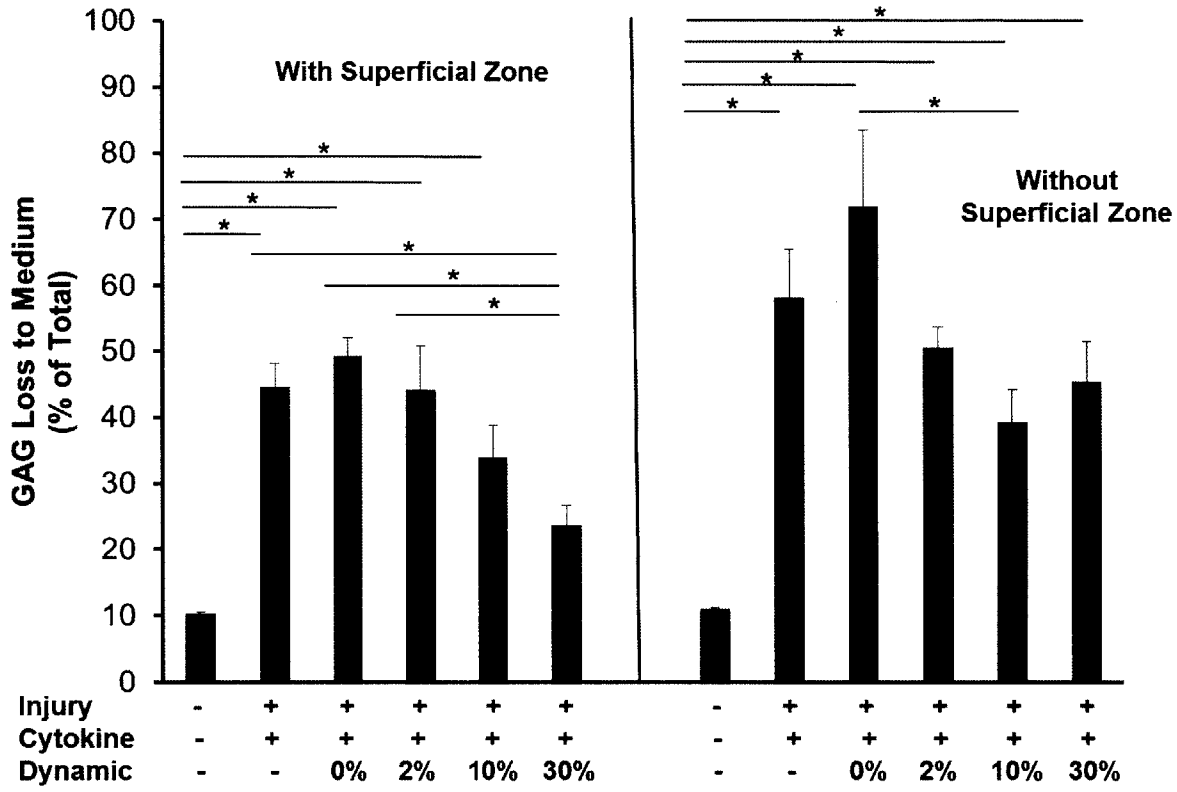

Figure 2S.3 Percent sGAG loss to the medium of bovine cartilage explants with or without the superficial zone in respond to 16-day treatments. Cytokines: TNF-α (10 ng/ml), IL-6 (20 ng/ml), sIL-6R (100 ng/ml). Values are mean ± SEM, N = 6 disks; * = $P < 0.05$.

CHAPTER 3

Effects of Insulin-like Growth Factor-1 and Dexamethasone on Cytokine-Challenged Cartilage: Relevance to Post Traumatic Osteoarthritis

Contents

ABSTRACT

Objective. The inflammatory cytokine interleukin-1 is elevated after traumatic joint injury and plays a critical role in mediating cartilage tissue degradation, suppressing matrix biosynthesis, and inducing chondrocyte apoptosis, events associated with progression to posttraumatic osteoarthritis (PTOA). This study explored the effects of a combination therapy involving insulin-like growth factor 1 (IGF-1) and dexamethasone (Dex) to block these multiple degradative effects of IL-1 challenge to articular cartilage.

Methods. Young bovine and adult human articular cartilage were treated with IL-1α in the presence or absence of IGF-1, Dex, or their combination. Loss of sulfated glycosaminoglycans (sGAG) and collagen were evaluated by the DMMB and hydroxyproline assay, respectively. Matrix biosynthesis was measured via radiolabel incorporation, chondrocyte gene expression was studied using qRT-PCR, and cell viability was examined by fluorescence staining.

Results. The combination of IGF-1 and Dex significantly inhibited IL-1α induced sGAG and collagen loss, rescued the suppressed matrix biosynthesis, and inhibited the loss of chondrocyte viability caused by IL-1α treatment of young bovine cartilage. In adult human cartilage, only IGF-1 rescued matrix biosynthesis and only Dex inhibited sGAG loss and improved cell viability; however, IGF-1 + Dex together showed combined beneficial effects.

Conclusions. Our findings suggest that the combination of IGF-1 and Dex has greater beneficial effects than either molecule alone on preventing cytokine-mediated cartilage

degradation in both young bovine and adult human cartilage. Our results support the use of this combination therapy as a potential treatment option to ameliorate cartilage degradation associated with PTOA.

3.1 INTRODUCTION

Osteoarthritis (OA) is a chronic joint disease characterized by articular cartilage degradation, along with synovial membrane inflammation, subchondral bone remodeling, and severe joint pain. Among the many known risk factors of OA, traumatic injury greatly predisposes the damaged joint to OA development at a younger age, and the resulting post-traumatic OA (PTOA) is a major sub-category of the total OA population. The impact mechanical loading can cause direct damage on the cartilage itself and/or rupture the surrounding soft tissue such as the anterior cruciate ligament (ACL). Immediately and weeks after the injury, synovial fluid concentrations of pro-inflammatory cytokines such as interleukin-1 (IL-1), tumor necrosis factor-α (TNF-α), and IL-6 are highly upregulated (1, 2), during which time increased cartilage matrix fragments and chondrocyte apoptosis have also been detected (3, 4). These pro-inflammatory cytokines eventually drop to the levels found in chronic OA (5) but continue to distort the delicate balance between anabolic and catabolic processes in normal cartilage homeostasis. Therefore, one of the main objectives in the treatment of OA is to restore this imbalance and halt the disease progression.

Even though significant efforts have been invested in developing potential therapeutics to achieve the above goal, currently there is no disease modifying OA drug

(DMOAD) capable of altering the course of the disease with structural and clinical benefits. Given the critical role of pro-inflammatory cytokines in OA development, IL-1 receptor antagonists (IL-1RA) and TNF-α blockers, as well as inhibitors that target cytokine-mediated matrix metalloproteinases (MMPs) or ADAMTSs (a disintegrin-like and metalloproteinase with thrombospondin motif) have been developed (6). Another category of potential DMOADs raised increasing attention is the anabolic growth factor family that regulates cartilage matrix production and cell proliferation and counteracts the catabolic processes induced by cytokines. For example, bone morphogenetic protein 7 (BMP-7) and fibroblast growth factor 18 (FGF-18) have been studied in clinical trials based on their strong anabolic potential in cartilage tissue repair (7).

Insulin-like growth factor 1 (IGF-1) is one of the most well-known anabolic growth factors for its powerful induction of cartilage matrix synthesis, as well as its capacity to abolish cartilage catabolism stimulated by cytokines (8, 9). In chondrocyte, IGF-1 binds to the IGF-1 receptor and transduces signal via the IRS-1/PI3K/Akt pathway, which regulates protein synthesis (10). In addition, IGF-1 provides pro-survival signals and was shown *in vitro* to rescue chondrocyte apoptosis (11) and after mechanical injury (12).

Dexamethasone (Dex) is a potent synthetic glucocorticoid (GC) that has been widely used intra-articularly to relieve inflammation for the treatment of OA and other types of arthritis (13). Long-term use of Dex has been considered as a potential treatment for chronic OA (14) but negative side-effects such as osteoporosis have been noticed, which may be resulted from high dose usage (15) or ineffective local delivery method (16). In vitro, Dex has been shown to significantly block cytokine-induced cartilage

degradation and alleviate suppressed matrix biosynthesis via GC receptor-dependent pathways (17). However, the ability of Dex to modulate cytokine-mediated cartilage degeneration in the presence of an anabolic growth factor such as IGF-1 is still largely unknown. Furthermore, whether this combination therapy can provide additional beneficial effects than the mono therapy remains to be elucidated, and the answer to this question may have significant clinical implications.

In this study, we propose to take advantage of the pro-anabolic and anti-catabolic potential of IGF-1 and Dex with a combination treatment and explore their effects on IL-1α-challenged adult human and young bovine cartilage *in vitro*. We hypothesize that this combination therapy can help to regain the lost balance between cartilage anabolism and catabolism in the presence of the inflammatory cytokine. In additional to matrix biosynthesis and degradation, we hypothesize the cytokine-induced chondrocyte cell death can be rescued by this combination therapy. Furthermore, we propose to examine the hypothesis that the effects of IGF-1 and Dex were consequences of their direct transcriptional regulation by comparing changes at the protein level to their effects on the transcriptional level.

3.2 MATERIALS AND METHODS

Bovine cartilage harvest and culture. Cartilage disks were harvested from the femoropatellar grooves of 1-2-week-old calves (obtained from Research '87, Boylston, MA). A total of 15 joints from 14 animals were used. Briefly, a 3-mm dermal punch was used to core full-thickness cartilage cylinders, and the top 1-mm disk containing intact

superficial zone was obtained with a blade. For each experiment, disks from different treatment groups were matched for anatomic location along the joint surface. Then, disks were equilibrated in serum-free medium (low-glucose DMEM; 1g/L) supplemented with 10 m*M* HEPES buffer, 0.1 m*M* nonessential amino acids, 0.4 m*M* proline, 20 g/ml ascorbic acid, 100 units/ml penicillin G, 100 g/ml streptomycin, and 0.25 g/ml amphotericin B for 2-3 days (5% CO_2; 37°C).

Adult human cartilage tissue. Cartilage from adult human knee and ankle joints was obtained postmortem from the Gift of Hope Organ and Tissue Donor Network (Itasca, IL). All procedures were approved by the Rush University Medical Center Institutional Review Board (ORA Number: 08082803-IRB01-AM01) and the Committee on the Use of Humans as Experimental Subjects at MIT. A total of 11 joints from 7 humans were used. Eight ankle joints (Collin's grade 1/2) were from 5 different donors, age between 64 and 74 year old. Three knee joints were from 3 different donors (19-year-old: Grade 0; 54-year-old: Grade 2; 66-year-old: Grade 1). One donor provided an ankle/knee pair. Full-thickness (~1-2 mm) cartilage disks cored with a 3-mm punch were harvested from the talar domes of ankles and the tibial plateau of knees, only unfibrillated cartilage were used. Explants were equilibrated for 2-3 days in high-glucose DMEM (4.5 g/L) containing the same supplements as the bovine culture medium with the addition of 1 m*M* pyruvate.

Selection study with IL-1α. A preliminary IL-1α dose study (with 1, 2, 5, and 10 ng/ml IL-1α) showed that IGF-1 was most effective in rescuing IL-1α-induced sGAG loss and suppressing biosynthesis at the lowest concentration of IL-1α (data not shown), and therefore, 1 ng/ml of IL-1α was used from hereafter. To select the best combination

of potential therapeutics, bovine disks (from 2 joints of the same animal) were treated with or without 1 ng/ml of IL-1α for 8 days, and with a single or a combination of two of the followings: IGF-1, BMP (Bone morphogenetic protein)-2, BMP-4, BMP-7, FGF-2 (all at 100 ng/ml), and Dex (100 nM).

Biosynthesis, sGAG, and biochemical analysis. Cartilage disks were radiolabeled with 5 μCi/ml ^{35}S-sulfate (Perkin-Elmer, Norwalk, CT) for 36-48 hours. When terminated, disks were washed in PBS, weighted, and digested with proteinase K (Roche, Indianapolis, MN). Radiolabel incorporation was measured using a liquid scintillation counter, and normalized to DNA (measured via Hoechst 33258 dye-binding assay (18) for bovine explants, and to wet weight for human explants. The dimethylmethylene blue assay (19) was used to determine the sGAG content in the digested cartilage explants and medium.

Collagen degradation. Medium and proteinase K digested cartilage samples were analyzed for collagen content using the hydroxyproline assay (20). Briefly, 50-200 μl, depends on the time-point or treatment, of media or cartilage digests were reacted with 200 μl 12N HCl overnight at 110° C. The hydrolysate was then dried on a heating plate and the residue was re-suspended in the assay buffer (375 μl, 23.8 mM citric acid, 88.2 mM sodium acetate, 85 mM sodium hydroxide, and 0.12 v/v% glacial acetic acid, pH 6.0), transferred in duplicate (150 μl) along with the hydroxyproline standards to a 96-well plate. 75 μl of chloramine T reagent (0.57 g chloramine T, 13.0 ml n-propanol, 26.6 ml 10X assay buffer, 10.4 ml DI wa1ter) was then added and allowed to react for 20 min at room temperature. 75 μl of DMBA reagent (1.2 g dimethylaminobenzaldehyde, 4.8 ml n-propanol, and 2.1 ml perchloric acid) was added and the plate was heated at

60°C for 15 min. After the plate was cooled to room temperature, absorbance was determined at 560 nm with a microplate reader. The collagen content in each sample was calculated using the hydroxyproline standard curve (0-40 μg/ml) and data were expressed as percent of total collagen.

Cell viability. After termination in culture, cartilage disks were cut into 100-200 μm-thick slices (3 mm-long × 1 mm-wide cross-sections from superficial surface to 1-mm deep) with a scalpel blade. The slices were incubated for 2-3 min in the dark in PBS containing fluorescein diacetate (FDA; 4 μg/ml) and propidium iodide (PI; 40 μg/ml) (both from Sigma), for viable and non-viable cell staining, respectively. Then the slices were washed twice with PBS and imaged with a Nikon fluorescence microscope with a 4x objective. 1-2 slices were imaged (2 images/slice) for each sample. For human cartilage disks, cell viability was quantified using the imaging software FIJI (ImageJ). The numbers of viable and non-viable cells were counted over each entire slice via the Image-based Tool for Counting Nuclei (ITCN version 1.6) plug-in, and data were expressed as percent of total viable cells.

Gene expression analyses. Bovine cartilage disks from 5 animals (6 disks per condition per animal) were treated for 4 days and stored in -80°C after flash-freezing. The 6 disks from each condition were pooled and pulverized using a custom pulverizer cooled with liquid nitrogen. Each sample was homogenized in TRIzol reagent, and then separated using phase-gel tubes (Eppendorf, Hamburg, Germany). The supernatant was purified following the Qiagen RNeasy mini kit protocol (Qiagen, Chatsworth, CA). Equal amounts of mRNA from each condition were reverse transcribed using the AmpliTaq-Gold Reverse Transcription kit (Applied Biosystems, Foster City, CA). Primer pairs used

were previously reported (21, 22) except for caspase-3: forward 5'-GAAGTCTGACTGGAAAACCC-3', reverse 5'- GAAGTCTGCCTCAACTGGTA-3'. Real-time PCR were performed using the Applied Biosystems 7700HT instrument with SYBR Green Master Mix (Applied Biosystems). As described previously (21), the expression data for each gene were calculated from the threshold cycle (Ct) value, and normalized to the internal housekeeping gene 18S.

Statistical analysis. Student's t test was used to examine the differences between any two treatment groups in the growth factor/Dex selection study. Bovine and human sGAG loss and biosynthesis data, bovine collagen loss data, as well as bovine gene expression data were log-transformed and analyzed by the linear mixed effect model with animal as a random factor, followed by Tukey's test for pair-wise comparisons. Human viability data were analyzed by the linear mixed effect model with the joint type as a fixed variable and donor as a random factor, followed by Tukey's test for pair-wise comparisons. P values less than 0.05 were considered statistically significant.

3.3 RESULTS

Combination therapy selection. The effects of each mono-therapy or combination therapy were evaluated in an 8-day study using bovine explants (Figure 1A&B). Compared to untreated controls (Figure 1A), IL-1α (1 ng/ml) significantly increased sGAG loss ($p = 0.0048$), which was reduced by the mono-therapy with IGF-1 ($p = 0.0215$) or Dex ($p = 0.0269$). As a comparison, mono-therapy with IGF-1 ($p =$

0.0287) or βFGF ($p = 0.0008$) was able to rescue IL-1α-suppressed ^{35}S sulfate incorporation (Figure 1B). Among the combination therapies, only BMP-7 + βFGF failed to reduce IL-1α-induced sGAG loss ($p = 0.0732$). The combination of IGF-1 and Dex showed the strongest reduction in sGAG loss as well as rescued ^{35}S sulfate that is higher ($p = 0.036$) than BMP-7 + βFGF but not significantly different from the other combination therapies. Therefore, the combination therapy of IGF-1 + Dex was selected to be the target of interest for the rest of this study.

The beneficial effects of this combination therapy was further confirmed with 3 independent 8-day experiments (3 different bovine animals) using IL-1α in the presence or absence of IGF-1, Dex, or both. As shown in Figure 1C&D, either IGF or Dex was able to reduce IL-1α-induced sGAG loss or rescue suppressed ^{35}S sulfate incorporation, even though Dex showed less rescuing effect on ^{35}S sulfate incorporation than IGF-1 ($p < 0.0001$). However, the IGF-1 + Dex combination showed significant further reduction in sGAG loss ($p < 0.0001$ vs. either IGF-1 or Dex) and higher ^{35}S sulfate ($p = 0.001$ vs. IGF-1, $p < 0.0001$ vs. Dex).

The effects of IGF-1 and Dex on Collagen Degradation. Bovine explants were cultured in IL-1α medium for 25 days to study the kinetics of sGAG and collagen release. As shown in Figure 2A, IL-1α induced significantly more sGAG loss than the untreated controls (77.0% vs. 8.6%, $p < 0.0001$) for the first 10 days, during which collagen release is negligible in both control and IL-1α treatments. On Day 12, when 84.5% sGAG was depleted from the IL-1α-treated disks, the same disks released significantly more collagen than the untreated controls (6.9% vs. 1.1%, $p = 0.0378$). By Day 25, the collagen loss reached 68.8% for IL-1α treatment vs. 2.1% for controls ($p < 0.0001$).

Next, we examined the effects of IGF-1 and Dex on IL-1α-induced collagen release after sGAG depletion during a 24-day study (3 independent experiments with 3 bovine animals). Except for the control, only IL-1α was added to the treatment medium for the first 12 days, resulting in 74.1% sGAG loss (Figure 2B). On Day 12, IGF-1, Dex, or both were introduced to the treatment medium in the presence of IL-1α. By Day 24, IGF-1 + Dex treatment significantly reduced sGAG loss compared to IL-1α alone ($p < 0.0001$), IGF-1 treatment ($p < 0.0001$), or Dex treatment ($p = 0.0004$).

The accumulated collagen release during Day 12-24 showed that IL-1α alone induced 58.0% vs. 1.1% in the untreated controls ($p < 0.0001$) (Figure 2C). This increase in collagen loss was markedly attenuated by IGF-1 to 23.8% ($p < 0.0001$), and was further reduced by Dex to 14.2% ($p = 0.008$ vs. IL-1α + IGF-1). The combination treatment showed the lowest collagen loss of 7.9% ($p = 0.028$ vs. IL-1α + Dex). Collagen release kinetics revealed that the effects of IGF-1 or Dex became significantly different from IL-1α on Day 18 (Figure 2D), while IGF-1 + Dex treatment showed earlier effects on Day 15. Furthermore, the combination treatment completely arrested collagen release between Day 15-24 compared to the untreated controls ($p = 0.0447$).

IGF-1 and Dex rescued bovine chondrocyte viability in the presence of IL-1α. Bovine disks were cultured in IL-1α medium with or without Dex for 8, 16, and 24 days (Figure 3A). Significant increase in cell death (red-stained cells) can be observed as early as 8 days after IL-1α treatment, and by Day 24, disks had undergone serious degeneration and significant shrinkage in tissue dimensions (Figure 3A, bottom-middle column). In contrast, the addition of Dex completely prevented IL-1α-induced cell death and its effects sustained over 24 days. In a separate experiment (Figure 3B), IGF-1, Dex, or both

successfully rescued IL-1α-induced cell death when they were introduced on Day 0, but no rescuing effects were observed when added on Day 8.

Bovine chondrocyte gene expression. Chondrocyte gene expression in bovine explants was evaluated by qPCR after 4-day treatments and was shown in Figure 4. The matrix genes aggrecan and collagen II were severely suppressed by IL-1α ($p < 0.0001$ for both genes). The addition of IGF-1, Dex, or both significantly rescued aggrecan expression compared to IL-1α alone, and the effect of Dex was greater than that of IGF-1 ($p < 0.0001$). In contrast, only the combination treatment rescued collagen II expression ($p = 0.01$). ADAMTS-4 expression was upregulated by IL-1α ($p < 0.0001$ vs. control), and was suppressed by IGF-1, Dex, or both. IL-1α also increased ADAMTS-5 expression by more than 200 fold, which was then downregulated by IGF-1 or Dex, and their combination showed a further reduction from either treatment ($p = 0.015$ vs. IGF-1, and $p < 0.0001$ vs. Dex). The elevated proprotein convertase PACE-4 and Furin mRNA levels under IL-1α treatment were significantly suppressed by IGF-1 and Dex, respectively (data not shown). The matrix metalloproteinases MMP-3 and MMP-13 were similarly upregulated by a few hundreds fold by IL-1α ($p < 0.0001$ vs. control for both genes). IGF-1 had no significant effect on either gene ($p = 0.103$ for MMP-3, $p = 0.057$ for MMP-13), whereas Dex or the combination markedly reduced both genes ($p < 0.0001$ for both genes). The mRNA of COX-2 was upregulated by IL-1α ($p < 0.0001$ vs. control), but then suppressed by IGF-1 ($p = 0.04$ vs. IL-1α), and further reduced by Dex ($p < 0.0001$ vs. IGF-1). IL-1α significantly increased the expression of iNOS ($p < 0.0001$ vs. control), but IGF-1, Dex, or their combination had no additional effect. Dex completely blocked the effect of IL-1α on IL-6 expression, whereas IGF-1 showed no effect at all.

The apoptosis executioner gene caspase-3 was increased upon IL-1α treatment, but was significantly reduced by Dex or Dex + IGF-1; however, IGF-1 by itself had no suppressive effect.

Effects of IGF-1/Dex on human cartilage degradation and biosynthesis.

Cartilage disks were obtained from 8 human ankle joints of 5 donors and 3 knee joints of 3 donors. Accumulated sGAG losses were evaluated in a 17-day study (8 independent experiments, 5 for ankle and 3 for knee) along with ^{35}S sulfate incorporation rates measured during Day 15-17. For both ankle and knee cartilage, IL-1α treatment increased sGAG loss compared to the untreated control (Figure 5A&C, $p < 0.0001$ for both). The addition of IGF-1, however, had no impact on reducing the elevated sGAG release. In contrast, Dex completely blocked sGAG loss compared to IL-1α alone ($p < 0.0001$ for both ankle and knee) to a level not significantly different from the untreated control ($p = 0.0762$ for ankle and $p = 0.5418$ for knee). The combination treatment showed similar effects as Dex.

Compared to the untreated control, ^{35}S Sulfate incorporation was also suppressed by IL-1α treatment in both ankle and knee cartilage (Figure 5 B&D, $p < 0.0001$ for both). IGF-1 rescued ^{35}S incorporation in the ankle ($p < 0.0001$) and knee ($p = 0.0196$), whereas Dex showed no rescuing effects. The combination of IGF-1 and Dex significantly increased biosynthesis but the effect was similar to the IGF-1 treatment ($p = 0.3936$) in the ankle. However, IGF-1 + Dex had no impact on biosynthesis in the knee compared to the IL-1α treatment ($p = 0.3194$) but its effect is also not significantly different from the IGF-1 treatment ($p = 0.7764$).

Only Dex rescued chondrocyte viability in human cartilage. Chondrocyte viability in human ankle and knee cartilage explants were evaluated 17 days after treatments. Two ankle joints (Collin's grade 1) from a 64-yr-old female donor, and an ankle (Collin's grade 1)/knee (Collin's grade 2) pair from a 66-yr-old female donor were used. As shown in Figure 6A, representative images indicated significant cell death occurred under IL-1α treatment, especially in the superficial zone, and only Dex treatment rescued cell death. Quantitative results in Figure 6B revealed similar trends for both ankle and knee cartilage disks. Specially, IL-1α induced significant cell death compared to the untreated control ($p = 0.0007$ for ankle, $p < 0.0001$ for knee). The addition of IGF-1 showed no improvement on overall viability for both types of joints. In ankle cartilage, Dex rescued majority of cells to the level of the untreated control ($p = 0.9244$). As a comparison, Dex had no effect compared to IL-1α treatment in knee cartilage but significant over IGF-1 treatment ($p = 0.0027$). The combination of IGF-1 and Dex, however, showed significant reduction from Dex treatment to values similar as the corresponding IGF-1 treatment for both ankle and knee cartilage. A closer look at the depth-dependent cell viability in ankle cartilage revealed that majority of cell death occurred in the superficial and middle zones when challenged with IL-1α (Figure 6C). Again, only the addition of Dex rescued cell death throughout the entire depth of the cartilage disks.

3.4 DISCUSSION

The objective of this study was to explore the effects of the IGF-1 + Dex combination on IL-1α-challenged articular cartilage *in vitro*. Our results demonstrated that IGF-1 and Dex complemented each other in adult human cartilage, specifically IGF-1 promoted matrix biosynthesis while Dex blocked matrix loss, and the resulting beneficial effects cannot be achieved by either molecule alone. In young bovine cartilage, both IGF-1 and Dex provided pro-anabolic and anti-catabolic effects but the combinational effects were additive or synergistic. Furthermore, Dex prevented IL-1α-induced chondrocyte cell death in both adult human and young bovine cartilage, while IGF-1 only offered protection in young bovine cartilage. Lastly, the changes at the protein level were consequences of direct transcriptional upregulation by IGF-1 and Dex on aggrecan and collagen II gene expression, and suppression on MMPs, aggrecanases ADAMTS-4 and -5 mRNA, as well as proprotein convertase Furin and PACE 4.

Besides their inhibitory effects on aggrecanase transcription, the mechanisms by which IGF-1 + Dex prevent proteoglycan degradation in the presence of IL-1α may involve inflammatory mediators such as COX-2 and iNOS. COX-2 catalyzes the synthesis of prostaglandin E_2 (PGE_2) and is inducible upon IL-1 stimulation. Our results showed that the elevated COX-2 mRNA was markedly suppressed by IGF-1 + Dex. This COX-2 dependent mechanism may contribute to the overall reduction in cartilage degradation achieved by the combination therapy. In fact, Hardy et al (23) demonstrated that COX-2 is partially responsible for IL-1β-mediated human OA cartilage degradation, and Dex attenuated both COX-2 activity and proteoglycan loss. In contrast to their effects on COX-2, IGF-1 + Dex had no significant effects on iNOS expression. This is consistent with previous studies that showed NO release was strongly suppressed by Dex in both

primary human chondrocytes and bovine explants (17, 24), even though the mRNA express+ion level of iNOS was not blocked by Dex.

The sGAG and collagen loss kinetics study revealed that aggrecan protects the collagen network from IL-1α mediated proteolysis, as shown previously (25). IGF-1 was known to partially suppress MMPs mRNA (26) and collagenase activation, and block collagen release when co-incubate with IL-1α (27). Here, we have shown that IGF-1 is capable of blocking collagen loss even after the majority of sGAG was depleted by IL-1α, suggesting direct suppressive effects of IGF-1 on collagenases. Furthermore, we have shown that Dex had even more pronounced protective effects on collagen by significantly abrogating MMP-3 and MMP-13 expression, consistent with previous studies (28, 29). When combined with IGF-1, they together provide complete protection for collagen that cannot be achieved by either one alone.

The strong IL-6 mRNA induction by IL-1α suggests that the effects of IL-1α were augmented by IL-6, which is strongly suppressed by Dex. Guerne et al (24) showed that Dex (100 nM) rescued the inhibition of PG synthesis by IL-6/sIL-6 or IL-6 in primary human chondrocyte. However, the effect of Dex is more likely to counteract the suppressive effect of cytokine on matrix biosynthesis instead of directly promoting matrix synthesis, since Dex by itself inhibits aggrecan synthesis (data not shown).

One of the surprise findings of this study is that Dex prevented IL-1α-induced chondrocyte cell death in both young bovine and adult human cartilage. To date, there is no report on the effects of Dex on chondrocyte apoptosis induced by inflammatory cytokines. In the absence of inflammatory cytokines, however, Dex is known to induce apoptosis in proliferative chondrocytes cell lines (30, 31), primary chondrocytes (32), as

well as terminally differentiated hypertrophic chondrocytes (33). In contrast, Dex was shown to prevent apoptosis in terminally differentiated cell line (34) and did not compromise cell viability in long-term culture of young bovine cartilage explants (35). The complexity of Dex signaling on cell apoptosis was further evident by studies that showed strong pro-apoptotic effects of Dex in hematological cells, osteoblasts (36), while Dex offers anti-apoptotic effects in epithelial (37), fibroblasts (38), and in carcinoma cells when inflammatory cytokines or anticancer drugs are present (39, 40). Dex can even transduce pro- and anti-apoptotic signals in the same cell type, depending on the stress environment (41, 42). These findings suggest that the pro-apoptotic or anti-apoptotic nature of Dex is cell type-, cell differentiation stage-, dose-, as well as stimulus-dependent. Therefore, when cartilage is challenged with IL-1α, one can speculate that Dex interferes with cytokine-induced apoptotic signaling network, as supported by the downregulated caspase-3 mRNA expression by Dex in the current study. Our preliminary data further corroborate the anti-apoptotic role of Dex in the presence of IL-1α by showing blocked caspase-3 activity at the protein level (data not shown), and the anti-apoptotic mechanisms of Dex are investigated in the ongoing studies.

Compared to the young bovine cartilage, the anti-catabolic and pro-survival potential of IGF-1 were lost when examined in adult human ankle and knee cartilage. Substantial evidences in the literature showed that OA and aging chondrocytes response poorly to IGF-1 (43, 44), while the exact mechanisms are still unknown, possible explanations that have been suggested include the presence of extracellular IGF-1 binding proteins (45, 46), as well as altered intracellular signaling by mediators such as reactive oxygen species (47). Yin et al (10) demonstrated that oxidative stress is

responsible for inhibiting Akt phosphorylation and stimulating MEK-ERK MAPK signaling in human OA chondrocytes, and as a result, IGF-1 signaling was blocked along with proteoglycan synthesis. In the current study, however, the fact that IGF-1 was capable of significantly rescuing IL-1α-suppressed proteoglycan biosynthesis in human cartilage without affecting proteoglycan degradation may suggest that: 1) the extracellular IGF-1 binding proteins did not prevent IGF-1 signaling (48); 2) the Akt signaling pathway can be activated by IGF-1; 3) Akt-independent signaling pathways responsible for regulating proteoglycan degradation and chondrocyte survival are altered in human chondrocytes. Whether the aberrant survival signaling pathway in response to IGF-1 has compromised the anti-apoptotic effect of Dex is still inconclusive, since our results also showed that IGF-1 did not interfere with the anti-apoptotic potential of Dex when human ankle and knee cartilage were stimulated with TNFα and IL-6 (data not shown).

In this study, we examined a potential combination therapy with IGF-1 and Dex and demonstrated their beneficial effects in reversing IL-1α-suppressed biosynthesis and blocking cytokine-induced proteoglycan and collagen degradation in young bovine explants. Furthermore, IGF-1 + Dex strongly inhibit cell death induced in an inflammatory environment. Importantly, we have shown that each therapeutic has its unique role in cytokine-challenged adult human cartilage: IGF-1 offers stimulation on proteoglycan biosynthesis while Dex modulates cartilage catabolism. Consequently, this combination is required to restore the imbalance between anabolic and catabolic processes in OA. The advantageous effects of this combination therapy can be further expanded with improved IGF-1 function (49) as well as appropriate *in vivo* delivery

method, i.e. intra-articular injection with nanoparticles, and thus may stimulate interests for clinical studies to target the treatment of early stage PTOA.

3.5 ACKNOWLEDGEMENTS

This work has been supported by NIH Grants AR060331 and grant from Merrimack Pharmaceuticals to MIT. The funding sources had no involvement in the design, collection, analysis and interpretation of data, nor in the writing and submission of this manuscript.

3.6 FIGURES

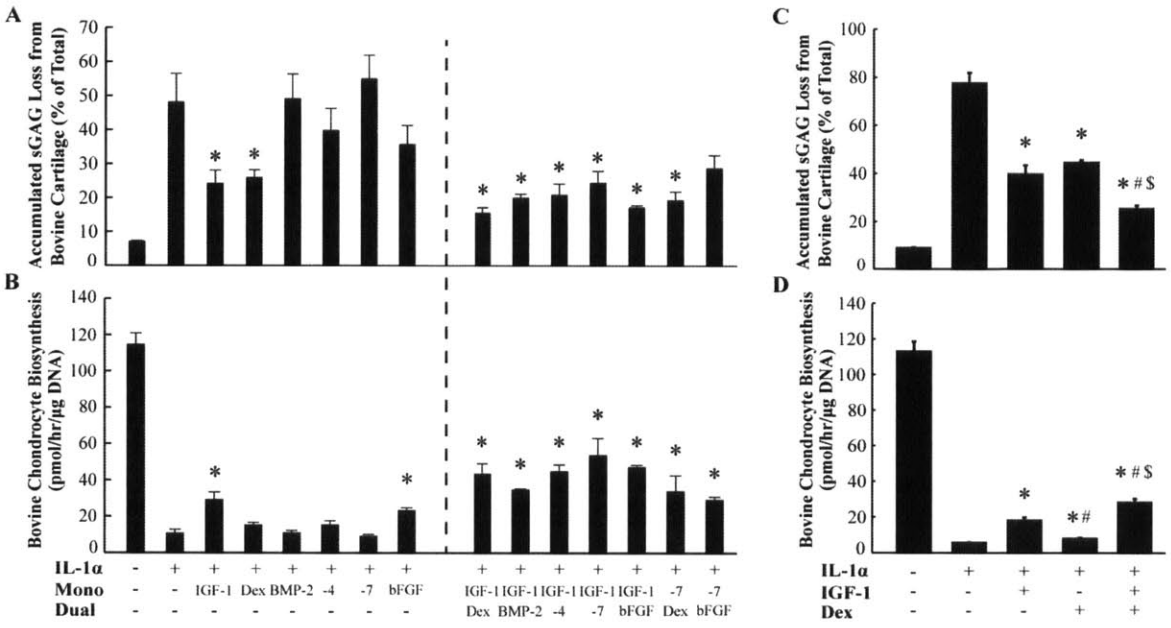

Figure 3.1 **A,** Percent sGAG loss from immature bovine cartilage in an 8-day experiment. Disks were subject to either mono or dual therapy in the presence of IL-1α (1 ng/ml); N = 6 disks. **B,** Normalized sulfate incorporation rate measured during Day6-8 of the same disks in A. **C,** Percent sGAG loss in response to 8-day treatements; N = 18 disks from 3 independent experiments. **D,** Normalized sulfate incorporation rate measured during Day6-8 of the same disks in C. Values are mean and SEM, * vs. IL-1α alone; # vs. IL-1α + IGF-1; $ vs. IL-1α + Dex, $P < 0.05$.

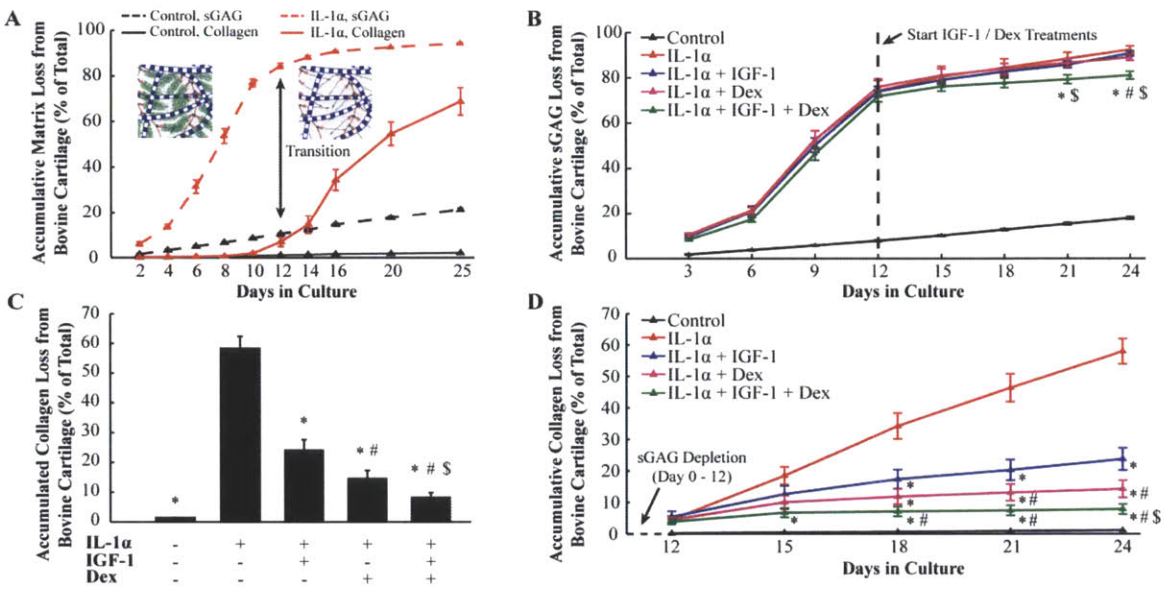

Figure 3.2 **A,** Kinetics of sGAG and collagen loss from immature bovine cartilage in response to 25-day treatment with 1 ng/ml IL-1α; N = 6 disks. **B,** Kinetics of sGAG loss from immature bovine cartilage in response to 24-day treatments. IL-1α (1 ng/ml) was added on Day 0 while IGF-1 and Dex were introduced on Day 12 after majority of sGAG was depleted; N = 18-20 disks from 3 independent experiments. **C,** Accumulated collagen loss to the medium from Day 12 to 24 of disks in B. **D,** Kinetics of collagen loss of disks in B. Values are mean and SEM, * vs. IL-1α alone; # vs. IL-1α + IGF-1; $ vs. IL-1α + Dex, $P < 0.05$.

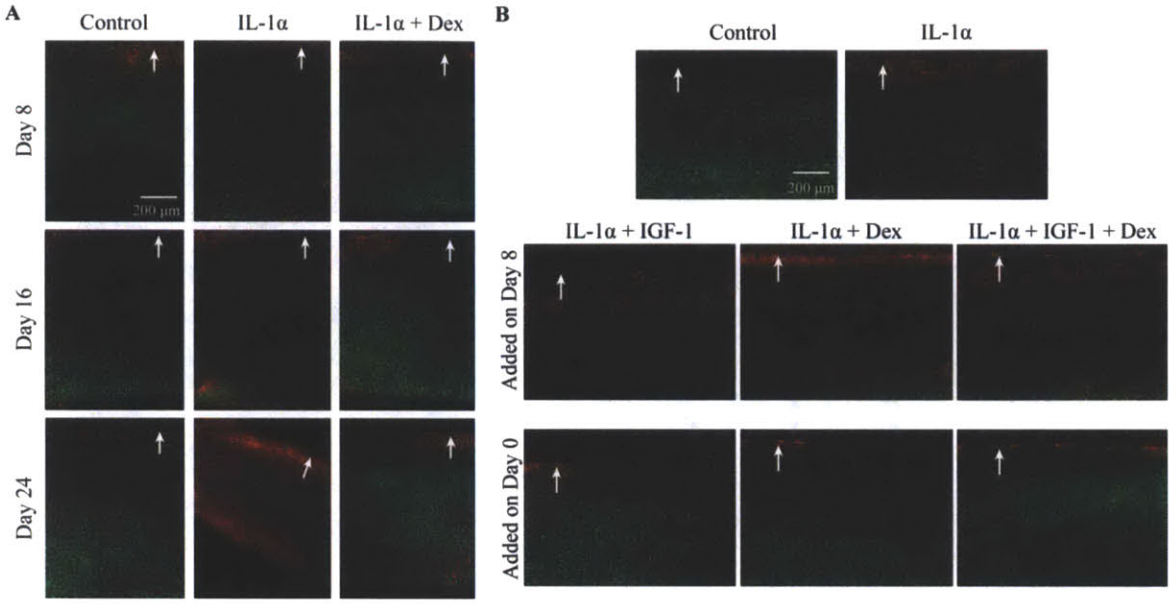

Figure 3.3 **A,** Bovine chondrocyte viability in cartilage disks in response to 8, 16, or 24-day treatments. Cells were fluorecently labeled with fluorescein diacetate (green, viable) and propidium iodide (red, non-viable). **B,** Bovine chondrocyte viability evaluated on Day 16 after treatments. Disks were treated with IL-1α (1ng/ml) for the first 8 days, and switched to 1 pg/ml IL-1α between Day 8 and Day 16. IGF-1, Dex, or both were added either on Day 8 (middle panel) or Day 0 (bottom panel). White arrow: superficial surface. Scale bar = 200 μm.

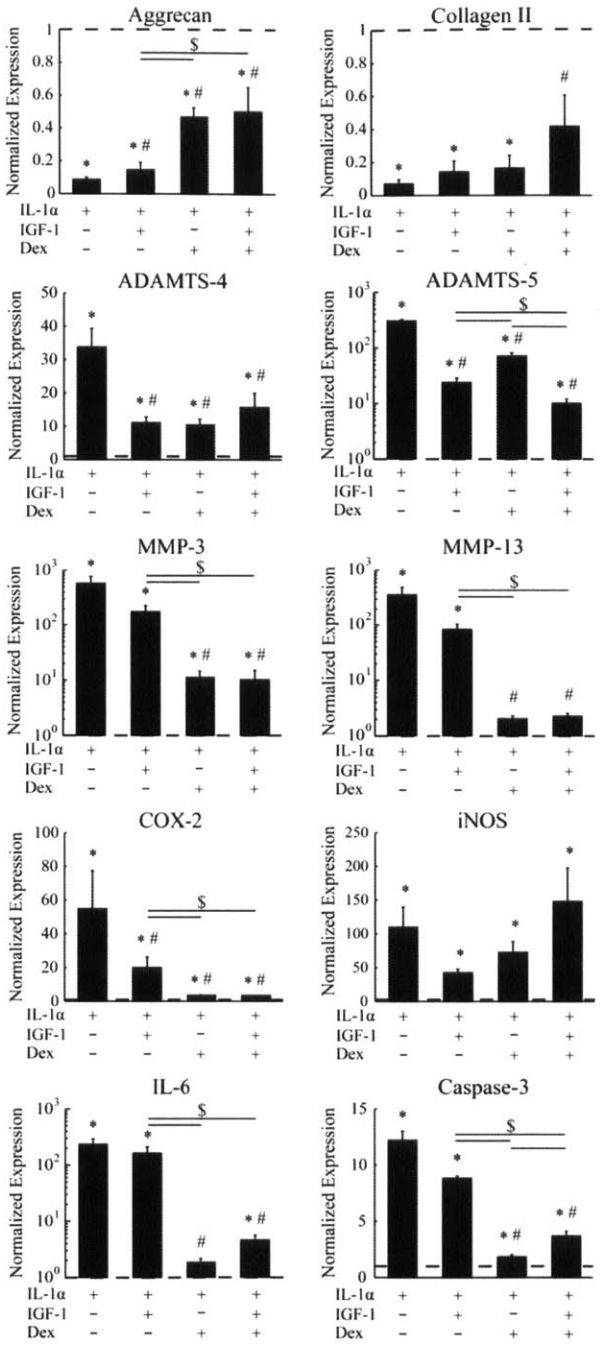

Figure 3.4 The effects of IGF-1/Dex on bovine chondrocyte gene expression after 4-day treatment with IL-1α (1ng/ml). For each condition, 6 cartilage disks from the same animal were pooled for mRNA extraction; n = 5 animals. Gene expression levels were normalized to that of the 18S gene and then normalized to the untreated control condition which had an expression level = 1 (dotted line). Data are presented as mean ± SEM, * vs. untreated control; # vs. IL-1α alone; $ = comparisons between IGF-1, Dex, or both treatments. $p < 0.05$.

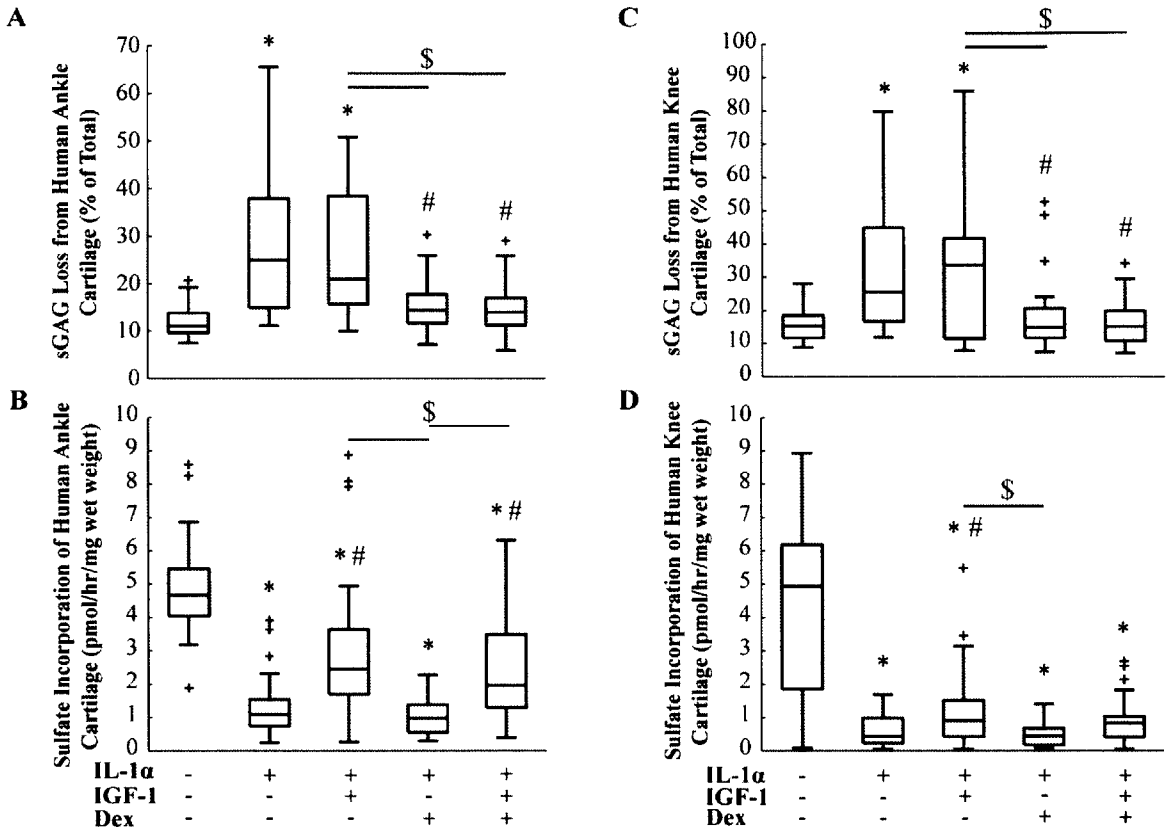

Figure 3.5 **A,** Percent sGAG loss from adult human ankle cartilage in response to 17-day treatments, N = 40 disks from 5 donors (1 independent experiment per donor). **B,** Normalized sulfate incorporation rate during Day 15-17 of the same disks in A. **C,** Percent sGAG loss from adult knee cartilage in response to 17-day treatments, N = 24 disks from 3 donors (1 independent experiment per donor). **D,** Normalized sulfate incorporation rate during Day 15-17 of the same disks in C. Data are presented in box-whisker plots with outliers (+). * vs. untreated control; # vs. IL-1α alone; $ = comparisons between IGF-1, Dex, or both treatments. $p < 0.05$.

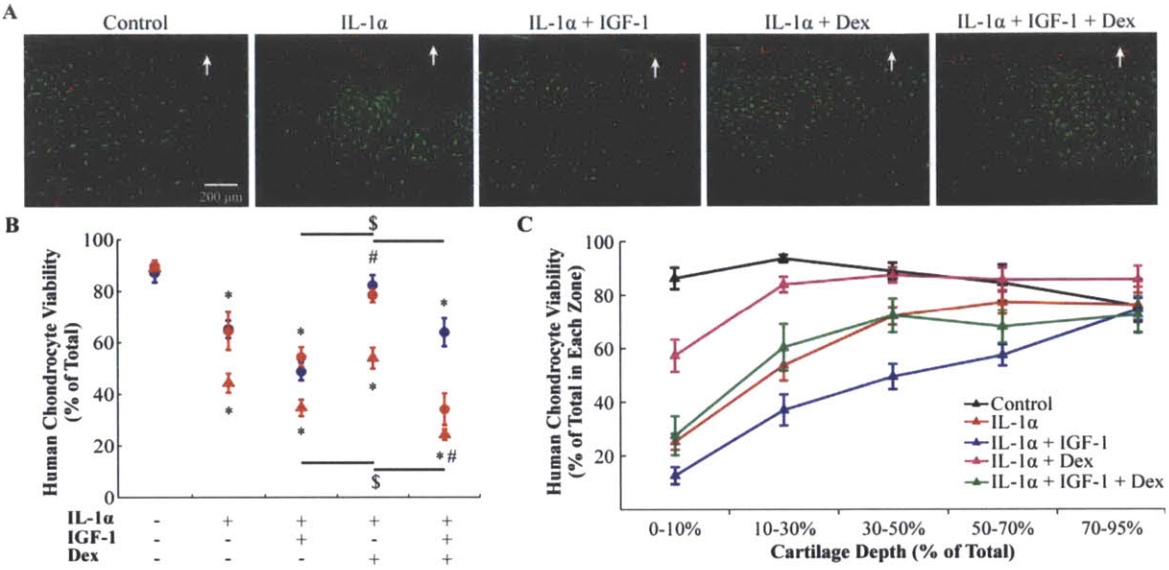

Figure 3.6 **A,** Representative images of fluorescently stained adult human ankle cartilage on Day 17 after treatments. Cells were labeled with fluorescein diacetate (green, viable) and propidium iodide (red, non-viable). White arrow: superficial surface. Scale bar = 200 μm. **B,** Quantified percent viability from red/green images of 2 adult human ankles and 1 human knee cartilage. Blue circle: 64-yr-old female ankle (N = 6 disks, 1-2 slices/disks); red circle: 66-yr-old female ankle (N = 4 disks); red triangle: same 66-yr-old female knee (N = 12 disks). Data are presented as mean ± SEM, * vs. untreated control; # vs. IL-1α alone; $: comparisons between IGF-1, Dex, and IGF-1+Dex, statistical significance was separately indicated for the ankles (above circles) and knee (below triangles). **C,** Depth-dependent cell viability in the 64-yr-old female ankle cartilage. Each slice of a disk was divided into 5 zones, with 0-10% as the superficial zone. The deepest 5% depth was discarded due to cutting-induced cell death.

3.7 REFERENCES

1. Higuchi H, Shirakura K, Kimura M, Terauchi M, Shinozaki T, Watanabe H, et al. Changes in biochemical parameters after anterior cruciate ligament injury. Int Orthop. 2006;30(1):43-7.
2. Elsaid KA, Fleming BC, Oksendahl HL, Machan JT, Fadale PD, Hulstyn MJ, et al. Decreased lubricin concentrations and markers of joint inflammation in the synovial fluid of patients with anterior cruciate ligament injury. Arthritis Rheum. 2008;58(6):1707-15.
3. Johnson DL. Distal femoral shaft fracture: a complication of endoscopic anterior cruciate ligament reconstruction--a case report. Am J Sports Med. 1998;26(2):344.
4. Catterall JB, Stabler TV, Flannery CR, Kraus VB. Changes in serum and synovial fluid biomarkers after acute injury (NCT00332254). Arthritis Res Ther. 2010;12(6):R229.
5. Irie K, Uchiyama E, Iwaso H. Intraarticular inflammatory cytokines in acute anterior cruciate ligament injured knee. Knee. 2003;10(1):93-6.
6. Kapoor M, Martel-Pelletier J, Lajeunesse D, Pelletier JP, Fahmi H. Role of proinflammatory cytokines in the pathophysiology of osteoarthritis. Nat Rev Rheumatol. 2011;7(1):33-42.
7. Hunter DJ. Pharmacologic therapy for osteoarthritis--the era of disease modification. Nat Rev Rheumatol. 2011;7(1):13-22.
8. Tyler JA. Insulin-like growth factor 1 can decrease degradation and promote synthesis of proteoglycan in cartilage exposed to cytokines. Biochem J. 1989;260(2):543-8.
9. Sah RL, Chen AC, Grodzinsky AJ, Trippel SB. Differential effects of bFGF and IGF-I on matrix metabolism in calf and adult bovine cartilage explants. Arch Biochem Biophys. 1994;308(1):137-47.
10. Yin W, Park JI, Loeser RF. Oxidative stress inhibits insulin-like growth factor-I induction of chondrocyte proteoglycan synthesis through differential regulation of phosphatidylinositol 3-Kinase-Akt and MEK-ERK MAPK signaling pathways. J Biol Chem. 2009;284(46):31972-81.
11. Lo MY, Kim HT. Chondrocyte apoptosis induced by collagen degradation: inhibition by caspase inhibitors and IGF-1. J Orthop Res. 2004;22(1):140-4.
12. D'Lima DD, Hashimoto S, Chen PC, Lotz MK, Colwell CW. Prevention of chondrocyte apoptosis. J Bone Joint Surg Am. 2001;83-A Suppl 2(Pt 1):25-6.
13. Mina R, Melson P, Powell S, Rao M, Hinze C, Passo M, et al. Effectiveness of dexamethasone iontophoresis for temporomandibular joint involvement in juvenile idiopathic arthritis. Arthritis Care Res (Hoboken). 2011;63(11):1511-6.
14. Stein A, Yassouridis A, Szopko C, Helmke K, Stein C. Intraarticular morphine versus dexamethasone in chronic arthritis. Pain. 1999;83(3):525-32.
15. Ishida Y, Heersche JN. Glucocorticoid-induced osteoporosis: both in vivo and in vitro concentrations of glucocorticoids higher than physiological levels attenuate osteoblast differentiation. J Bone Miner Res. 1998;13(12):1822-6.
16. Gerwin N, Hops C, Lucke A. Intraarticular drug delivery in osteoarthritis. Adv Drug Deliv Rev. 2006;58(2):226-42.
17. Lu YCS, Evans CH, Grodzinsky AJ. Effects of short-term glucocorticoid treatment on changes in cartilage matrix degradation and chondrocyte gene

expression induced by mechanical injury and inflammatory cytokines. Arthritis Research & Therapy. 2011;13(5).
18. Kim YJ, Sah RL, Doong JY, Grodzinsky AJ. Fluorometric assay of DNA in cartilage explants using Hoechst 33258. Anal Biochem. 1988;174(1):168-76.
19. Farndale RW, Buttle DJ, Barrett AJ. Improved quantitation and discrimination of sulphated glycosaminoglycans by use of dimethylmethylene blue. Biochim Biophys Acta. 1986;883(2):173-7.
20. WOESSNER JF. The determination of hydroxyproline in tissue and protein samples containing small proportions of this imino acid. Arch Biochem Biophys. 1961;93:440-7.
21. Fitzgerald JB, Jin M, Dean D, Wood DJ, Zheng MH, Grodzinsky AJ. Mechanical compression of cartilage explants induces multiple time-dependent gene expression patterns and involves intracellular calcium and cyclic AMP. J Biol Chem. 2004;279(19):19502-11.
22. Wheeler CA, Jafarzadeh SR, Rocke DM, Grodzinsky AJ. IGF-1 does not moderate the time-dependent transcriptional patterns of key homeostatic genes induced by sustained compression of bovine cartilage. Osteoarthritis Cartilage. 2009;17(7):944-52.
23. Hardy MM, Seibert K, Manning PT, Currie MG, Woerner BM, Edwards D, et al. Cyclooxygenase 2-dependent prostaglandin E-2 modulates cartilage proteoglycan degradation in human osteoarthritis explants. Arthritis and Rheumatism. 2002;46(7):1789-803.
24. Guerne PA, Desgeorges A, Jaspar JM, Relic B, Peter R, Hoffmeyer P, et al. Effects of IL-6 and its soluble receptor on proteoglycan synthesis and NO release by human articular chondrocytes: comparison with IL-1. Modulation by dexamethasone. Matrix Biology. 1999;18(3):253-60.
25. Pratta MA, Yao WQ, Decicco C, Tortorella MD, Liu RQ, Copeland RA, et al. Aggrecan protects cartilage collagen from proteolytic cleavage. Journal of Biological Chemistry. 2003;278(46):45539-45.
26. Im HJ, Pacione C, Chubinskaya S, van Wijnen AJ, Sun YB, Loeser RF. Inhibitory effects of insulin-like growth factor-1 and osteogenic protein-1 on fibronectin fragment- and interleukin-1 beta-stimulated matrix metalloproteinase-13 expression in human chondrocytes. Journal of Biological Chemistry. 2003;278(28):25386-94.
27. Hui W, Rowan AD, Cawston T. Insulin-like growth factor 1 blocks collagen release and down regulates matrix metalloproteinase-1,-3,-8, and-13 mRNA expression in bovine nasal cartilage stimulated with oncostatin M in combination with interleukin 1 alpha. Annals of the Rheumatic Diseases. 2001;60(3):254-61.
28. Sadowski T, Steinmeyer J. Effects of non-steroidal antiinflammatory drugs and dexamethasone on the activity and expression of matrix metalloproteinase-1, matrix metalloproteinase-3 and tissue inhibitor of metalloproteinases-1 by bovine articular chondrocytes. Osteoarthritis and Cartilage. 2001;9(5):407-15.
29. Richardson DW, Dodge GR. Dose-dependent effects of corticosteroids on the expression of matrix-related genes in normal and cytokine-treated articular chondrocytes. Inflammation Research. 2003;52(1):39-49.

30. Heino TJ, Chagin AS, Takigawa M, Savendahl L. Effects of alendronate and pamidronate on cultured rat metatarsal bones: Failure to prevent dexamethasone-induced growth retardation. Bone. 2008;42(4):702-9.
31. Chrysis D, Zaman F, Chagin AS, Takigawa M, Sävendahl L. Dexamethasone induces apoptosis in proliferative chondrocytes through activation of caspases and suppression of the Akt-phosphatidylinositol 3'-kinase signaling pathway. Endocrinology. 2005;146(3):1391-7.
32. Van Offel JF, Schuerwegh AJ, Bridts CH, Stevens WJ, De Clerck LS. Effect of bisphosphonates on viability, proliferation, and dexamethasone-induced apoptosis of articular chondrocytes. Ann Rheum Dis. 2002;61(10):925-8.
33. Silvestrini G, Ballanti P, Patacchioli FR, Mocetti P, Di Grezia R, Wedard BM, et al. Evaluation of apoptosis and the glucocorticoid receptor in the cartilage growth plate and metaphyseal bone cells of rats after high-dose treatment with corticosterone. Bone. 2000;26(1):33-42.
34. Mushtaq T, Farquharson C, Seawright E, Ahmed SF. Glucocorticoid effects on chondrogenesis, differentiation and apoptosis in the murine ATDC5 chondrocyte cell line. J Endocrinol. 2002;175(3):705-13.
35. Bian L, Stoker AM, Marberry KM, Ateshian GA, Cook JL, Hung CT. Effects of dexamethasone on the functional properties of cartilage explants during long-term culture. Am J Sports Med. 2010;38(1):78-85.
36. Weinstein RS, Chen JR, Powers CC, Stewart SA, Landes RD, Bellido T, et al. Promotion of osteoclast survival and antagonism of bisphosphonate-induced osteoclast apoptosis by glucocorticoids. J Clin Invest. 2002;109(8):1041-8.
37. Spiecker M, Darius H, Liao JK. A functional role of I kappa B-epsilon in endothelial cell activation. J Immunol. 2000;164(6):3316-22.
38. Gascoyne DM, Kypta RM, Vivanco M. Glucocorticoids inhibit apoptosis during fibrosarcoma development by transcriptionally activating Bcl-xL. J Biol Chem. 2003;278(20):18022-9.
39. Messmer UK, Pereda-Fernandez C, Manderscheid M, Pfeilschifter J. Dexamethasone inhibits TNF-alpha-induced apoptosis and IAP protein downregulation in MCF-7 cells. Br J Pharmacol. 2001;133(4):467-76.
40. Herr I, Gassler N, Friess H, Büchler MW. Regulation of differential pro- and anti-apoptotic signaling by glucocorticoids. Apoptosis. 2007;12(2):271-91.
41. Kaufer D, Ogle WO, Pincus ZS, Clark KL, Nicholas AC, Dinkel KM, et al. Restructuring the neuronal stress response with anti-glucocorticoid gene delivery. Nat Neurosci. 2004;7(9):947-53.
42. Ekert P, MacLusky N, Luo XP, Lehotay DC, Smith B, Post M, et al. Dexamethasone prevents apoptosis in a neonatal rat model of hypoxic-ischemic encephalopathy (HIE) by a reactive oxygen species-independent mechanism. Brain Research. 1997;747(1):9-17.
43. Guerne PA, Blanco F, Kaelin A, Desgeorges A, Lotz M. Growth factor responsiveness of human articular chondrocytes in aging and development. Arthritis Rheum. 1995;38(7):960-8.
44. Loeser RF, Shanker G, Carlson CS, Gardin JF, Shelton BJ, Sonntag WE. Reduction in the chondrocyte response to insulin-like growth factor 1 in aging and

osteoarthritis: studies in a non-human primate model of naturally occurring disease. Arthritis Rheum. 2000;43(9):2110-20.
45. Martin JA, Ellerbroek SM, Buckwalter JA. Age-related decline in chondrocyte response to insulin-like growth factor-I: the role of growth factor binding proteins. J Orthop Res. 1997;15(4):491-8.
46. De Ceuninck F, Caliez A, Dassencourt L, Anract P, Renard P. Pharmacological disruption of insulin-like growth factor 1 binding to IGF-binding proteins restores anabolic responses in human osteoarthritic chondrocytes. Arthritis Res Ther. 2004;6(5):R393-403.
47. Loeser RF, Carlson CS, Del Carlo M, Cole A. Detection of nitrotyrosine in aging and osteoarthritic cartilage: Correlation of oxidative damage with the presence of interleukin-1beta and with chondrocyte resistance to insulin-like growth factor 1. Arthritis Rheum. 2002;46(9):2349-57.
48. Morales TI. The quantitative and functional relation between insulin-like growth factor-I (IGF) and IGF-binding proteins during human osteoarthritis. J Orthop Res. 2008;26(4):465-74.
49. Miller RE, Grodzinsky AJ, Cummings K, Plaas AH, Cole AA, Lee RT, et al. Intraarticular injection of heparin-binding insulin-like growth factor 1 sustains delivery of insulin-like growth factor 1 to cartilage through binding to chondroitin sulfate. Arthritis Rheum. 2010;62(12):3686-94.

3.8 SUPPLEMENTAL DATA

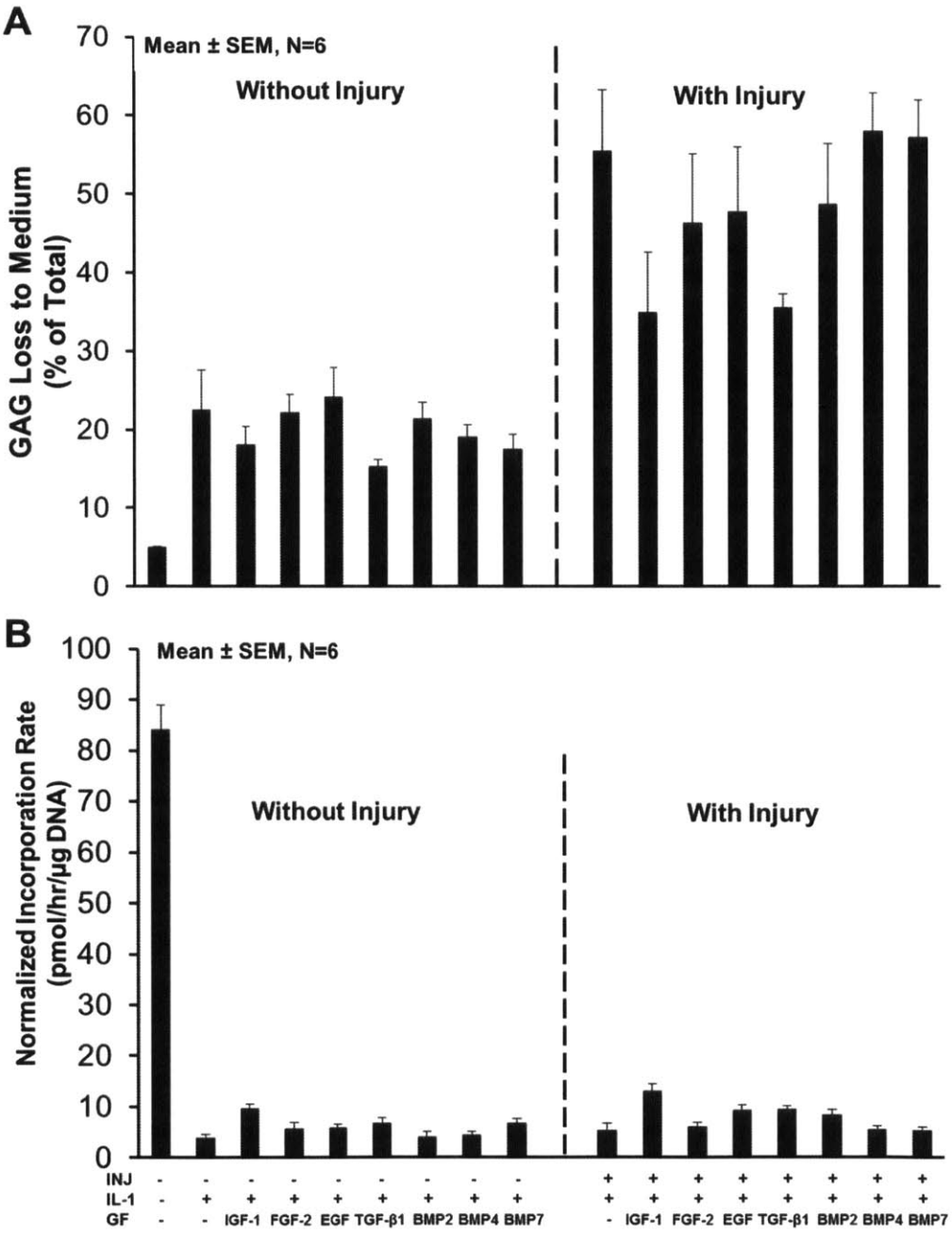

Figure 3S.1 **A,** Percent sGAG loss from immature bovine cartilage in a 4-day experiment. Disks were subject to mono growth factor therapy with or without initial injury in the presence of IL-1α (10 ng/ml). Concentration used: IGF-1 (100 ng/ml), FGF-2 (10 ng/ml), EGF (10 ng/ml), TGF-β1 (10 ng/ml), BMP-2, -4, -7 (all 100 ng/ml); N = 6 disks. **B,** Normalized sulfate incorporation rate measured during Day2-4 of the same disks in A.

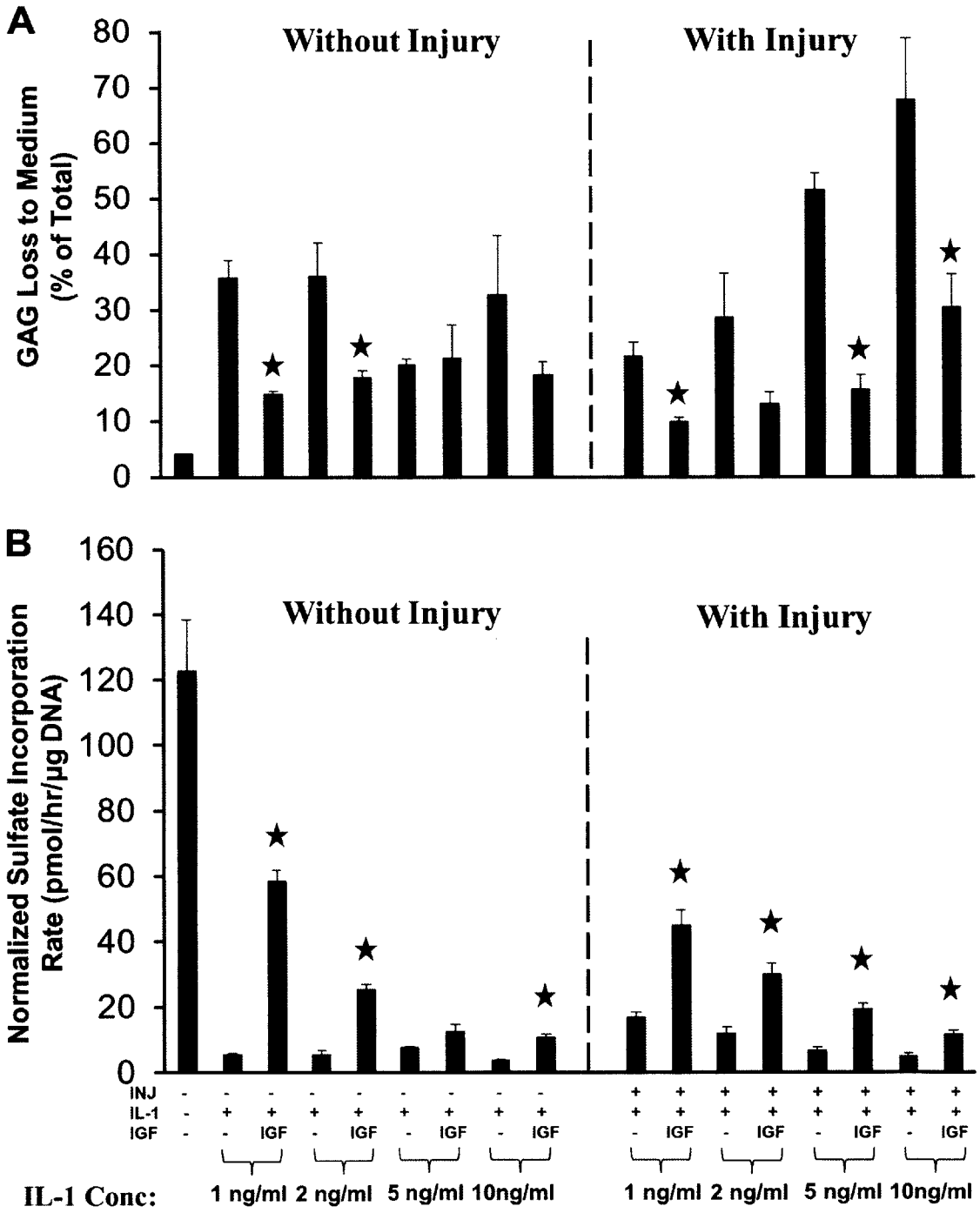

Figure 3S.2 The effect of IL-1α dose on IGF-1 A, Percent sGAG loss from immature bovine cartilage in a 4-day experiment. Disks were subject to IGF-1 with or without initial injury. N = 4 disks. **B,** Normalized sulfate incorporation rate measured during Day2-4 of the same disks in A. ★ $p < 0.05$.

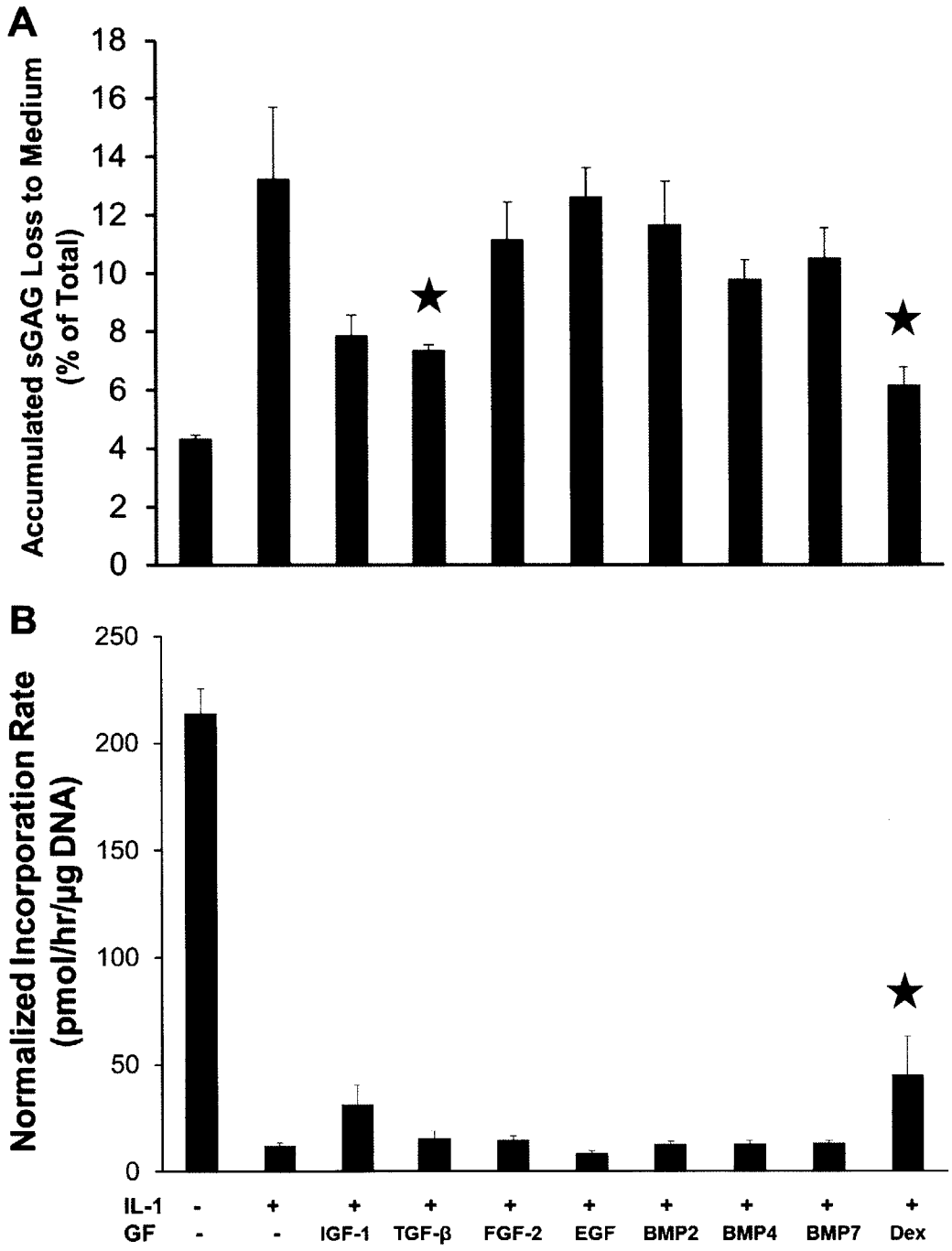

Figure 3S.3 **A,** Percent sGAG loss from immature bovine cartilage in a 4-day experiment. Disks were subject to mono growth factor therapy with or without initial injury in the presence of IL-1α (1 ng/ml). Concentration used: IGF-1 (100 ng/ml), FGF-2 (10 ng/ml), EGF (10 ng/ml), TGF-β1 (10 ng/ml), BMP-2, -4, -7 (all 100 ng/ml), Dex (100 nM); N = 6 disks. **B,** Normalized sulfate incorporation rate measured during last 4 hours of culture of the same disks in A. ★ $p < 0.05$.

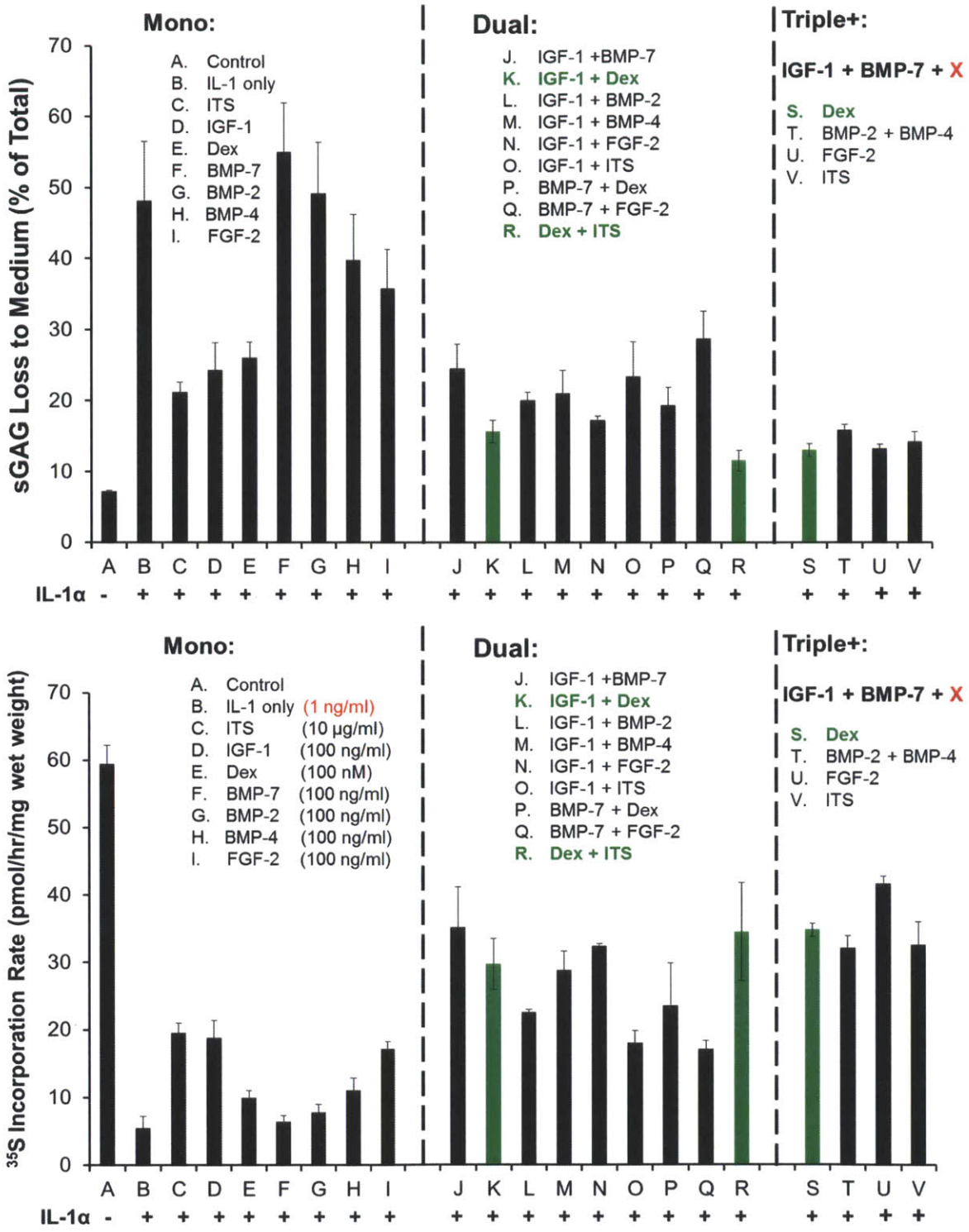

Figure 3S.4 **A,** Percent sGAG loss from immature bovine cartilage in an 8-day experiment. Disks were subject to mono, dual, or triple therapy in the presence of IL-1α (1 ng/ml); N = 6 disks. **B,** Normalized sulfate incorporation rate measured during Day6-8 of the same disks in A.

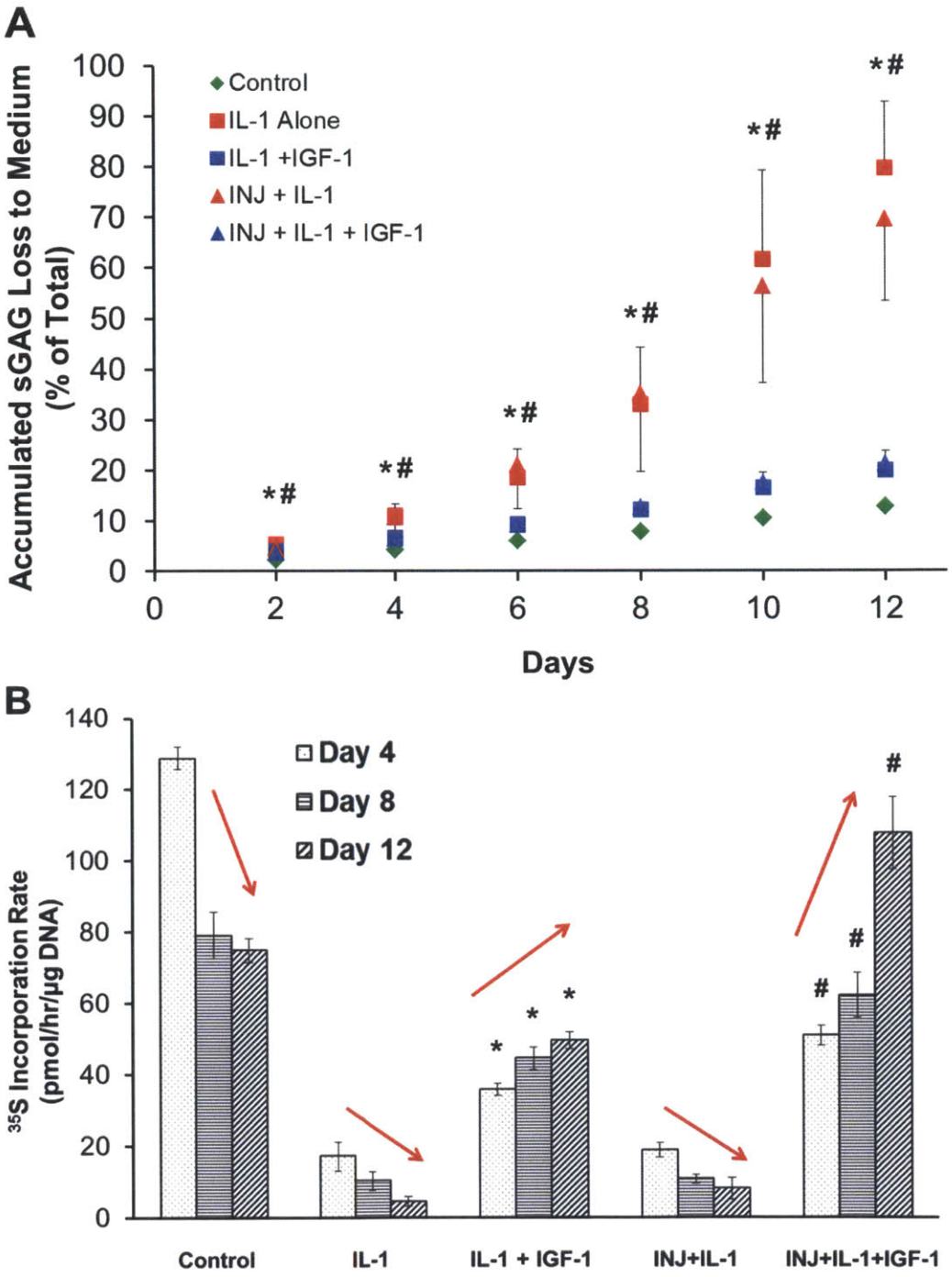

Figure 3S.5 **A,** Percent sGAG loss from immature bovine cartilage in a 12-day experiment. Disks were subject to IGF-1 therapy with or without initial injury in the presence of IL-1α (1 ng/ml). IGF-1: 100 ng/ml. **B,** Normalized sulfate incorporation rate measured during last 2 days of culture of 4-, 8-, and 12-day experiments. Red arrow indicates significant trend by linear regression. Data are mean ± SEM, N = 6 disks. * vs. IL-1 alone; # vs. Inj + IL-1, $p < 0.05$.

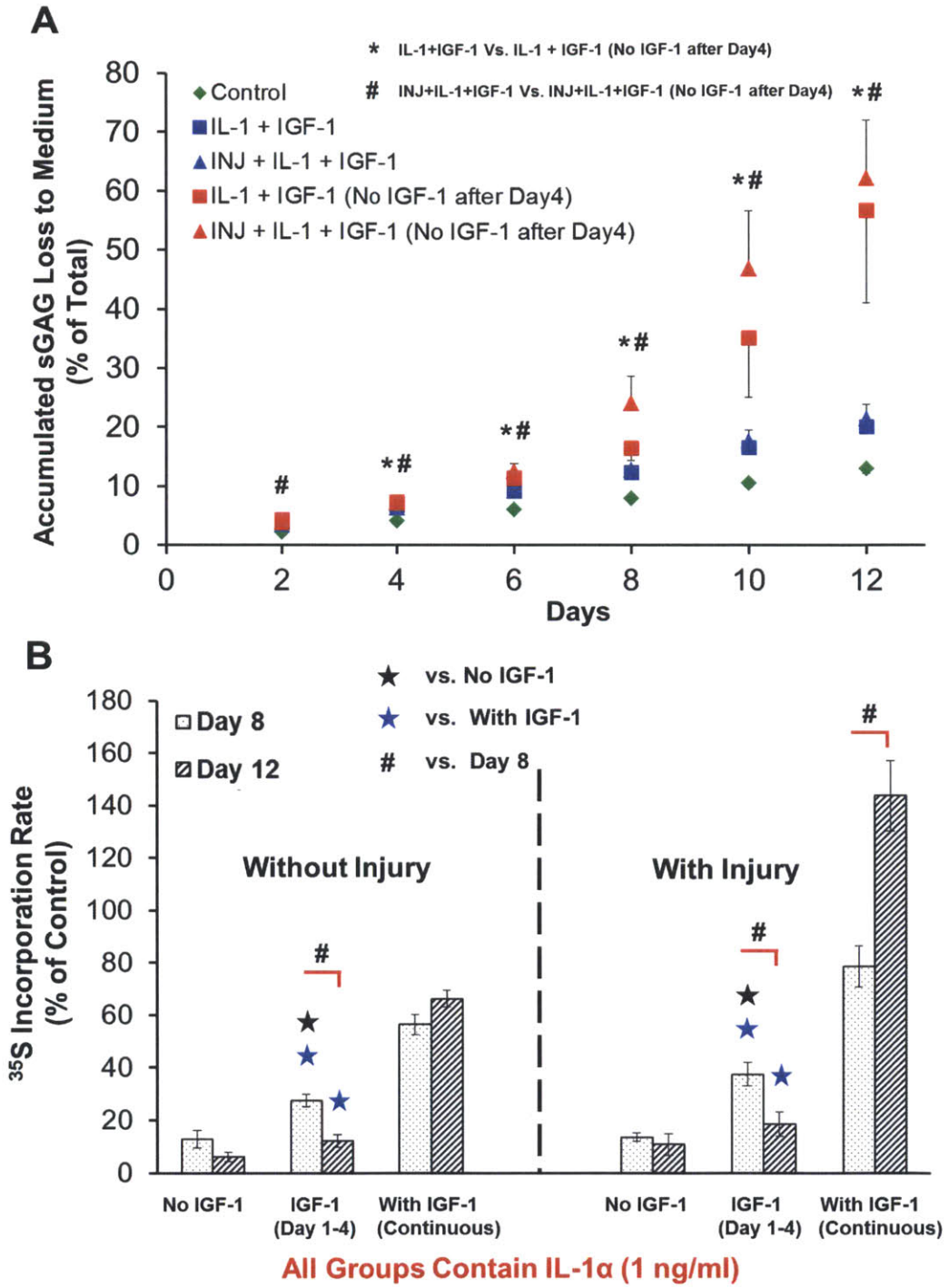

Figure 3S.6 The sustained effects of IGF-1 on reducing IL-1-induced sGAG loss and rescuing IL-1-suppressed biosynthesis. **A,** Percent sGAG loss from immature bovine cartilage in a 12-day experiment. Disks were subject to IGF-1 therapy with or without initial injury in the presence of IL-1α (1 ng/ml). IGF-1: 100 ng/ml. Data are mean ± SD, N = 6 disks. **B,** Normalized sulfate incorporation rate measured during last 2 days of culture of 8- and 12-day experiments. Data are mean ± SEM, N = 6 disks. $p < 0.05$.

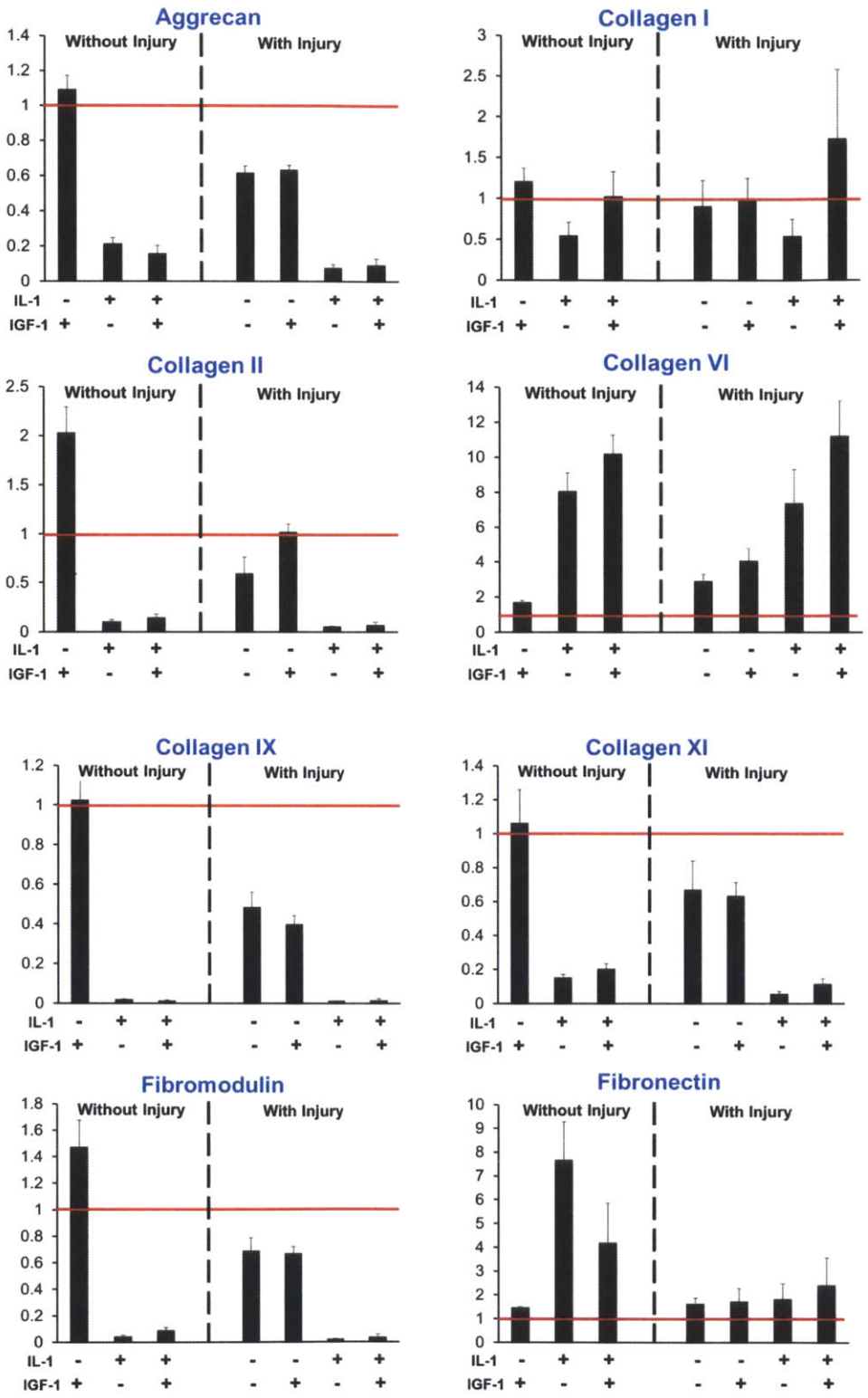

Figure 3S.7 Normalized bovine chondrocyte gene expression in response to 4-day treatments. Red line indicates the untreated control with expression level = 1. N = 5 animals

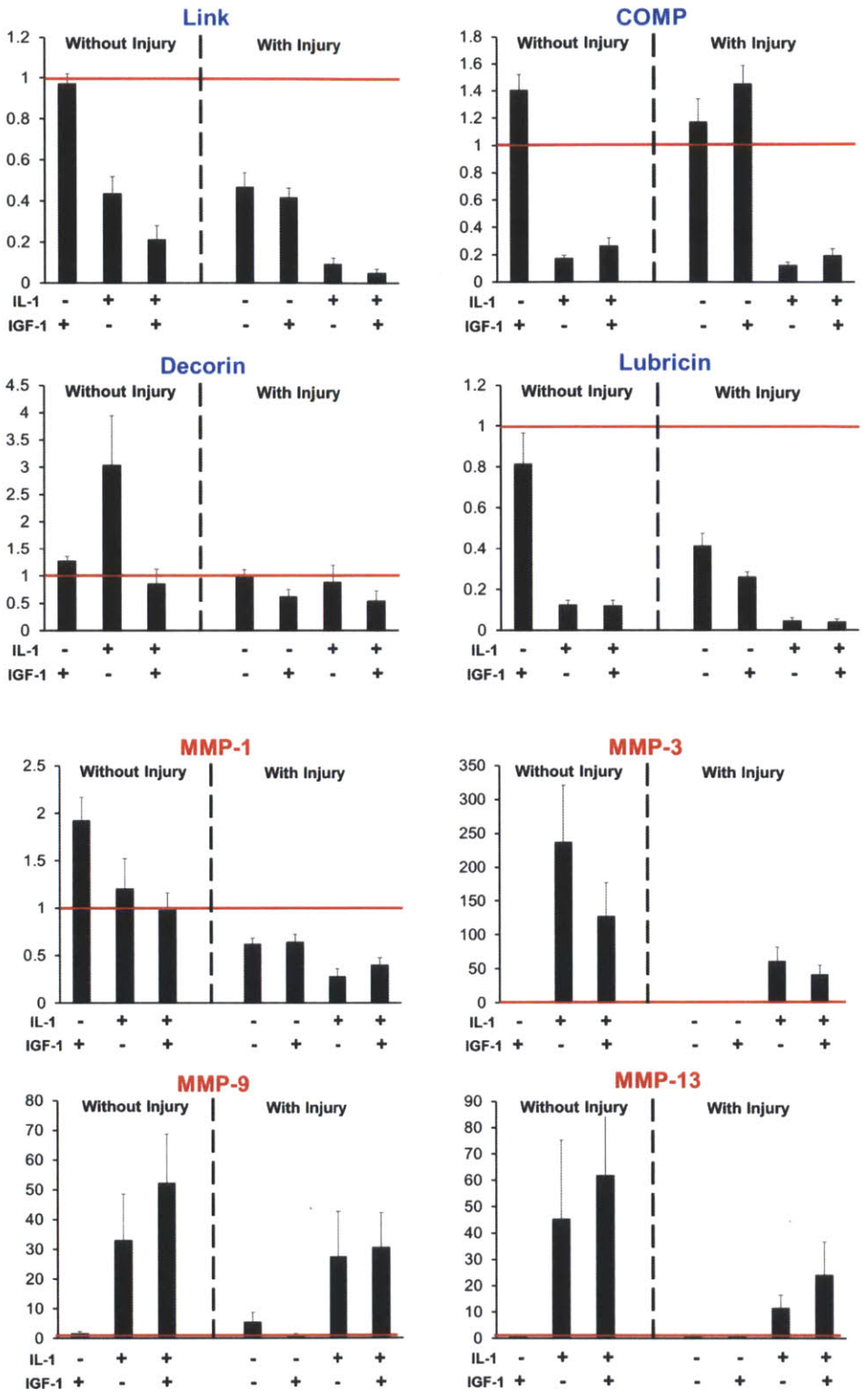

Figure 3S.8 Normalized bovine chondrocyte gene expression in response to 4-day treatments. Red line indicates the untreated control with expression level = 1. N = 5 animals

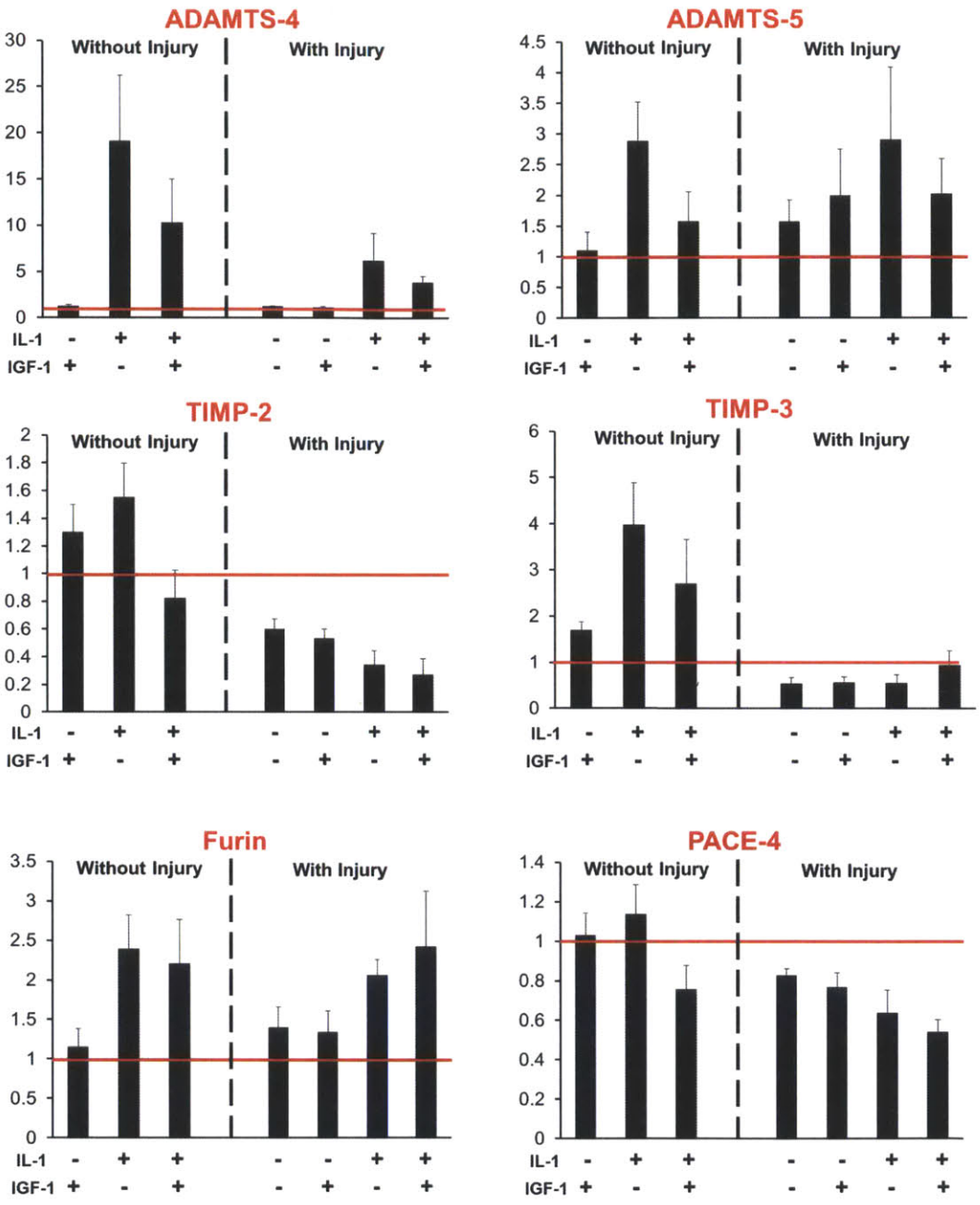

Figure 3S.9 Normalized bovine chondrocyte gene expression in response to 4-day treatments. Red line indicates the untreated control with expression level = 1. N = 5 animals

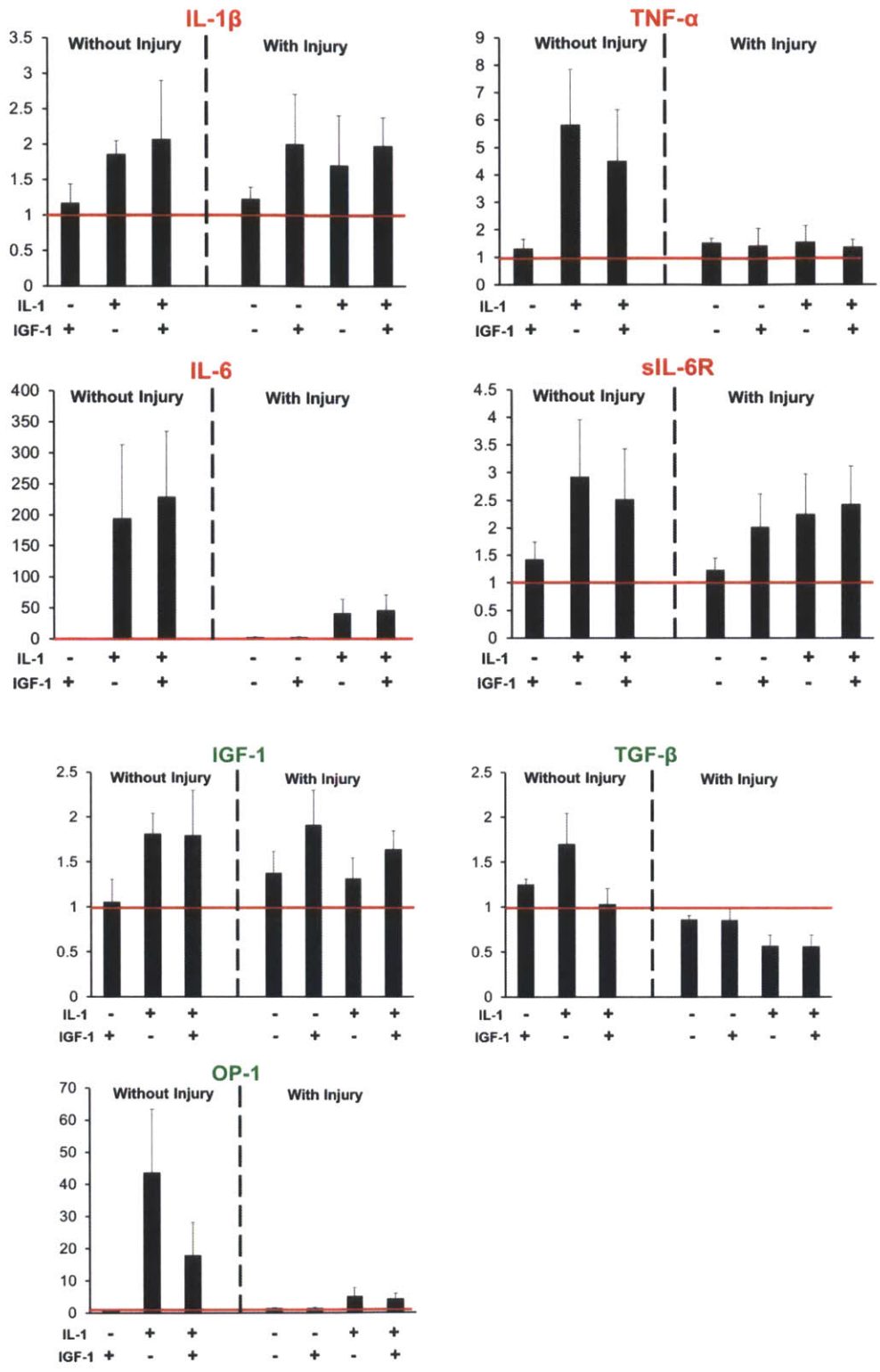

Figure 3S.10 Normalized bovine chondrocyte gene expression in response to 4-day treatments. Red line indicates the untreated control with expression level = 1. N = 5 animals

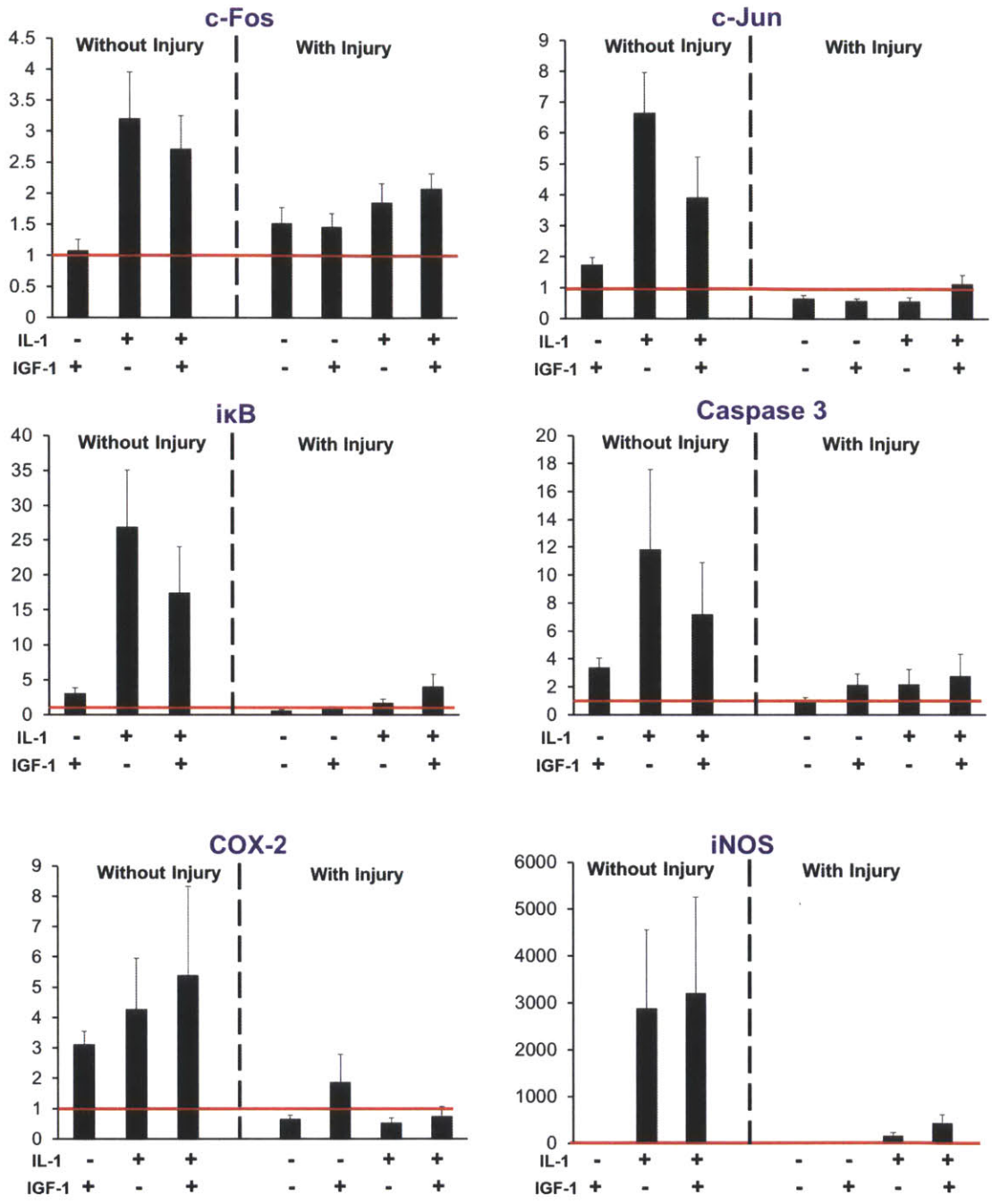

Figure 3S.11 Normalized bovine chondrocyte gene expression in response to 4-day treatments. Red line indicates the untreated control with expression level = 1. N = 5 animals

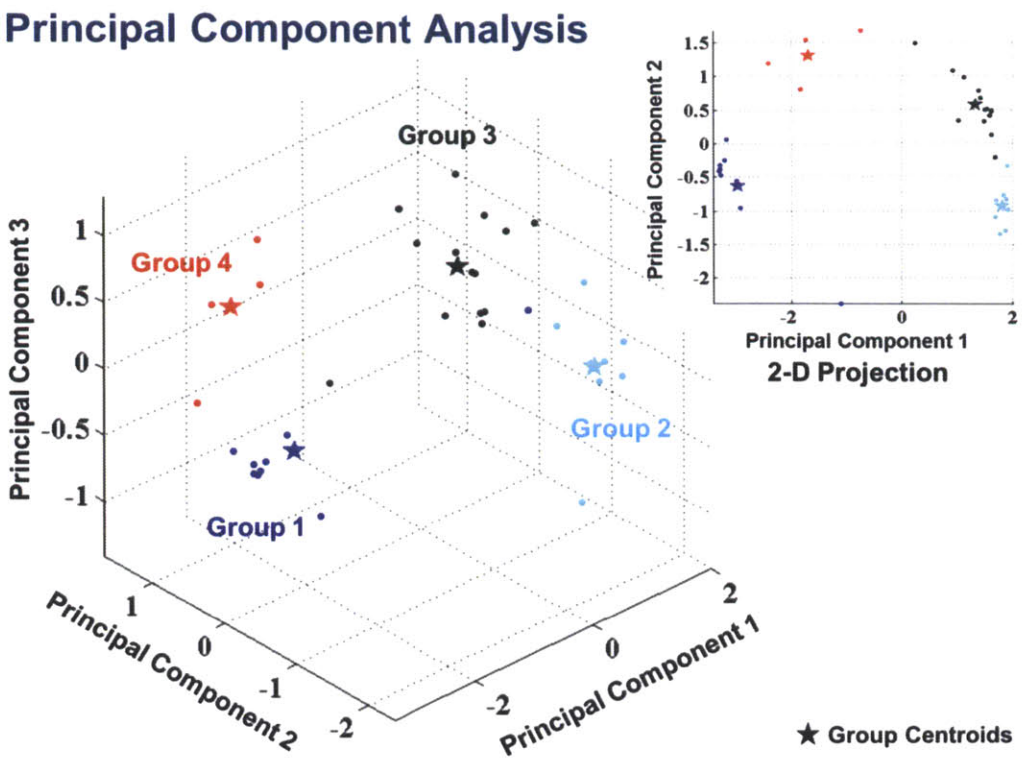

K-means Clustering

Group	Grouped Genes (use averaged gene expression of 4 independent experiments)
1	Aggrecan, Collagen I, Collagen II, Collagen IX, Collagen XI, Fibromodulin, Link, COMP, Lubricin
2	Collagen VI, MMP9, ADAMTS5, Furin, IL-1β, sIL-6R, IGF-1, c-Fos
3	Fibronectin, Decorin, MMP3, MMP13, ADAMTS4, TIMP3, TNF-α, IL-6, OP-1, c-Jun, iκB, Caspase3, COX-2, iNOS
4	MMP1, TIMP2, PACE4, TGF-β

Black: Match with at least 3 out of 4 experiments
Blue: Match with 2 out of 4 experiments
Red: Could be switched between Group 2 and 3

Group	Centroid Coordinates
1	(-2.94, -0.63, -0.01)
2	(1.81, -0.93, -0.29)
3	(1.33, 0.57, 0.11)
4	(-1.67, 1.30, 0.21)

p-value*	Centroid 1	Centroid 2	Centroid 3
Centroid 2	2.94×10^{-7}	-	-
Centroid 3	2.73×10^{-7}	3.32×10^{-7}	-
Centroid 4	2.47×10^{-3}	4.27×10^{-5}	1.76×10^{-3}

* Two sample Student's t-test was used to compare the Euclidean distance between the projection coordinates of pairs of centroids

Figure 3S.12 Principal component analysis and k-means clustering revealed distinct groups of genes. Data are taken from Figures 3S.7-11.

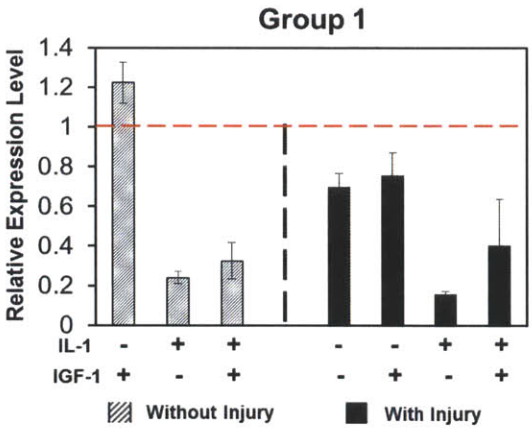

- **Group 1 (matrix proteins) expression suppressed by both IL-1 and Injury**
- **IGF-1 can partially rescue this suppression**

p-value*	IGF-1	IL-1	INJ	IGF-1 and INJ	IL-1 and INJ	IGF-1 and IL-1
Aggrecan	-	<0.0001	<0.0001	-	-	-
Collagen I	0.038	-	-	-	-	-
Collagen II	0.006	<0.0001	<0.0001	-	-	-
Collagen IX	-	<0.0001	<0.0001	-	0.049	-
Collagen XI	0.027	<0.0001	<0.0001	-	-	0.018
Fibromodulin	-	<0.0001	<0.0001	-	0.049	-
Link	0.033	<0.0001	<0.0001	-	0.031	-
COMP	0.002	<0.0001	-	-	0.043	-
Lubricin	-	<0.0001	<0.0001	-	-	-

* significance of the fixed effects from the linear mixed-effects model; - indicates p-value >0.05

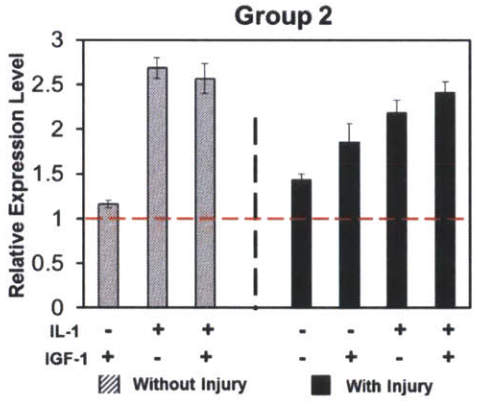

- **Group 2 gene expression upregulated by only IL-1**
- **INJ and IGF-1 have no effect**

p-value*	IGF-1	IL-1	INJ	IGF-1 and INJ	IL-1 and INJ	IGF-1 and IL-1
Collagen VI	<0.0001	<0.0001	<0.0001	-	<0.0001	-
MMP9	-	<0.0001	-	-	-	-
ADAMTS5	-	0.003	-	-	-	-
Furin	-	<0.0001	-	-	-	-
IL-1β	-	0.012	-	-	-	-
sIL-6R	-	0.002	-	-	-	-
IGF-1	-	-	-	-	0.021	-
c-Fos	-	<0.0001	-	-	0.001	-

* significance of the fixed effects from the linear mixed-effects model; - indicates p-value >0.05

Figure 3S.13 Principal component analysis and k-means clustering revealed distinct groups of genes. Data are taken from Figures 3S.7-11.

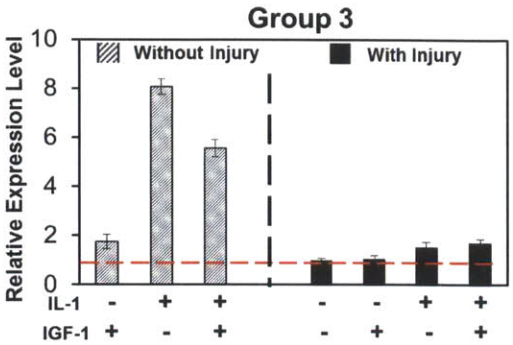

- **Group 3 gene expression upregulated by IL-1, but abrogated by INJ**
- **IGF-1 may alleviate this upregulation in selective genes**

p-value*	IGF-1	IL-1	INJ	IGF-1 and INJ	IL-1 and INJ	IGF-1 and IL-1
Fibronectin	-	0.001	0.016	-	0.001	-
Decorin	0.011	-	0.001	-	-	-
MMP3	-	<0.0001	0.002	-	0.004	-
MMP13	-	<0.0001	0.014	-	0.008	-
ADAMTS4	-	<0.0001	0.006	-	0.005	-
TIMP3	-	0.02	<0.0001	-	-	-
TNFα	-	0.002	0.009	-	0.002	-
IL-6	-	<0.0001	0.042	-	<0.0001	-
OP-1	-	<0.0001	0.001	-	<0.0001	-
c-Jun	-	<0.0001	<0.0001	-	0.002	-
iκB	0.02	<0.0001	<0.0001	-	0.005	-
Caspase3	0.023	<0.0001	<0.0001	-	0.007	-
COX-2	0.004	-	<0.0001	-	0.001	-
iNOS	-	<0.0001	0.003	-	<0.0001	0.018

* significance of the fixed effects from the linear mixed-effects model; - indicates p-value >0.05

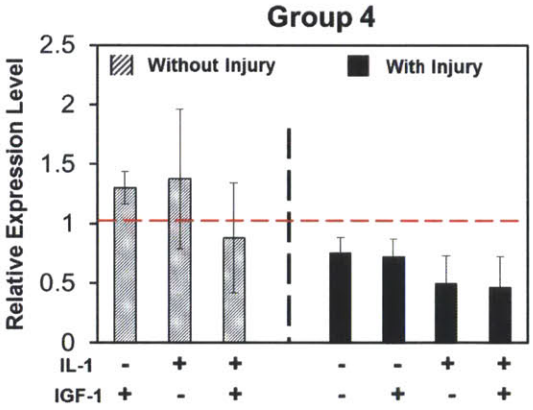

- **Group 3 gene expression suppressed by INJ**
- **IL-1 may have mixed effect**

p-value*	IGF-1	IL-1	INJ	IGF-1 and INJ	IL-1 and INJ	IGF-1 and IL-1
MMP1	-	<0.0001	<0.0001	-	-	-
TIMP2	-	0.01	<0.0001	-	0.034	-
PACE4	0.036	0.006	<0.0001	-	-	-
TGF-β	-	0.049	<0.0001	-	0.007	-

* significance of the fixed effects from the linear mixed-effects model; - indicates p-value >0.05

Figure 3S.14 Principal component analysis and k-means clustering revealed distinct groups of genes. Data are taken from Figures 3S.7-11.

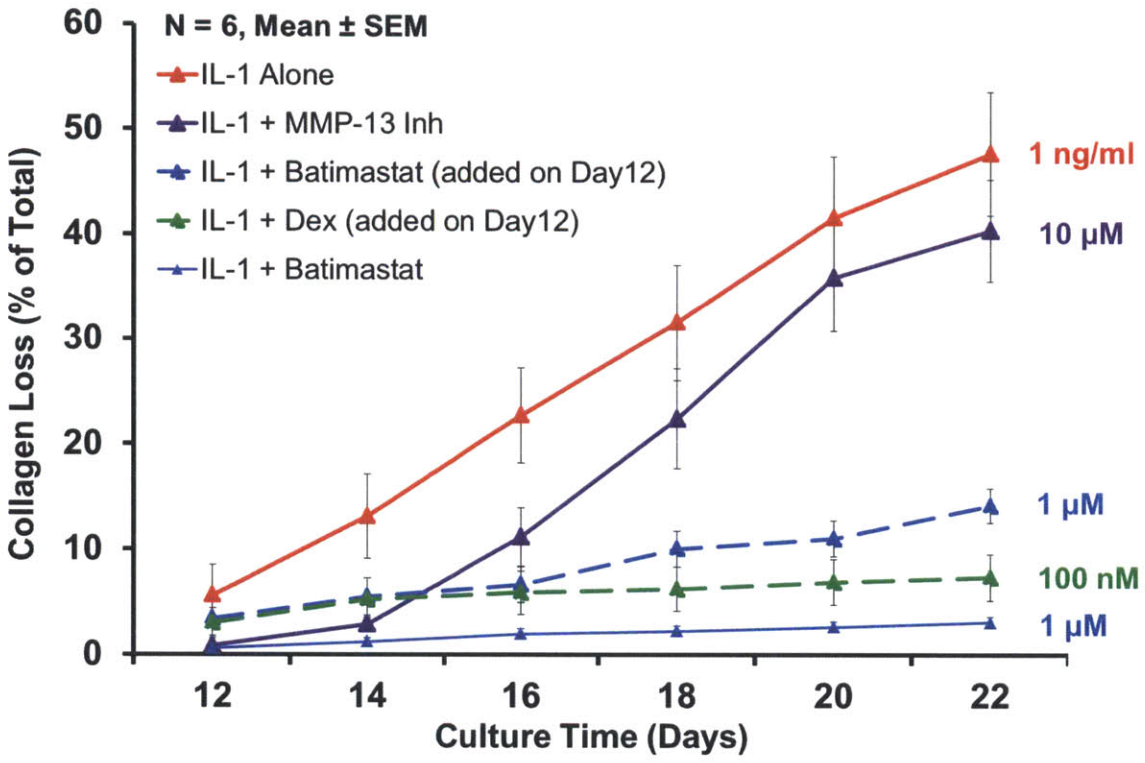

Figure 3S.15 **A,** Kinetics of collagen loss from immature bovine cartilage in response to 22-day treatments. IL-1α (1 ng/ml) was present in all treatment medium for Day 0-22. Batimastat (1µM) was added either on Day 0 or Day 12, MMP-13 inhibitor (10 µM) was added on Day 0, and Dex (100 nM) was added on Day 12 after majority of sGAG was depleted. Data are mean ± SEM, N = 6 disks.

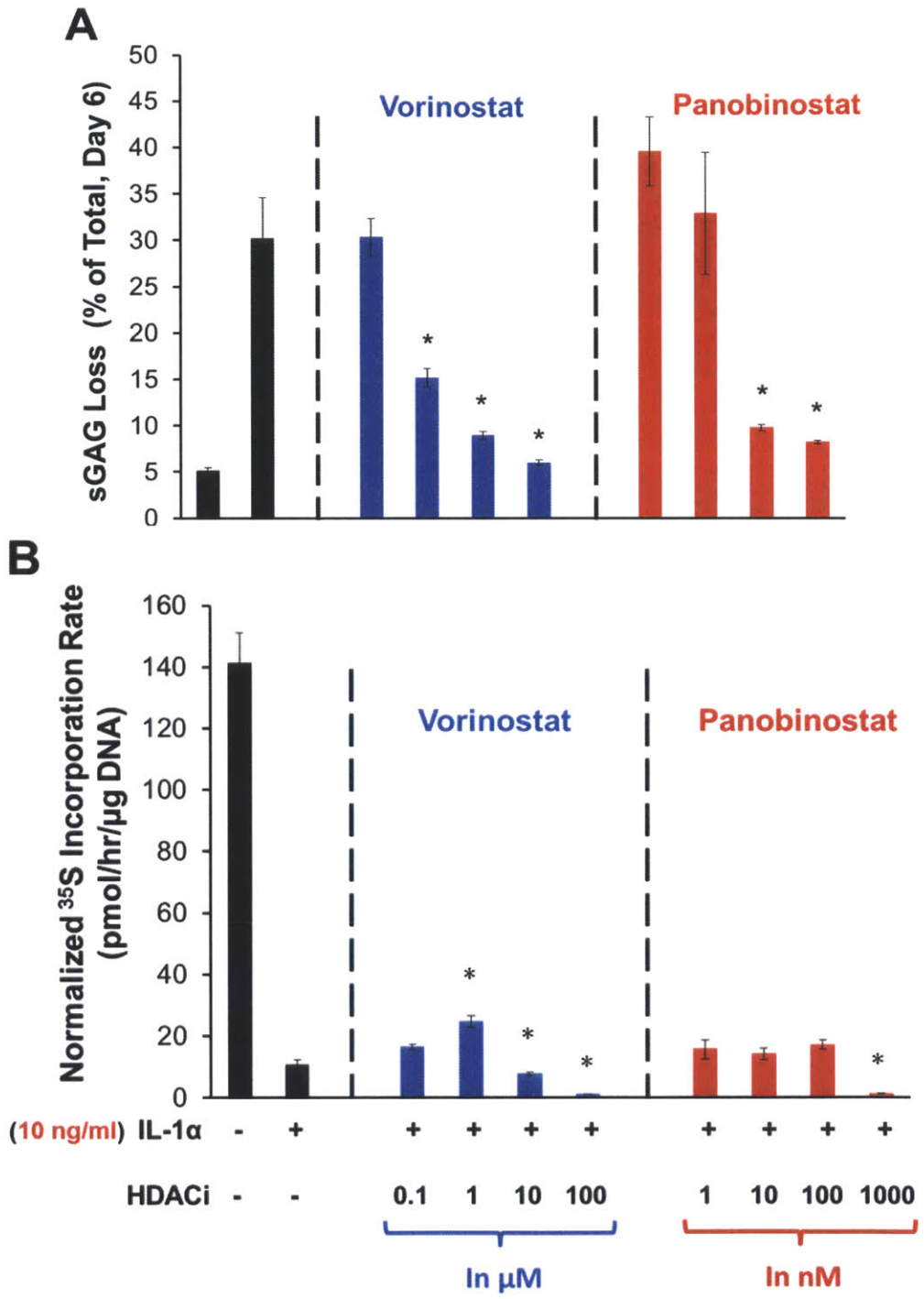

Figure 3S.16 Effects of HDAC inhibitors on proteoglycan biosynthesis and degradation in young bovine cartilage explants. **A,** Accumulated percent sGAG loss to the medium in respond to 6-day treatments. **B,** Averaged biosynthesis rate during day 4-6 culture of the same explants in A. Data are mean ± SEM, N = 6 disks; * vs. IL-1α alone, $p < 0.05$.

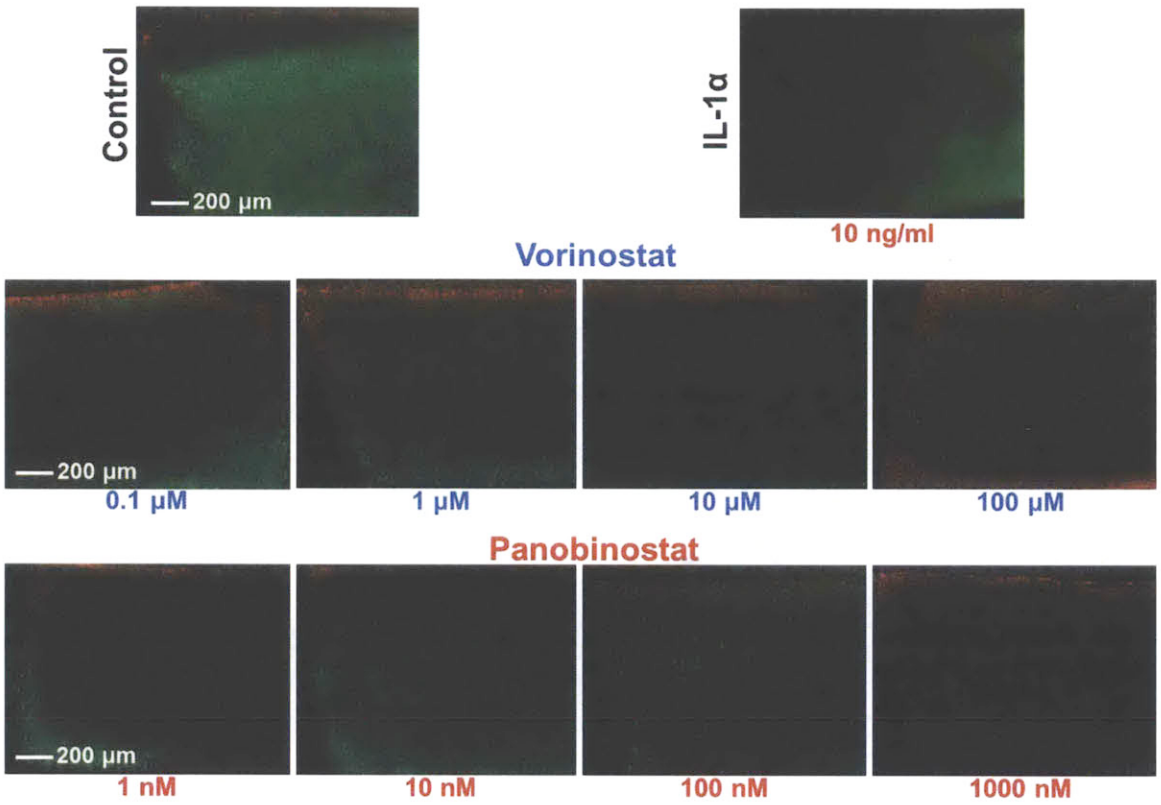

Figure 3S.17 Representative images of the effects of HDAC inhibitors on chondrocyte viability in young bovine cartilage explants after 4-day treatments.

CHAPTER 4

Dexamethasone Suppresses Interleukin-1 alpha Induced Chondrocyte Apoptosis via Caspase-dependent Pathways

Contents

4.1 INTRODUCTION

Apoptosis is a process of programmed cell death (PCD) with distinct characteristics such as membrane blebbing, cell shrinkage, chromatin condensation, and DNA fragmentation. Generally, the mechanisms of apoptosis are classified into two distinct pathways: the extrinsic or death receptor pathway and the intrinsic or mitochondrial pathway (1). In both pathways, caspases (Cysteine-dependent aspartate-directed proteases) are the essential players involved in the initiation and execution phases of apoptosis. Caspases are expressed as zymogens (procaspases) in the cytoplasm and upon activation can cleave cellular substrates, leading to downstream biochemical and morphological changes that are characteristic of apoptosis. Even though distinct in features, the two apoptosis pathways are often interconnected and can influence each other (2). Caspase-dependent apoptosis pathways are considered one of the main mechanisms leading to PCD, however, caspase-independent apoptosis pathways (3) and other forms of PCD (4, 5) contribute to the complex cell fate determination process.

The extrinsic pathway was activated when death-inducing signals such as TNF-α and Fas ligand bind to their membrane receptors, which trigger the recruitment of adapter proteins TRADD or FADD and form the death-inducing signaling complex (DISC) (6). The inactive initiator caspases procaspase-8 and procaspase-10 are then activated at the DISC site. The active caspase-8 can initiate apoptosis directly but it can also cleave the BID (BH3 interacting-domain death agonist, a Bcl-2 family protein) , which translocates to the mitochondria membrane and participates in the intrinsic pathway to amplify the pro-apoptotic signals. The intrinsic pathway can also be initiated by negative cellular stress such as accumulation of free radicals, lack of nutrients or hormones, radiation, and

others, which result in the loss of mitochondrial trans-membrane potential and release of cytochrome c into the cytosol. Cytochrome c binds and activates Apaf-1 as well as procaspase-9. The mitochondrial pathway was regulated by a complex, dynamic network of the Bcl-2 family proteins (7), include pro-apoptotic proteins Bax, Bak, Bad, Bik, Bid, Bim, Noxa, and pro-survival proteins Bcl-2, Bcl-xL, Mcl-1 and others. How a cell decides whether or not to initiate apoptosis through the interplay between Bcl-2 proteins in response to apoptotic signals is still not well understood.

Chondrocyte apoptosis is one of the hallmarks of cartilage degeneration and is believed to play a critical role in the pathogenesis of OA (8). Increased apoptotic chondrocytes have been found in OA patients (9, 10) as well as after joint injury (11). Significantly elevated concentrations of pro-inflammatory cytokines such as IL-1, TNF-α, and IL-6 were also detected in the synovial fluid of patients with ACL injury (12-14). In vitro, substantial evidences showed that IL-1 can induce chondrocyte apoptosis, which was shown to be mediated by the production of NO and PEG2 through activation of the ERK1/2, p38 MAPK, and NF-κB pathways and was caspase-dependent (15, 16). Suppression of NO and PGE2 synthesis in turn inhibited IL-1β-induced apoptosis, likely to be associated with mitochondria-mediated pathways (17-19). A recent study has also shown the possibility of TNF-α induction by IL-1 drives apoptosis initiation via the extrinsic pathway (20).

Dexamethasone (Dex) is a potent synthetic glucocorticoid (GC) that has been widely used intra-articularly to relieve inflammation for the treatment of rheumatoid arthritis (RA) and other types of arthritis (21). Dex suppresses many of the IL-1 induced catabolic processes such as upregulation of ADAMTSs and MMPs, synthesis of

inflammatory mediators COX-2, PGE2, and NO, and matrix degradation (22, 23) (also see Chapter 3). However, the potential of Dex as an OA drug candidate has been dampened by reports that suggest it can induce chondrocyte apoptosis, especially in proliferative chondrocytes (24, 25). However, contradictory studies have shown that Dex was able to prevent cell apoptosis (26) or maintain cell viability over long-term culture (27). As discussed in Chapter 3.4, the pro-apoptotic or anti-apoptotic nature of Dex largely depends on the cell type, stimuli, culture system, and dose. Moreover, what role does Dex play on regulating chondrocyte apoptosis in the presence of pro-inflammatory cytokines have not been studied.

The objectives of this study are 1). Examine whether Dex alone treatment induce cell apoptosis in high-density cultured monolayer chondrocytes; 2). Study the effects of Dex on chondrocyte cell viability/apoptosis in the presence of IL-1α; 3). Explore the mechanisms of Dex-mediated cell survival/death.

4.2 MATERIALS AND METHODS

Bovine chondrocyte isolation and culture. Cartilage slices were harvested from the chondyles of 1-2-week-old calves (obtained from Research '87, Boylston, MA). Cartilage was digested in pronase for 1 hour at 37°C, followed by collagenase digestion in serum-free medium overnight at 37°C. On the next day, isolated chondrocytes were collected by filtering through a 40-μm cell strainer, and then pelleted at 800 g for 10 min. Cells were washed twice with PBS and re-suspended in culture medium. The initial cell viability was evaluated by Trypan-Blue staining to ensure >80% viable cells obtained.

Chondrocytes were plated at a high density of $1X10^6$ cells/cm^2 in 48-well or 6-well plates, and equilibrated for 24 hours before treatments in serum-free medium (low-glucose DMEM; 1g/L) supplemented with 10 m*M* HEPES buffer, 0.1 m*M* nonessential amino acids, 0.4 m*M* proline, 20 g/ml ascorbic acid, 100 units/ml penicillin G, 100 g/ml streptomycin, and 0.25 g/ml amphotericin B for 2-3 days (5% CO_2; 37°C).

Cell viability staining. Cultured chondrocytes in 48-well plates were incubated with fluorescein diacetate (FDA; 4 μg/ml) and propidium iodide (PI; 40 μg/ml) (both from Sigma), for viable and non-viable cell staining, respectively. After 2 min incubation, cells were washed twice with PBS and imaged with a Nikon fluorescence microscope with a 20x objective. Four fields were imaged for each sample well, and cell viability was quantified using the imaging software FIJI (ImageJ). The numbers of viable and non-viable cells were counted via the Image-based Tool for Counting Nuclei (ITCN version 1.6) plug-in, and data were expressed as percent of total viable cells.

Caspase-3 Activity Assay. Caspase-3 activity was determined using the EnzChek Caspase-3 Assay kit #2 (Invitrogen), procedures follow manufacturer's protocol with slight modifications. After treatments, medium was collected and the attached cells were washed with cold PBS. Cell lysis buffer (RIPA buffer, Cell Signaling Technologies) was added to each well and cells were scraped off and transferred to an eppendorf tube. Cells were sonicated for 30 s/cycle for 5 cycles, and the lysed cells were centrifuged at 13,200 rpm for 10 min at 4°C to collect the supernatant. Total protein content was determined using the BCA assay. 50 μl of the cell lysate or the collected medium was added to 50 μl substrate solution containing 2.5 nmol of the Z-DEVD-R110 substrate into a 96-well plate. Readings were taken kinetically every 5 min for 1 hour using a fluorometer

(Perkin-Elmer). Caspase-3 activity in the cell lysate was expressed as the fluorescent unit per min per μg of protein, whereas the activity in the medium was reported as the fluorescent unit per min.

Caspase-8 and -9 Activity Assays. Caspase-8 and caspase-9 activities were measured in the same cell lysates using the Caspase-8 Colorimetric Assay (R&D systems) and the Caspase-9 Colorimetric Assay Kit (Sigma), procedures follow manufacturer's protocols. Briefly, chondrocytes in 6-well plates were grown for 48 hours, and the attached cells were scraped off the plate into a 15-ml tube along with the culture medium. Cells were collected after centrifuging for 2 min at 850g, and then the pellet was washed with cold PBS. Cell lysis buffer was added to each sample and then transferred to an eppendorf tube. Cells were sonicated for 30 s/cycle for 5 cycles, and the lysed cells were centrifuged at 12,000 g for 15 min at 4°C. The supernatant was collected and the total protein content was determined using the BCA assay (Thermo Scientific). 50 μl of the cell lysate was added to 50 μl substrate solution containing 200 μM of Ac-IETD-pNA (caspase-8 substrate) or Ac-LEHD-pNA (Caspase-9 substrate) into a 96-well plate. The initial absorbance was measured using a spectrophotometer at 405 nm. The plate was incubated at 37°C for 1.5 hour, and the final reading was taken at 405 nm. To calculate each caspase activity, the background absorbance was deducted from both the initial and final readings, and the difference between the initial and final reading was converted to pmol of pNA using a standard curve. Data were then normalized by protein content over the time of incubation, and expressed as pmol of pNA per mg of protein per min.

Gene expression analyses. Chondrocytes were cultured for 6, 24, 48, and 96 hours, after removal of the culture medium, cells were washed with cold PBS, and stored

in -80°C after flash-freezing. On the extraction day, cells were thawed on ice and lysed in the TRIzol reagent with homogenization. Samples were added with chloroform, vertexed, and centrifuged at 13,200 rpm for 10 min. The supernatant was further purified following the Qiagen RNeasy mini kit protocol (Qiagen, Chatsworth, CA). Equal amounts of mRNA from each condition were reverse transcribed using the AmpliTaq-Gold Reverse Transcription kit (Applied Biosystems, Foster City, CA). Bovine primers were designed using the PRIMER-BLAST tool. Caspase-3: forward 5'-GAAGTCTGACTGGAAAACCC-3', reverse 5'-GAAGTCTGCCTCAACTGGTA-3', caspase-8: forward 5'-GGATGATGACATGACTTTGC-3', reverse 5' CCTGCTCACAGATTCTTTTC-3'; caspase-9: forward 5'-CATGATCGAGGACATTCAGA-3', reverse 5'-CAAGCAGGAGATGAACAAAG-3'; Bax: forward 5'-CTTTTGCTTCAGGGTTTCAT-3', reverse 5'-CCATGTTACTGTCCAATTCA-3'; Bak1: forward 5'-GCCTATGAGTACTTCACCAA-3', reverse 5'-AATCTTCGTACCACAAACTG-3'; Bik: forward 5'-TACACCTTCCTACAAAACCA-3', reverse 5'-TAGGGGAAAAACAAGCTGTA-3'. Real-time PCR were performed using the Applied Biosystems 7700HT instrument with SYBR Green Master Mix (Applied Biosystems). As described previously (28), the expression data for each gene were calculated from the threshold cycle (Ct) value, and normalized to the internal housekeeping gene 18S.

Multiplex Luminex. To examine which of the upstream signaling pathways is responsible for the anti-apoptotic effect of Dex, we studied the Akt, MAPK JNK, MAPK ERK1/2, and NF-κB/iκB pathways using the Bio-Plex Pro™ Magnetic Cell Signaling Assays (Bio-Rad). All procedures and reagents used follow the manufacturer's instructions.

Antibodies for phosph-Akt (Ser^{473}), phospho-JNK (Thr^{183}/Tyr^{182}), phosphor-ERK1/2 (Thr^{202}/Tyr^{204}, Thr^{185}/Tyr^{187}), phospho-IκB-α (Ser^{32}/Ser^{36}) were purchased with the Bio-Plex kit. Human cartilage harvested from both the knee and ankle joints (all Collin's grade 1) of a 57-year-old female donor were digested in pronase for 1 hour at 37°C, followed by collagenase digestion in 10% FBS high-glucose DMEM medium overnight at 37°C. Chondrocytes were plated into 96-well plates at a density of $1X10^6$ cells/cm^2 for 24 hours in 10% FBS medium, followed by 24-hour serum starvation. After treatments for 10, 30, 60 min, or 6 hours, cells were washed twice with cold PBS and were stored at -80°C after flash-freezing. On the next day, thawed samples were lysed on ice with the provided cell lysis buffer supplemented with 2 mM PMSF. Cells were sonicated for 30 s/cycle for 5 cycles, and the lysed cells were centrifuged at 13,200 rpm for 10 min at 4°C to collect the supernatant. Protein concentration was determined using the BCA assay and then was adjusted to 200 μg/ml. Equal amount of total proteins (5 μg) and positive control for each phosphor-protein were loaded into the 96-well assay plates containing multiplexed magnetic beads coated with primary antibodies. The plates were incubated overnight at room temperature with shaking. On the next day, the plates were washed and incubated with detection antibodies for 30 min at RT, then incubated with streptavidin-PE for 10 min, and the plates were read with a MAGPIX instrument (Luminex). Data are expressed as the fluorescent intensity for each phosphor-protein.

Statistical analysis. Bovine gene expression data were log-transformed and analyzed by the linear mixed effect model with animal as a random factor, followed by Bonferroni's test for pair-wise comparisons. Bovine chondrocyte viability data were analyzed by the linear mixed effect model with animal as a random factor, followed by

Bonferroni's test for pair-wise comparisons. Bovine IL-1α dose, Dex dose, and Human luminex data were analyzed by two- or three-way ANOVA, followed by Tukey's test for pair-wise comparisons. P values less than 0.05 were considered statistically significant.

4.3 RESULTS

Caspase-3 activation by IL-1α, a dose and time course study. Bovine chondrocyte treated with 1 or 10 ng/ml of IL-1α over 24-, 48-, and 96-hour time course revealed a dose- and time-dependent caspase-3 activation mediated by IL-1α (Figure 1). Initially, no significant caspase-3 activity was measured at either 24 or 48 hour time points for both concentrations of IL-1α. In comparison, the positive control staurosporine-treated samples showed significant activation, measured both in the cell lysates and medium, starting from 24 hour ($p < 0.0001$ vs. untreated control). By 96-hour, significant caspase-3 activity was induced by 10 ng/ml IL-1α ($p = 0.0018$ vs. untreated control in the lysates) but not by 1 ng/ml ($p = 0.1413$ vs. untreated control). The positive control, however, showed decreased caspase-3 activity ($p = 0.0001$ vs 10 ng/ml IL-1α) in the lysates at 96-hour.

The effets of Dex dose on caspase-3 activation. The effects of Dex dose on caspase-3 activation were evaluated in a 4-day study in the presence or absence of IL-1α. As shown in Figure 2, Dex alone treatments did not induce caspase-3 activation in the cell lysates nor found in the medium at any of dose tested. Consistent with Figure 1, IL-1α at 10 ng/ml significantly increased caspase-3 activity in the lysates ($p < 0.0001$ vs. untreated control) as well as in the medium ($p < 0.0001$ vs. untreated control). The

addition of Dex significantly suppressed the activated caspase-3 activity by IL-1α ($p < 0.0001$ vs. IL-1α for all Dex concentrations) in the lysates to the control level. Similarly, IL-1α induced caspase-3 activity was largely abolished by Dex in the medium even though significantly above the untreated control. Staurosporine-treated samples showed active caspase-3mostly in the medium.

Dex rescued IL-1α-induced cell death. Chondrocyte remained >80% viable after 4-day treatment in the control medium (Figure 4). Dex alone treatment at either 10 nM or 100 μM did not induce significant cell death compared to the untreated control ($p = 1$ for both Dex concentrations). IL-1α at 10 ng/ml almost completely eliminated all viable cells ($p < 0.0001$ vs. untreated control). When Dex was added at 10 nM, ~34 ± 5.3% (Mean ± 95% Confidence interval) cells remained viable, which was significantly larger than the IL-1α alone treatment ($p < 0.0001$). Moreover, 100 μM Dex showed significantly greater cell rescuing effect than 10 nM ($p < 0.0001$), but still lower than the untreated control (66.5 ± 2.6% vs. 85.6 ± 6.8%, $p < 0.0001$). Staurosporine treatment yielded an overall viability of 4.0 ± 0.8%, which is not difference from the IL-1α alone treatment.

Dex suppressed caspase-depenent apoptotic pathways gene expression. Since the elevated caspase-3 activity by IL-1α was significantly inhibited by Dex treatments (Figure 2), we further explored which of the intrinsic or extrinsic apoptotic pathway was regulated by Dex at the gene expression level. As shown in Figure 4, Dex alone treatments at either 10 nM or 100 μM significantly suppressed the endogenously expressed caspase-3 expression starting from 6 hour. IL-1α alone significantly upregulated caspase-3 expression 6-16 folds over the 6-24 hour time course. Both the low

and high dose of Dex significantly reduced the caspase-3 upregulation. Similar to caspase-3, caspase-8 expression was suppressed by Dex alone treatments. The caspase-8 upregulation by IL-1α was partially blocked by Dex. Interestingly, caspase-9 was not suppressed by Dex alone treatment (except for 10 nM at 6 hour). IL-1α activation of caspase-9 started at 24 hour, which was later than both caspase-3 and caspase-8. The addition of Dex did not have significant suppressive effect on caspase-9 expression until 96 hour. A further look at the expression of pro-apoptotic proteins Bax and Bak, both are upstream of caspase-9, revealed that Dex significantly repressed Bak at 6 and 24 hour in the presence of IL-1α. Dex at high dose also inhibited IL-1α upregulated Bax expression at 6 hour. However, the suppressive effects of Dex on Bax and Bak expression were lost at the later time points, even though both genes remained elevated by IL-1α treatment. In comparison, Dex alone treatment significantly reduced Bik expression, and completely blocked the pro-apoptotic gene Bik from 6-24 hour in the presence of IL-1α.

Dex regulated multiple signaling pathways in a time-dependent manner. Multiple intracellular signaling pathways regulate cell apoptosis. Here we studied the effects of Dex, in the presence or absence of IL-1α, on the phosphorylation of the JNK MAPK, Akt, ERK MAPK, and iκB-α pathway in human chondrocytes. As shown in Figure 5, JNK (Thr^{183}/Tyr^{182}) phosphorylation was significantly increased at 30 and 60 min after treatment with IL-1α. Dex inhibited JNK activation back to the untreated control level at 60 min. In general, Akt (Ser^{473}) phosphorylation was not induced by IL-1α treatment (except for 60 min in knee cell), and Dex had no effects either by itself or in the presence of IL-1α. ERK1/2 (Thr^{202}/Tyr^{204}, Thr^{185}/Tyr^{187}) was activated by IL-1α at 30 and 60 min for both ankle and knee cells, and the addition of Dex had suppressive effect

at 60 min for the knee cells. IL-1α also triggered the activation of iκB-α (Ser^{32}/Ser^{36}) as early as 10 min after treatment, which was not inhibited by Dex. Interestingly, IL-1α stimulated iκB-α phosphorylation level dropped at 30 min, but then re-surged at 60 min. The addition of Dex had significantly suppressive effect on iκB-α activation at 6 hour and 60 min for ankle and knee cells, respectively.

4.4 DISCUSSION

In the present study, we investigated the role of Dex on chondrocyte apoptosis in the presence or absence of IL-1α. Results indicated that Dex can significantly inhibit IL-1α-induced chondrocyte apoptosis and rescue decreased cell viability in a dose-dependent manner, while Dex alone did not induce significant cell apoptosis or compromise overall cell viability. The effects of Dex were mediated by inhibition on caspase-dependent apoptosis pathways, and likely to be the result of regulation on the JNK MAPK and NF-κB/iKB-α signaling pathways.

Activation of caspase-3 by IL-1 have been widely reported and the use of caspase-3 specific inhibitor has direct suppressive effect on the subsequent apoptosis (29-31), suggesting the IL-1-mediated chondrocyte apoptosis is caspase-dependent. Our results at both the gene and protein level agree well with the literature. However, even though a near-complete caspase-3 inhibition was achieved by Dex treatment, the fact that viability was not completely rescued suggested the presence of other active executioner

caspases such as caspase 6 or 7. Caspase-independent apoptosis pathways cannot be ruled out either.

Gene expression study showed that both caspase-8 and caspase-9 expression were activated by IL-1α with caspase-8 being upregulated first. A closer look at the Bcl-2 family proteins, which are upstream of caspase-8 activation, showed that the pro-apoptotic genes Bax, Bak, and Bik were all upregulated at the early 6 hour, while caspase-8 activation was found to be significant after 24 hour. Dex initially blocked Bax and Bak expression but it effects were lost after 24 hour, which is consistent with the elevated caspase-9 expression. Complete blockage of Bik expression by Dex had no inhibitory effect on the downstream caspase-9 gene expression. Bik was shown to interact with and inhibit the activity of the pro-survival Bcl-2 and Bcl-xL proteins and result in the induction of Bax-dependent pathway (32). Our data showed that Bcl-2 and Bcl-xL gene expression profiles were not upregulated by the addition treatment with Dex, further studies are needed to examine the protein level regulation of these Bcl-2 family proteins by Dex.

In our study, no serum or growth factors such as Insulin-like growth factor 1 (IGF-1) were used in our culture medium, and as a result, the Akt pathway was not activated in the untreated control. Under this serum-free condition, IL-1α had no stimulatory or suppressive effect on Akt phosphorylation, which is in contrast to studies that used serum as medium supplement where IL-1 was reported to suppress Akt activation (33). Dex treatment in the presence or absence of IL-1α had no additional effects, and therefore it is unlikely the downstream anti-apoptotic effect of Dex in the presence of IL-1α was through pro-survival signal activation via the Akt pathway.

It is likely that IL-1α directly activate caspases through receptor binding, but rather the indirect consequence of induction of other mediators such as NO. NO is an important mediator of chondrocyte apoptosis through the disruption of normal mitochondria function (34). Previous studies as well as studies in Chapter 3 of this thesis have shown that IL-1α significantly upregulates iNOS gene expression and the subsequent NO production. While Dex was unable to suppress the iNOS at the gene level, it was shown that Dex was able to block NO production at the protein level (23). Further studies with the use of NO inhibitor or adding NO directly to the culture in the presence of IL-1α and Dex could test the hypothesis that Dex inhibits NO-mediated apoptosis pathways.

The present study examined the anti-apoptotic role of Dex in the presence of the pro-inflammatory cytokine IL-1α using high-density cultured monolayer bovine and human chondrocyte. Our results showed that Dex alone treatment with high dose (100 μM) did not induce significant cell apoptosis or compromise cell viability. In the presence of IL-1α, Dex was able to inhibit the caspase-dependent extrinsic and intrinsic pathways both at the gene and protein levels, resulting in a significantly greater survival rate. The anti-apoptotic effects of Dex is likely to be mediated by the inhibition on the upstream JNK MAPK and NF-κB/iκB pathways but not the result of activation of the pro-survival Akt pathway.

4.5 ACKNOWLEDGEMENTS

This work has been supported by NIH Grants AR060331 and grant from Merrimack Pharmaceuticals to MIT. The funding sources had no involvement in the design, collection, analysis and interpretation of data, nor in the writing and submission of this manuscript.

4.6 FIGURES

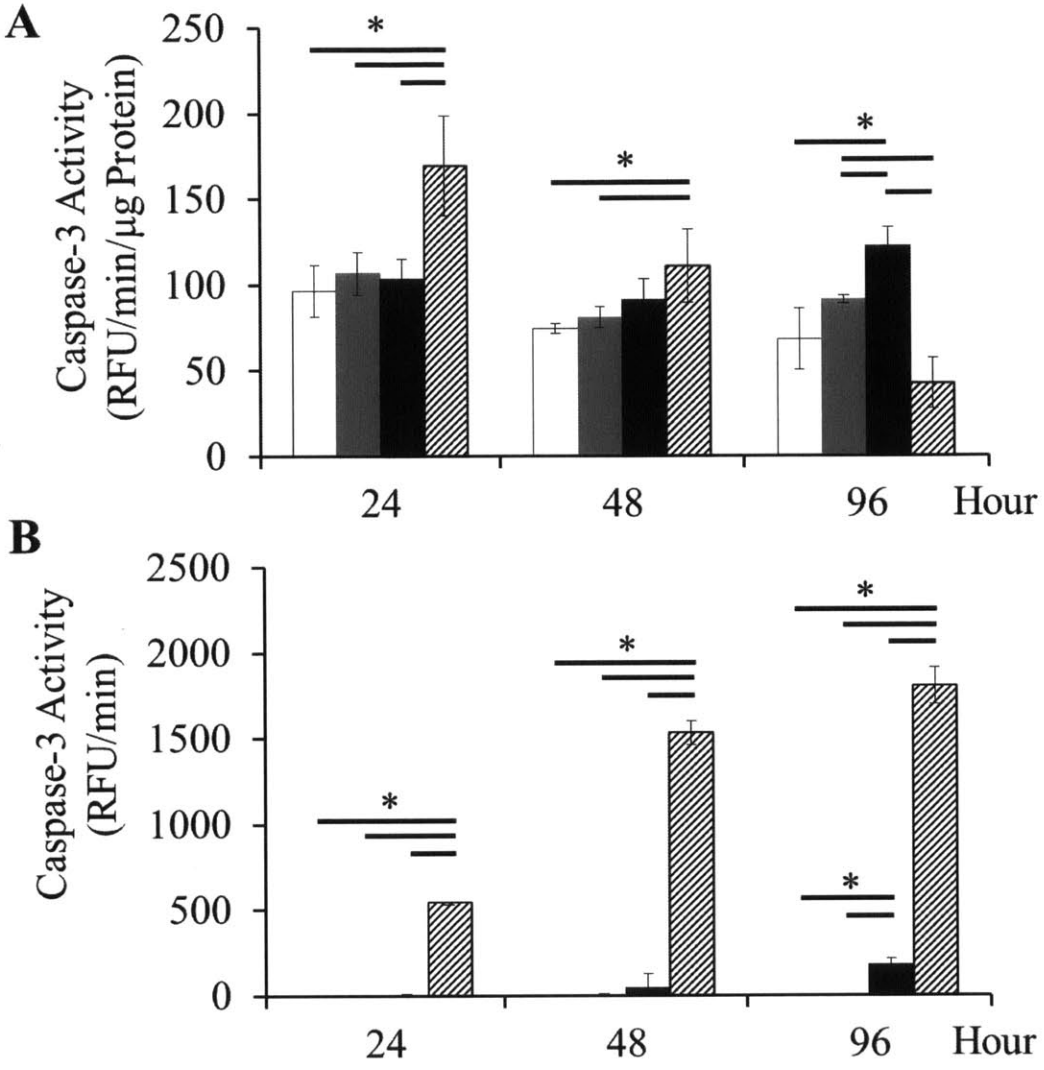

Figure 4.1 **A,** Normalized caspase-3 activity measured in total cell lysates after 24-, 48-, and 96-hour treatments. White bar: untreated control; gray bar: IL-1α (1 ng/ml); black bar: IL-1α (10 ng/ml); shaded bar: staurosporine (1 µM). **B,** Caspase-3 activity measured in the medium of the same samples in A. Data are mean ± 95% confidence interval; N = 3 replicates; $p < 0.05$.

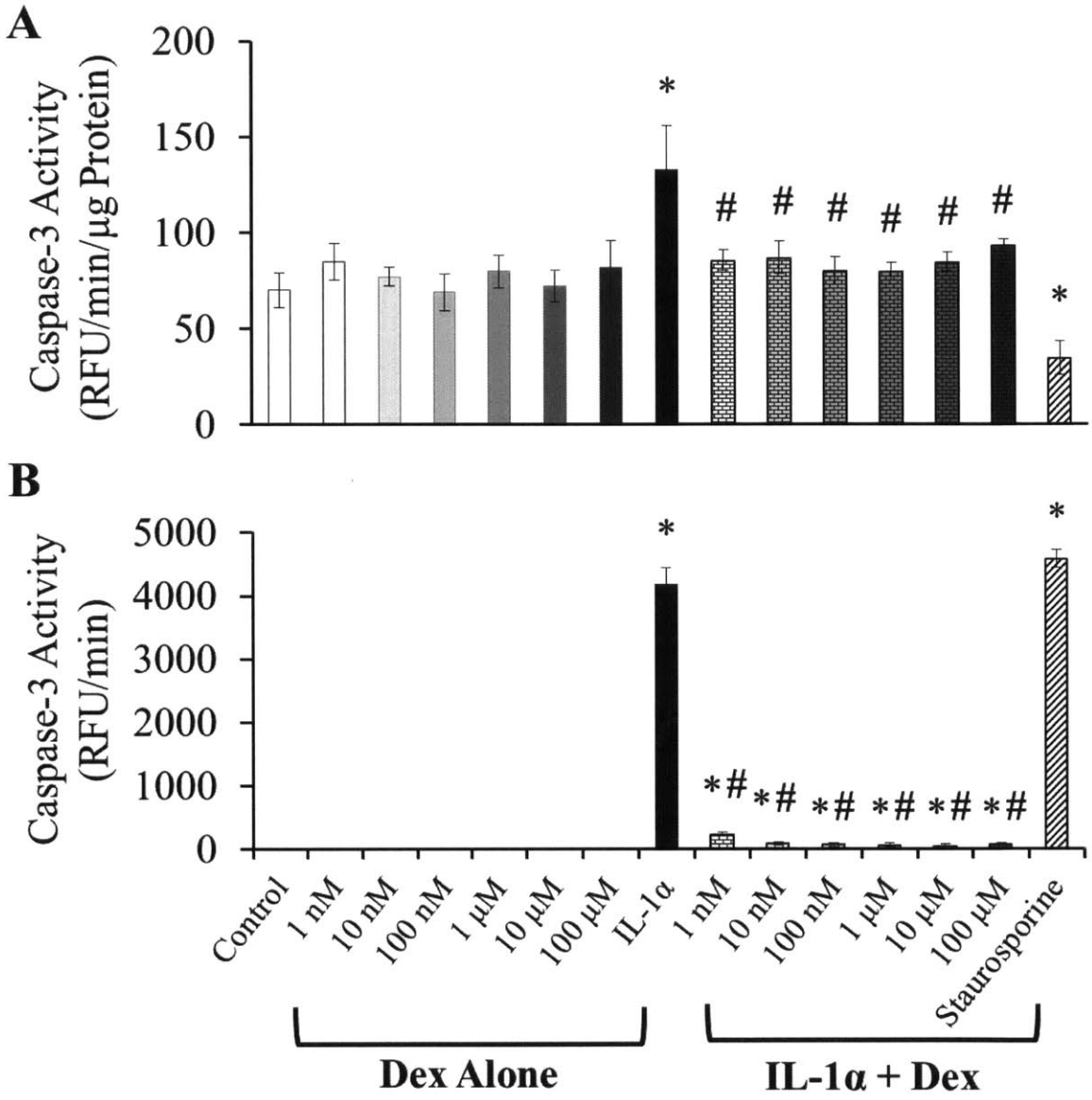

Figure 4.2 The dose effect of Dex on caspase-3 activity in the presence or absence of IL-1α (10 ng/ml). **A,** Normalized caspase-3 activity measured in total cell lysates after 96-hour treatments. Staurosporine (1 μM) was used as the positive control. **B,** Caspase-3 activity measured in the medium of the same samples in A. Data are mean ± 95% confidence interval; N = 6 replicates. * vs. untreated control; # vs. IL-1α alone; $p < 0.05$.

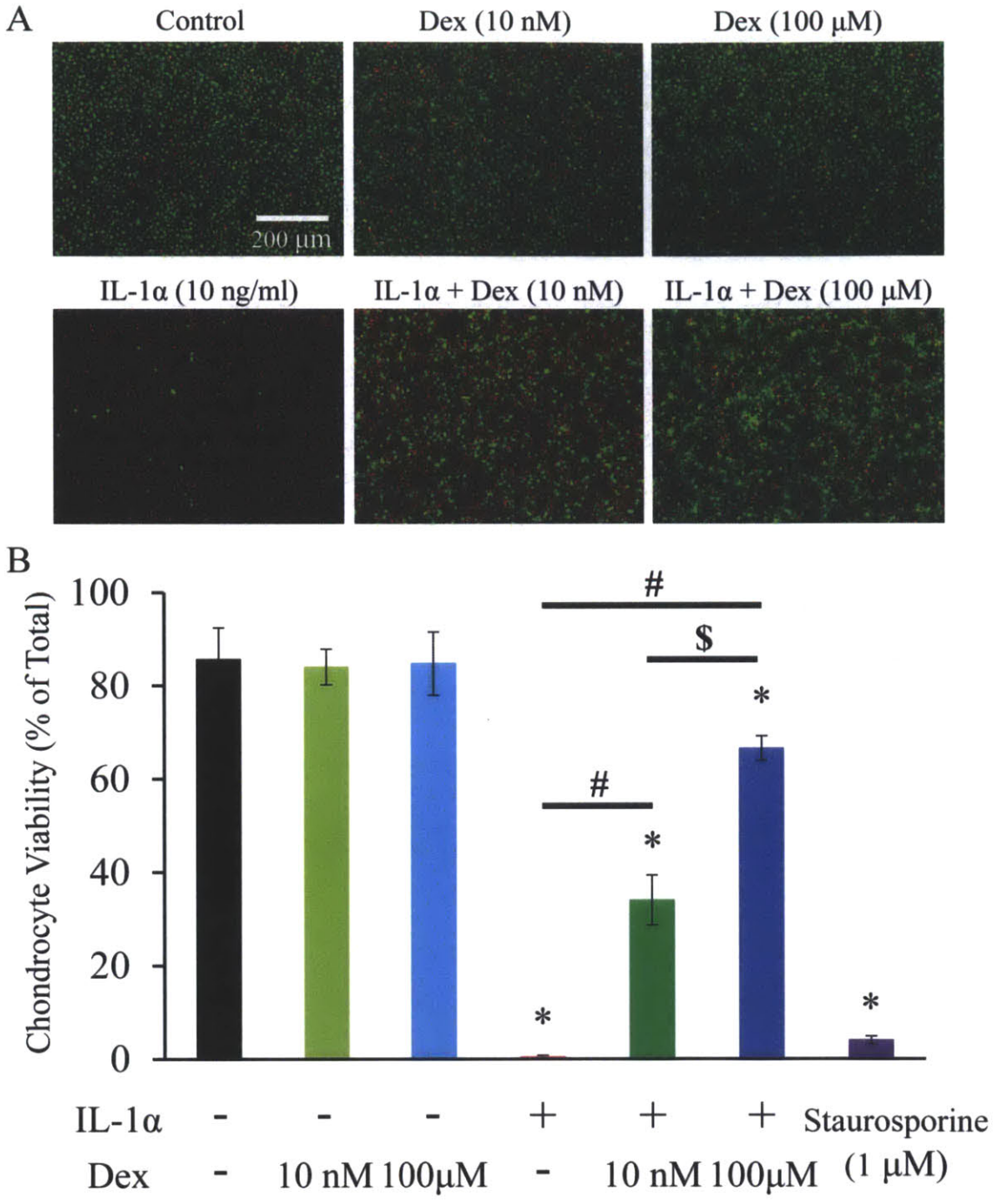

Figure 4.3 The effects of Dex on bovine chondrocyte viability in the presence or absence of IL-1α (10 ng/ml). Chondrocytes were fluorescently stained with fluorescein diacetate (green, viable) and propidium iodide (red, non-viable) after 4-day treatments. Images were taken with a Nikon fluorescence microscope with a 20X objective. The numbers of viable and non-viable cells were quantified with ImageJ. N = 4 replicates using chondrocytes from 2 different bovines. * vs. untreated control; # vs. IL-1α alone; $ vs. IL-1α + 10 nM Dex; $p < 0.05$.

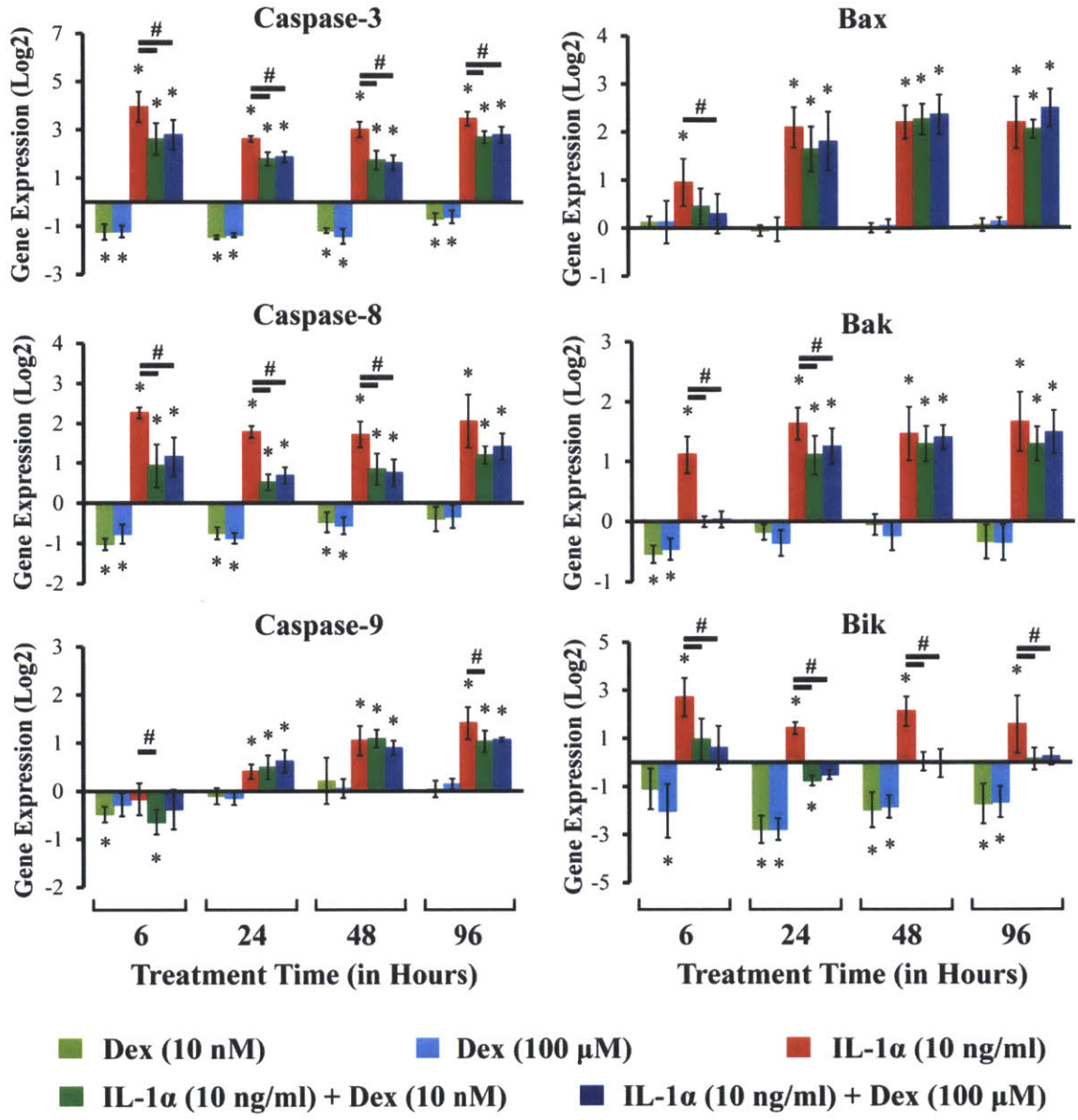

Figure 4.4 Normalized bovine chondrocyte gene expression (in $\log_2$ scale) in response to 6-, 24-, 48-, and 96-hour treatments. For each condition, 6 cartilage disks from the same animal were pooled for mRNA extraction; n = 5 animals. Gene expression levels were normalized to that of the 18S gene and then normalized to the untreated control condition which had a $\log_2$ expression level = 0. Data are presented as mean ± 95% confidence interval, * vs. untreated control; # vs. IL-1α alone; $p < 0.05$.

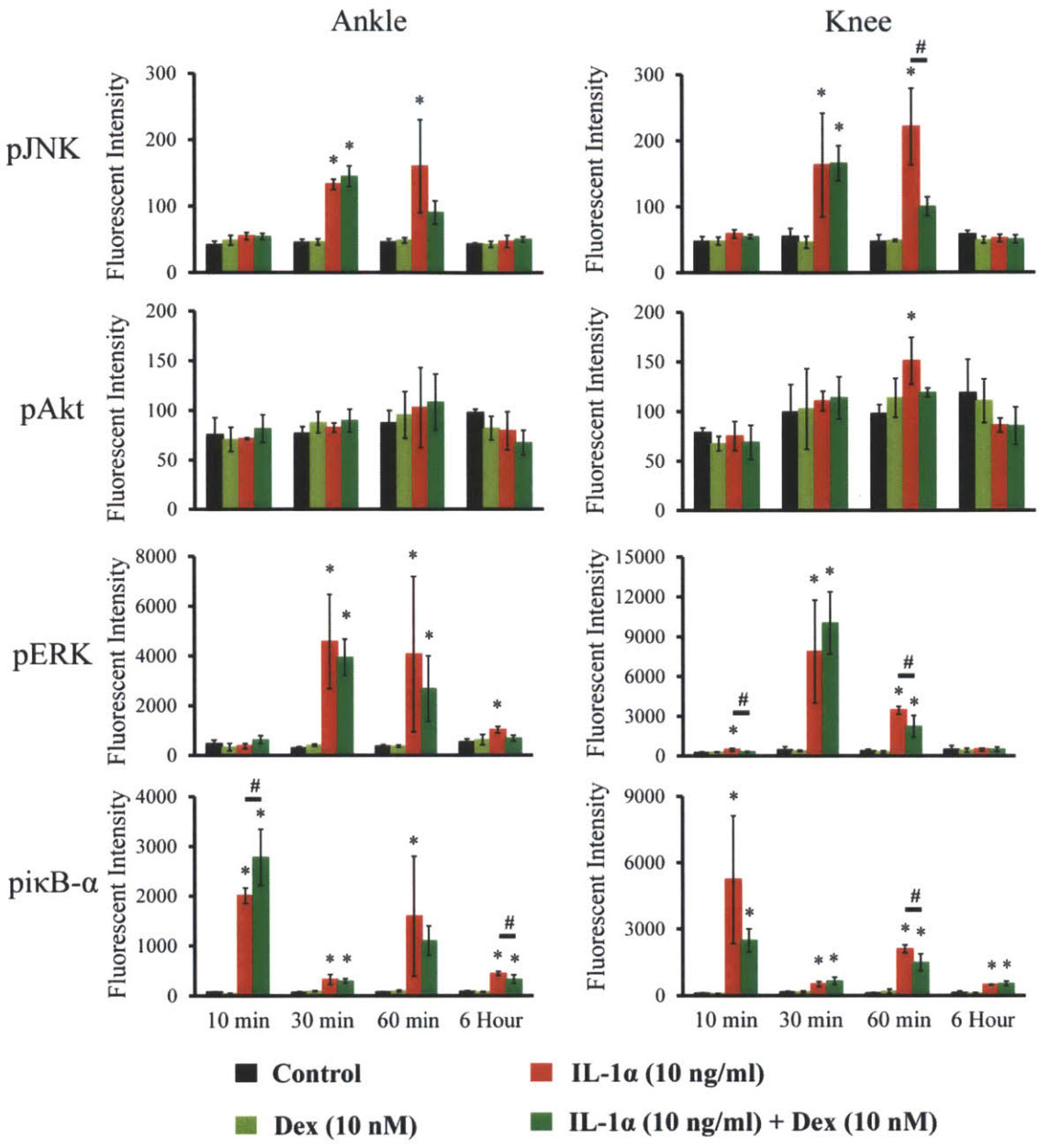

Figure 4.5 The effects of Dex on the phosphorylation of JNK, Akt, ERK, and iκB in the presence or absence of IL-1α. Chondrocytes were obtained from both knee and ankle cartilage and subjected to treatments for 10, 30, 60 min, or 6 hour. Total cell lysates were prepared and equal total proteins (5 μg) were loaded to the luminex magnetic plates. Data are presented as mean ± 95% confidence interval, * vs. untreated control; # vs. IL-1α alone; N = 3 replicates, $p < 0.05$.

4.7 REFERENCES

1. Elmore S. Apoptosis: a review of programmed cell death. Toxicol Pathol. 2007;35(4):495-516.
2. Igney FH, Krammer PH. Death and anti-death: tumour resistance to apoptosis. Nat Rev Cancer. 2002;2(4):277-88.
3. Bröker LE, Kruyt FA, Giaccone G. Cell death independent of caspases: a review. Clin Cancer Res. 2005;11(9):3155-62.
4. Sperandio S, de Belle I, Bredesen DE. An alternative, nonapoptotic form of programmed cell death. Proc Natl Acad Sci U S A. 2000;97(26):14376-81.
5. Castro-Obregón S, Rao RV, del Rio G, Chen SF, Poksay KS, Rabizadeh S, et al. Alternative, nonapoptotic programmed cell death: mediation by arrestin 2, ERK2, and Nur77. J Biol Chem. 2004;279(17):17543-53.
6. Lawen A. Apoptosis-an introduction. Bioessays. 2003;25(9):888-96.
7. García-Sáez AJ. The secrets of the Bcl-2 family. Cell Death Differ. 2012;19(11):1733-40.
8. Zamli Z, Sharif M. Chondrocyte apoptosis: a cause or consequence of osteoarthritis? Int J Rheum Dis. 2011;14(2):159-66.
9. Blanco FJ, Guitian R, Vázquez-Martul E, de Toro FJ, Galdo F. Osteoarthritis chondrocytes die by apoptosis. A possible pathway for osteoarthritis pathology. Arthritis Rheum. 1998;41(2):284-9.
10. Hashimoto S, Ochs RL, Komiya S, Lotz M. Linkage of chondrocyte apoptosis and cartilage degradation in human osteoarthritis. Arthritis Rheum. 1998;41(9):1632-8.
11. Johnson DL, Urban WP, Caborn DN, Vanarthos WJ, Carlson CS. Articular cartilage changes seen with magnetic resonance imaging-detected bone bruises associated with acute anterior cruciate ligament rupture. Am J Sports Med. 1998;26(3):409-14.
12. Elsaid KA, Fleming BC, Oksendahl HL, Machan JT, Fadale PD, Hulstyn MJ, et al. Decreased lubricin concentrations and markers of joint inflammation in the synovial fluid of patients with anterior cruciate ligament injury. Arthritis Rheum. 2008;58(6):1707-15.
13. Higuchi H, Shirakura K, Kimura M, Terauchi M, Shinozaki T, Watanabe H, et al. Changes in biochemical parameters after anterior cruciate ligament injury. Int Orthop. 2006;30(1):43-7.
14. Catterall JB, Stabler TV, Flannery CR, Kraus VB. Changes in serum and synovial fluid biomarkers after acute injury (NCT00332254). Arthritis Res Ther. 2010;12(6):R229.
15. Notoya K, Jovanovic DV, Reboul P, Martel-Pelletier J, Mineau F, Pelletier JP. The induction of cell death in human osteoarthritis chondrocytes by nitric oxide is related to the production of prostaglandin E2 via the induction of cyclooxygenase-2. J Immunol. 2000;165(6):3402-10.
16. Wang H, Wang Z, Chen J, Wu J. Apoptosis induced by NO via phosphorylation of p38 MAPK that stimulates NF-kappaB, p53 and caspase-3 activation in rabbit articular chondrocytes. Cell Biol Int. 2007;31(9):1027-35.

17. Dave M, Attur M, Palmer G, Al-Mussawir HE, Kennish L, Patel J, et al. The antioxidant resveratrol protects against chondrocyte apoptosis via effects on mitochondrial polarization and ATP production. Arthritis Rheum. 2008;58(9):2786-97.
18. Kim J, Xu M, Xo R, Mates A, Wilson GL, Pearsall AW, et al. Mitochondrial DNA damage is involved in apoptosis caused by pro-inflammatory cytokines in human OA chondrocytes. Osteoarthritis Cartilage. 2010;18(3):424-32.
19. Maneiro E, López-Armada MJ, de Andres MC, Caramés B, Martín MA, Bonilla A, et al. Effect of nitric oxide on mitochondrial respiratory activity of human articular chondrocytes. Ann Rheum Dis. 2005;64(3):388-95.
20. Qin J, Shang L, Ping AS, Li J, Li XJ, Yu H, et al. TNF/TNFR signal transduction pathway-mediated anti-apoptosis and anti-inflammatory effects of sodium ferulate on IL-1β-induced rat osteoarthritis chondrocytes in vitro. Arthritis Res Ther. 2012;14(6):R242.
21. Mina R, Melson P, Powell S, Rao M, Hinze C, Passo M, et al. Effectiveness of dexamethasone iontophoresis for temporomandibular joint involvement in juvenile idiopathic arthritis. Arthritis Care Res (Hoboken). 2011;63(11):1511-6.
22. Guerne PA, Desgeorges A, Jaspar JM, Relic B, Peter R, Hoffmeyer P, et al. Effects of IL-6 and its soluble receptor on proteoglycan synthesis and NO release by human articular chondrocytes: comparison with IL-1. Modulation by dexamethasone. Matrix Biology. 1999;18(3):253-60.
23. Lu YCS, Evans CH, Grodzinsky AJ. Effects of short-term glucocorticoid treatment on changes in cartilage matrix degradation and chondrocyte gene expression induced by mechanical injury and inflammatory cytokines. Arthritis Research & Therapy. 2011;13(5).
24. Van Offel JF, Schuerwegh AJ, Bridts CH, Stevens WJ, De Clerck LS. Effect of bisphosphonates on viability, proliferation, and dexamethasone-induced apoptosis of articular chondrocytes. Ann Rheum Dis. 2002;61(10):925-8.
25. Chrysis D, Zaman F, Chagin AS, Takigawa M, Sävendahl L. Dexamethasone induces apoptosis in proliferative chondrocytes through activation of caspases and suppression of the Akt-phosphatidylinositol 3'-kinase signaling pathway. Endocrinology. 2005;146(3):1391-7.
26. Mushtaq T, Farquharson C, Seawright E, Ahmed SF. Glucocorticoid effects on chondrogenesis, differentiation and apoptosis in the murine ATDC5 chondrocyte cell line. J Endocrinol. 2002;175(3):705-13.
27. Bian L, Stoker AM, Marberry KM, Ateshian GA, Cook JL, Hung CT. Effects of dexamethasone on the functional properties of cartilage explants during long-term culture. Am J Sports Med. 2010;38(1):78-85.
28. Fitzgerald JB, Jin M, Dean D, Wood DJ, Zheng MH, Grodzinsky AJ. Mechanical compression of cartilage explants induces multiple time-dependent gene expression patterns and involves intracellular calcium and cyclic AMP. J Biol Chem. 2004;279(19):19502-11.
29. Montaseri A, Busch F, Mobasheri A, Buhrmann C, Aldinger C, Rad JS, et al. IGF-1 and PDGF-bb suppress IL-1β-induced cartilage degradation through down-regulation of NF-κB signaling: involvement of Src/PI-3K/AKT pathway. PLoS One. 2011;6(12):e28663.

30. Ju XD, Deng M, Ao YF, Yu CL, Wang JQ, Yu JK, et al. Protective effect of sinomenine on cartilage degradation and chondrocytes apoptosis. Yakugaku Zasshi. 2010;130(8):1053-60.
31. Weng LH, Wang CJ, Ko JY, Sun YC, Su YS, Wang FS. Inflammation induction of Dickkopf-1 mediates chondrocyte apoptosis in osteoarthritic joint. Osteoarthritis Cartilage. 2009;17(7):933-43.
32. Gillissen B, Essmann F, Graupner V, Stärck L, Radetzki S, Dörken B, et al. Induction of cell death by the BH3-only Bcl-2 homolog Nbk/Bik is mediated by an entirely Bax-dependent mitochondrial pathway. EMBO J. 2003;22(14):3580-90.
33. Karna E, Miltyk W, Surazyński A, Pałka JA. Protective effect of hyaluronic acid on interleukin-1-induced deregulation of beta1-integrin and insulin-like growth factor-I receptor signaling and collagen biosynthesis in cultured human chondrocytes. Mol Cell Biochem. 2008;308(1-2):57-64.
34. Terkeltaub R, Johnson K, Murphy A, Ghosh S. Invited review: the mitochondrion in osteoarthritis. Mitochondrion. 2002;1(4):301-19.

CHAPTER 5

SUMMARY AND CONCLUSION

In Chapter 2, we implemented a previously-characterized *in vitro* injury model involving cytokines TNF-α and IL-6/sIL-6R with or without initial mechanical injury, and investigated the effects of intermittent unconfined dynamic compression (10%-30% strain amplitude) on both immature bovine and mature human cartilage. We demonstrated the anti-catabolic effects of moderate dynamic compression on injury/TNF + IL-6/sIL-6R-challenged immature bovine and adult human cartilage. Importantly, we discovered that there exists a threshold strain amplitude above which dynamic compression becomes detrimental to cell viability as well as upregulation of inflammatory genes and aggrecanase activity in the remaining viable cells. Together, these results provide evidence to support the concept that appropriate loading-rehabilitation post-joint injury can be beneficial at the cell level, but above threshold dynamic loading may further contribute to loss of cell and tissue function. Further studies exploring the effects of frequency and loading type (e.g., continuous vs. intermittent) are suggested to optimize the beneficial effects of dynamic loading.

In Chapter 3, we examined a potential combination therapy with IGF-1 and Dex and demonstrated their beneficial effects in reversing IL-1α-suppressed biosynthesis and blocking cytokine-induced proteoglycan and collagen degradation in young bovine explants. Furthermore, IGF-1 + Dex strongly inhibit cell death induced in an inflammatory environment. Importantly, we have shown that each therapeutic has its unique role in cytokine-challenged adult human cartilage: IGF-1 offers stimulation on proteoglycan biosynthesis while Dex modulates cartilage catabolism. Consequently, this combination is required to restore the imbalance between anabolic and catabolic processes in OA. The advantageous effects of this combination therapy can be further

expanded with improved IGF-1 function (49) as well as appropriate *in vivo* delivery method, i.e. intra-articular injection with nanoparticles, and thus may stimulate interests for clinical studies to target the treatment of early stage PTOA.

In Chapter 4, we examined the anti-apoptotic role of Dex in the presence of the pro-inflammatory cytokine IL-1α using high-density cultured monolayer bovine and human chondrocyte. Our results showed that Dex alone treatment with high dose (100 μM) did not induce significant cell apoptosis or compromise cell viability. In the presence of IL-1α, Dex was able to inhibit the caspase-dependent extrinsic and intrinsic pathways both at the gene and protein levels, resulting in a significantly greater survival rate. The anti-apoptotic effects of Dex is likely to be mediated by the inhibition on the upstream JNK MAPK and NF-κB/iκB pathways but not the result of activation of the pro-survival Akt pathway.

Appendix A

PROTOCOLS

Contents

A1. Protocol for Running Western Blots

1. Have a plan
    a. Volume of reagents to mix with sample volumes
        i. 4-12% 15 well 1.5 mm thick Invitrogen mini-gel tolds 25 uL per well max, usu do 20 uL
        ii. Purple sample buffer above western bench is 4x, so total volume per lane divided by 4.
        iii. 10x reducing agent, so total volume/10.
        iv. Volume of sample (5-10 ug seems standard, but can vary)
        v. Water to make up rest of volume
    b. Type of gel want to use (4-12% vs 10%) (smaller proteins get resolved better on bigger % gels, thicker gels allow to load more volume, fewer wells also leads to more volume)
    c. Order of lanes to run (put ladders on edges so know where gel ends)
    d. Antibody using, it's dilution, which animal to use for secondary
    e. If doing a strip and re-probe need to plan which antibody to do first (ie do NITEGE before G1 because G1 covers NITEGE).
2. Get a bucket of ice to keep samples and reducing agent cold.
3. Get NuPAGE Sample Reducing Agent (10x) off of Anna's shelf in the fridge in the injury room and a Novex Sharp pre-stained protein standards vial from the western shelf in the freezer in the injury room.
4. Set water to boil behind the shaker plate.
5. Make the running buffer: make 500 mL total, is 25 mL of 20x MOPS above western bench, then add rest of volume in DI water. Mix by covering top of graduated cylinder with parafilm and inverting. (If doing smaller proteins can use MES instead of MOPS)
6. Aliquot the appropriate amount of sample into new labeled tubes.
7. Make the sample buffer stock of 4x sample buffer, 10x reducing agent, and water. Add the appropriate volume to each sample. Vortex and spin down each sample tube. Set to boil for 5 mins (denatures proteins).
8. Get a gel from the cold room (right inside the door on the right)
9. Put the electrophoresis machine together
    a. The clear box with the gold post is the main unit
    b. Put the squarish piece with the 2 gold posts in, the side with the post facing down goes in the slot on the right.
    c. The piece with the lever goes in the back
    d. The blank plastic piece goes between the gold post piece and the lever piece, or could run a second gel here.
    e. The gel goes in the front of the gold post piece. **Take the white tape off of the gel before you put it in.
    f. Remove the comb from the gel, CAREFULLY.
    g. Tighten the lever in the back so the gel is held tight.
10. Pour running buffer behind the gel in the middle compartment between the gel and the back plate until the liquid level is over the white bar and covers all the

wires. If the buffer leaks out of the middle compartment into the outer parts, you did something wrong. Pour the rest on the buffer into the outer part of the box.

11. Use the special super-fine pipette tips (clear tips in a blue box) to squirt some buffer over the top of the lanes to make sure there's no gunk blocking them.
12. Once samples are done boiling, vortex them and spin them down again.
13. Load the protein standards ladders and your samples with the super-fine tips. Set the pipetter above the full volume you expect to pull up so you get everything. If the tip gets clogged, you can throw it out or cut it to try and salvage the sample. (Note: If running 2 gels at a time, you may want to run the gel in the cold room or on ice and add more running buffer outside the gel. You would want to load the samples in the cold room if you were going to run the gel there.)
14. Once all samples are loaded, put the top on the electrophoresis box (red to red, black to black) and plug the cords into the power supply (red to red, black to black). Run the gel at 200V for about 45 mins. If you don't see a bunch of bubbles when you turn the power on, something is wrong. Make sure protein of interest is going to be a bit away from the edge of the gel and separated well when you stop running the gel.
15. While the gel is running, make up the transfer buffer (1000 mL total)
    a. Measure out 3.03 g Tris base and 14.4 g glycine. (If have had problems with transfer in past can add 0.5 g SDS.)
    b. Add 800 mL water
    c. pH the solution to 8.3
    d. Add 200 mL methanol (stored under the waste fume hood).
16. After you're done running the gel (turn off the power supply and unplug it), you need to transfer the separated proteins to a membrane. To do this, get the aluminum tray and place a transfer cassette black side down, slide side up. Get 2 sponges and place 1 on the black part, one in the tray next to the cassette. Get 2 pieces of blotting paper from the top drawer on the left and put one on each sponge. Pour transfer buffer over each blotting paper.
17. Remove the gel from the electrophoresis machine and remove it from the plastic casing with the spackle applicator thing. You want the gel to stick to the side with the black writing when you pull the plastic pieces apart. Cut the comb and the two side pieces off the top of the gel with a razor blade.
18. Put the gel on top of the blotting paper and get the gel to come off the plastic and stick to the blotting paper. You want to make sure that the part of the gel you care about most (the top for full-length aggrecan) is fully on the blotting paper and not right on the edge. Cut off the bottom ridge of the gel. Add additional transfer buffer. Avoid any bubbles.
19. Assemble the transfer cell by placing the red and black plastic piece in the middle of the clear plastic box. Also make sure you have a green lid for the box and a small stir bar in the middle of the red and black piece.
20. Cut a piece of PVDF membrane (not nitrocellulose) to fit inside one of the little lids the blot will go into. The paper also should not be bigger than the gel or it messes up the voltage. Do not touch the white membrane, only the blue papers.
21. Saturate the white membrane only (not the blue papers) in methanol in a tip lid. Rinse with DI water in another tip lid.

22. Place the membrane on top of the gel, avoiding bubbles and avoiding moving the membrane once it's been laid down.
23. Place the other piece of blotting paper on top of the membrane, then add the other sponge. Roll over the sandwich with a 50 mL tube to squeeze out bubbles.
24. Maintain pressure on the stack while closing the cassette and sliding the top closed. Place the cassette into the transfer cell (black to black). You may need to jam it in a bit. Put an ice pack in the back of the transfer cell (from the top of the freezer/fridge in the tissue engineering room). Pour in a bunch of the transfer buffer (including the stuff in the aluminum tray), but not too full so you don't spill.
25. Take the transfer cell to the cold room. Add the rest of the transfer buffer, move the cell on top of the stir plate, and set the level to 2.5 (or maybe a little above to get the stir bar spinning). Put the top on the transfer cell (red to red, black to black) and plug the cords into the power supply (red to red, black to black). If one power supply doesn't work, try the other one. Other options are to switch lids and add more buffer. Set the voltage to 75V and transfer for 60 minutes (or a bit more if had problem before, can overtransfer small proteins).
26. To clean up the electrophoresis equipment, pour the MOPS buffer down the sink and rinse off all of the machine parts.
27. While the proteins are transferring, make up the blocking solution. Can either do milk or BSA in TBST or PBST. Usually do 5% milk in TBST. To make 50 mLs weigh out 2.5 g Carnation instant non-fat dry milk and add TBST. There is a volume effect, so don't add the full 50 mLs. Add some volume, mix it to break up the clumps and then sonicate it. Add the rest of the volume of TBST afterwards. (Note: TBST= Tris buffered saline + Tween, Tween is a detergent. Rachel makes up 10x TBS because it takes a long time to dissolve and pH. Make up 500 mL of 1x TBST at a time. Tween and is viscous so use wide mouth pipette tips. To make up 500 mL of TBST take 50 mL of 10x TBS and add 450 mL water. Then add 250 uL of Tween (is 0.5%).)
28. Once the transfer is complete, turn off the power supply and bring the transfer cell back to the western bench. Remove the cassette from the machine and open it, clear side up (?). Remove the PVDF membrane and place into one of the small lids so that the protein side (the side facing the gel) is up. Rinse the membrane off with TBST (about 8-10 mLs). Dump out the TBST and cover with 10 mL milk.
29. Place on stir table for 1 hour to block against non-specific binding.
30. To clean up the transfer materials, throw the gel into the big plastic jar (unless you want to do a Coomassie stain), throw away the blotting paper, and just rinse out everything else.
31. After the blocking is complete, make up the primary antibody solution. The total volume will be 8 mL because that's the minimum volume to cover the membrane in the small boxes. So, for a 1:1000 dilution add 8 uL of the antibody, or for a 1:2000 dilution add 4 uL of the antibody.
32. Put all 8 mL on the membrane and put it on a stir table in the cold room to incubate overnight.
33. The next morning, do one quick rinse with TBST and then wash the membrane 3 times in TBST on a stir table in the lab for 10 minutes each.

34. Make up the secondary antibody (1:2000 anti-rabbit for example) and incubate for 60 minutes at room temperature.
35. Do one quick rinse of the membrane with TBST to get the milk off. Wash the membrane 3 times with TBST for 10 minutes each again.
36. Set up the gel dock for visualizing the gel: Open the FluorChem software and set it to filter 1. Adjust so that you get all of the light coming in (top to 2.8) and adjust the focus so you see the inner square (middle is rough focus, bottom is fine focus).
37. Get the ECL kit from the fridge (chemiluminescence) and make up a 1:1 mix of the two solutions in the box. Make up 5 mL total to cover the whole membrane. **Only do this right before you're ready to use this solution!
38. Put the liquid directly on the membrane and let the ECL mix sit for 1 minute on the membrane. After the one minute is up, pick up the membrane with tweezers and dab one corner onto a paper towel.
39. Place the membrane on a plastic sheet, cover it without creating bubbles.
40. To image the membrane:
    a. Do a 1 minute supersensitive picture first, then a 5-10 minute at normal (longer if is grainy).
    b. Take a white image to see the ladders. Set to normal/high, autoexpose, expose preview, see the green light flash, and hit acquire image. Save. Remove from computer with USB key.
41. Save membrane in plastic wrap and keep in fridge. Or, to strip and re-probe:
    a. Rinse twice with TBST for 5 minutes each.
    b. Strip for 15 minutes with the stripping buffer (brown bottle on bottom shelf to left above western bench)
    c. Rinse twice with TBST for 5 minutes each.
    d. Block for 1 hour with milk.
    e. Incubate overnight with primary antibody in cold room, so go from step 31 back to 40.
42. To analyze the pictures in Photoshop:
    a. Image, adjust, invert
    b. Image, adjust, brightness/contrast and slide the contrast around
    c. You want the blot to be dark enough so you can tell where the gel is, not underexposed.
    d. Match up the MW standards with lane on end and put arrows where they are.
    e. To get the pictures into powerpoint:
        i. Image, mode, 8 bit
        ii. Save for web
        iii. Save as jpeg
        iv. Can import into powerpoint

<u>Coomassie Staining (for the gel or the membrane):</u>

- Coomassie dye is 1 g dye in 500 mL methanol, stir for 30 minutes (?think add water).

- Coomassie waste goes in the chemical hood.
- Dye goes on the gel on a stir plate for 30 mins, waste dye in container. Rinse gel a few times with DI water.
- Destaining solution is 7.5% acetic acid and 1% methanol in water. Cover the gel with destaining solution with a Kimwipe on one side. Rinse 2x with destaining solution and new Kimwipes.
- If taking pictures, let destain overnight. Flip down the white board in the imaging machine and select transluminator in the software.

A2. Protocol to Extract Aggrecan from Articulate Cartilage

1. Make up 4M guanidine HCl in 100 mM sodium acetate.
    a. First, figure out the amount of guanidine HCl powder and sodium acetate powder you need. Want to make about 1 mL of solution for every 1-2 plugs (assuming about 300 μg sGAG and 10 mg wet weight per plug).
    b. Measure out the sodium acetate powder and dissolve it in water to get 100 mM sodium acetate.
    c. Measure out the guanidine HCl powder IN THE FUME HOOD (it's a chaotropic agent, bad news).
    d. Add some volume of the 100 mM sodium acetate that is significantly less than the final volume you want to the guanidine powder. This is because the guanidine has a significant volume effect. The guanidine will dissolve easily. (Can pour extra sodium acetate solution down the sink.)
    e. pH the solution to 7.2
2. Add appropriate amount of protease complete tablet to inhibit proteases, add right before use.
3. Dice up samples with a scalpel and put them back in their 2 mL tubes.
4. Add 1 mL solution with protease inhibitor per 1-2 plugs.
5. Place tubes on rotating machine at 4C for 48 hours to extract aggrecan.
6. Spin the tubes down in the microcentrifuge at 13,000 x g for 30 mins.
7. Remove the supernatant and put it in a new 2 mL tube. Discard the pellet.
8. Measure the sGAG content of each sample. Note: the standards you use for the GAG assay must be made up in guanidine! If the amount of GAG is around 100, you must dilute the sample to be sure the measurement is not above the standard curve.
9. Make up 5 mM sodium acetate in absolute ethanol (200 proof=100%). Need enough to add 3x the volume of each sample to the sample.
10. Ethanol precipitation: Add 3x the volume of each sample of 5mM sodium acetate in 200 proof ethanol to each sample in a larger tube. Split up the sample mixed with ethanol into 2mL tubes. Store these tubes in the -20C freezer overnight.
11. Centrifuge at 13,000 x g for 30 minutes to pellet the sGAG.
12. Remove and discard the supernatant. *Dry is a Speedvac.* Or, if don't have, let sit in fume hood until ethanol has evaporated. The evaporation route takes a very long time.
13. Digest the sGAGs away, leaving the core protein exposed
    a. Make up Chase buffer. Will need enough to resuspend 100 ug GAG in 100 uL Chase buffer. To make 10 mL of solution do:
        i. 60 mg Tris base (MW 121.1), which is 0.05 M Tris
        ii. 41 mg sodium acetate (MW 82.03), which is 0.05 M
        iii. 37.2 mg EDTA (MW 372.2), which is 0.01 M
        iv. pH to 7.6
    b. Resuspend samples at 100 ug GAG in 100 uL Chase buffer. Mix well. The resuspension won't go any better after the digestion. This part generally seems to go horribly.

c. Digest the resuspended samples with protease-free chondroitinase ABC (30 mU/100 ug GAG) (Warner) for 3 hours in a water bath of 37C.
d. Add keratanase II (0.5 mU/100 ug GAG) and endobetagalactosidase (0.5 mU/100 ug GAG) (Seikagaku # 100455, #100812 respectively . . . 1 mU/uL when rehydrated). Note: Dilute 2.5 uL into 20 uL water, gives 0.5 mU/5 uL. Incubate 2-3 hours at 37C.

The extracted the aggrecan can be frozen and stored at -80 until use for western blot analysis.

A3. Cartilage RNA Extraction Protocol

Tissue preparation

0) You should prepare/label all required tubes before starting. Also make up the DNase used in step 6 of the RNA extraction protocol ahead of time and store in ice bath. All steps for the RNA extraction are taken from the QIAGEN RNeasy MiniKit for animal tissue. Pages 54-55. Obtain volumes of chloroform, 70% ethanol and RLT buffer (with β-Me added). Add 20mls of DI water to two 50ml tubes for for cleaning the homogenizer. Pre-spin Eppendorf phasegel tubes for 15 seconds.
1) Samples should be stored by either flash-freezing in liquid nitrogen and placing in a –80C freezer, or placing in RNA*later* solution and placing in –80C freezer. It is best if cartilage has been dissected into multiple 3x3x1mm pieces.
2) Place pulverizer and pole in container and bathe in liquid nitrogen repeatedly to cool. Remove two samples from the -80°C freezer and place in ice bath. Cool pulverizer again with liquid nitrogen.
3) Remove puliverizer and bend its arms downwards. Add cartilage samples to top of pulverizer (make sure metal stopper is in place). Place pole into top base. Hit pole firmly 8-10 times with a hammer, while holding pole and top of pulverizer.
4) Lift top of pulverizer and gently tap pole to release metal stopper. Place a 5ml polypropylene tube beneath pulverizer, turn pulverizer sideways and tap pole on side of bench to release the smashed cartilage into tube. Place in ice bath. Add 540µl of Trizol.**
5) Clean pulverizer with sterile gauss and if necessary re-cool with liquid nitrogen. Repeat steps 2 to 5 with next sample.
6) All samples should now be pulvierzed and have Trizol added. Set up the homogenizer so that the blade is flush with the sheath.
7) Place homogenizer in first 50ml water tube, turn on and rinse, turn off, remove and shake dry. Repeat in second water tube. The second water tube should still look clean at the end of the Tissue preparation protocol.
8) Place homogenizer into first sample, turn onto low speed, and slowly increase speed. Sample should be homogenized in less than 20 seconds. Place sample back in ice bath. Repeat steps 7 & 8 until finished.
9) Remove samples from ice bath and place onto 96 well frame. Remove lids and add 60µl of chloroform (final 10%) to each tube. Mix (should turn cloudy pink) and transfer sample to pre-spun phasegel tubes.
10) Spin phasegel tubes at maximum speed for 10 minutes at 4°C (room temperature also works).

** If performing more than 6 extractions then; once every 2 samples are pulverized place tubes in -80°C freezer (before adding Trizol). When all samples are done, remove all from freezer and add Trizol and continue with step 6.

RNA extraction

1) Make sure all QIAGEN reagents are ready. Buffer RPE should have ethanol added to the bulk volume when the kit is first used. Each month a 10ml aliquot of Buffer RLT mixed with 100X β-Mercaptoethanol must be made. β-Me is highly toxic and must remain in the chemical fume-hood.
2) The following steps are taken from the QIAGEN RNeasy Mini Protocol.
3) While the phasegel tubes are spinning add 250µl of 100% ethanol to a set of RNase-DNase free 1.5ml centrifuge tubes. Then add 350µl of RLT buffer (which contains β-Me).
4) Transfer the supernatant in a phasegel tube to the new centrifuge tube and immediately mix the supernatant, ethanol and RLT buffer. Transfer half the solution to the pink RNeasy spin column (less than 700µl). Repeat for each phasegel tube. Centrifuge spin columns for 15sec at 10,000 rpm, allowing 5sec for ramping up, then discard flow through. The RNA is now attached to the silica membrane in the pink tubes. Add the remaining sample from the centrifuge tube to the spin columns and spin again at 10,000rpm. Discard flow through.

   Steps 5 to 8 are the for **DNase digestion** to remove genomic DNA, and can be found in the QIAGEN RNeasy Mini Protocol (p98-99).
5) Pipette 350µl of Buffer RW1 into spin column and centrifuge for 15sec at 10,000rpm, allowing 5sec for ramping up. Discard flow-through into separate bin and reuse collection tube.
6) **Prepare ahead:** Make a mastermix of 10µl of DNase stock solution to 70µl of RDD Buffer per sample. Once dissolved DNase should be stored in the –20C freezer in aliquots. Thawed DNase aliquots should not be re-frozen, instead store in the 4°C fridge (generally choose aliquot size carefully).
7) Pipette 80µl aliquots of DNase mix directly onto the spin column membrane, tap gently to ensure the entire membrane is covered. Incubate on benchtop for 15 minutes at room temperature.
8) Pipette 350µl of Buffer RW1 into spin column and centrifuge for 15sec at 10,000rpm, allowing 5sec for ramping up. Discard flow-through and collection tubes into appropriate bins.

9) Place spin column into a new 2ml collection tube, add 500µl of Buffer RPE (with ethanol previously added), centrifuge for 15sec at 10,000rpm, allowing 5sec for ramping up. Discard flow-through into separate bin and reuse collection tube.
10) Pipette 500µl of Buffer RPE (with ethanol added) into spin column, centrifuge for 2 minutes at maximum speed. After spin remove spin column from collection tube and wipe the outside gently with sterile gauze to remove any residual ethanol, which may interfere with subsequent reactions (optional).
11) Place spin column into 1.5ml collection tube (supplied, rounded bottom). Add 50µl of Rnase-Dnase free dH_2O from QIAGEN kit. Spin at 10,000rpm for 1 minute, and then place immediately in ice bucket.
12) If proceeding directly to RT then keep in ice bath. If not then freeze RNA in -80°C immediately to minimize degradation.

A4. Reverse Transcription Protocol

1) If proceeding straight from a RNA extraction ensure that RNA is kept cold (but not frozen) by placing vials in an ice bucket and then placing in the 4°C fridge as calculation of RNA volumes can take some time. If RNA has been frozen and stored in the -80°C freezer then thaw it immediately before use, and then mix by pipetting.
2) Make a RT master mix using the following guide. Total reaction volume will be 60µl once RNA and H_2O have been added.

RT Reagents	**x1 60ul**	
10x PCR buffer	6	Mix thoroughly
MgCl2	6	
dNTP	6	
Random Hexamers	1.5	
dIH20	22.5	
Rnase Inhibitor	1.5	Keep cold, remove from freezer only when needed, mix thoroughly by pipetting, (do not vortex as enzymes are fragile).
Multiscribe Reverse Transcriptase	1.5	

3) Generally multiply all the above equations by the number of cartilage samples you have to create a master mix. A total volume of 60µl was chosen as this allow 60/1.5 = 40 aliquots to be taken from the same cDNA sample for PCR. Hence if you have less that 40 genes scale down the total volume.

4) Aliquot 45µl of the mastermix into X different tubes. Then add 15µl of RNA (different for each tube) to each one of the tubes and mix.

5) Load tubes into the thermocycler and follow these steps:

25°C 20 minutes	(hybridization)
42°C 30 minutes	(reverse transcription)
Hold 4°C	(wait for removal)

6) Although cDNA is significantly more stable than RNA and thus doesn't degrade as fast as RNA, quantitative RT-PCR aims to avoid degradation as much as possible. Hence, move cDNA into the -20°C as soon as possible after the thermocycler reaches 4°C.

A5. Protocol to Prepare Samples for PCR

1. Before casting day, need to label 4 of the 2 mL cryovial tubes for day 0 samples.
2. On the casting day, fill a container with some liquid nitrogen. Take 4 aliquots of 0.5-1 million cells when the cells have been resuspended for counting and place into the labeled tubes. If the volume that the cells are in is greater than 50 uL, spin them down to remove the liquid.
3. Flash freeze the cells as soon as possible in liquid nitrogen.
4. Once the liquid nitrogen stops boiling, remove the vials and store them at -80 until ready to isolate the RNA.
5. To take down gels for PCR, have a labeled 1.5 mL flip top tube for each gel. Place the gel into the tube and flash freeze it in liquid nitrogen. When all of the gels have been flash frozen, store them in the -80 until ready to isolate RNA. Ideally, this is done within 1 week of the take down.

Measuring RNA Levels on the Nanodrop Spectrophotometer

1. Bring the samples of RNA, 1 uL pipetter, pipet tips, RNase/DNase-free water, EtOH over to the Zhang lab.
2. Open the software ND1000. Click on the nucleic acid button.
3. Wipe off both sides of the tips of the machine with EtOH on a Kimwipe. Asks for water to start. Use 1 uL. Clean off machine with EtOH between each sample.
4. Set the sample type to RNA-40.
5. The RNA is in water, so use water as the blank. Do another blank again. The noise should be around 1 ng/mL.
6. The wavelength to read at is 260. Record the ratios and the ng/mL reading. The 260/280 ratio should be at 1.8 or above ideally (so is RNA and not other protein I think) and the 260/230 ratio should be low (so no solvent left), but is often between 2 and 3 I think. Clean off machine with EtOH between each sample.

Filling in the PCR plate, Putting it into the machine, and Getting the Data

1. Fill out the Excel template that calculates the amount of primer, water, SyberGreen master mix, and cDNA you need.
2. Make the two 96 well plates up (They have rounded wells, NOT the ones for the Maxy machine). One plate will have the Syber Green master mix (new boxes are in the freezer, once you thaw one just keep it in the fridge), which you just add straight from the bottle, and the cDNA. The other plate has the RNase/DNase-free water and the primer.
    a. To make primer aliquots take 10 uL of the forward primer, 10 uL of the reverse primer, and 180 uL of RNase/DNase free water (because the resuspended primers are at 20x). You can then split this stock up into 4-5 aliquots and freeze them in the -20.

b. If you have to resuspend the lyophilized primers, you add water so that they are at 100 uM, so add 10*(nmole) uL of water to the stock. Ex. If there's 31.4 nmoles of primer, add 314 uL of water.

3. Once the 96 well plates are made, pipet the appropriate volumes into the 384 well plate. Use the multichannel pipetter and the tips from the RED BOX, not the blue box. They are much more accurate. Keep the 384 well plate on ice (Pyrex dish, filled with ice, with plastic wrap over it) while you fill it out.
4. Put a plastic cover from the bottom drawer on the plate. These plastic covers are different from other ones in the lab, (made for high temp and optically clear for machine) do not use the others! Seal it well with the plastic squeegee thing. Tear off the perforated edges
5. Centrifuge the plate in the centrifuge in the Zhang lab with the plate attachments. Try 200 x g for 1 minute just to get all the bubbles out. Can go higher if needed.
6. Blow off the bottom of the plate with canned air. Dust can mess up the readings.
7. Open the SDS 2.3 software. (If the software is open, close it out and restart it.)
8. Click on the new document icon. The default setting is fine. The assay is "Standard Curve" for a 384 well plate with a blank template.
9. Go to Instrument, Real Time, Open and the window will open and an arm will swing out to put the plate into. Close the window to get the plate in the machine.
10. Under the Thermocycler setting you can see the protocol. The default is fine, it should read 50/2, 95/10, 40 repeats of 95/.15 60/1.
11. Add a dissociation stage of 95/.15, 60/.15 and slowly go to 95/.15
12. Set the sample volume to 10 uL. It's unclear what happens if you don't do this.
13. Click on the Setup tab (next to the Instrument) tab and hit Add Detector (this is the gene you're amplifying) and copy it to the plate document. All of the detectors should be SYBR because we use SYBR green.
14. Draw on the plate which genes are where. For the water spots label the task as "NTC" for no template control.
15. Mark the empty wells by clicking "Omit wells."
16. Set the passive reference to ROX.
17. Save the file to the place you want it to go. It will save as it runs and you can save it at the end too.
18. Go to the Instrument tab, Real Time, Start.
19. Takes about 2 hours to run.
20. The data will save to a file automatically. To get it off the computer, use a USB key.
21. Open the file in the SDS software on your computer. Export the spreadsheet of data it creates. Open the txt file in Excel. You can then check that the cells are in order (it automatically does A1, A10, A11, etc so you have to sort by well number to get A1, A2, A3, etc) and copy over the Ct number and name of the condition into the PCR data analysis template.
22. Find the efficiency correlation by taking 2 to the power of Ct times the slope of the standard curve for that particular gene. Normalize to 18s by dividing by the eff-corr number for that sample of a particular gene by the eff-corr number for that sample in 18s. Then normalize to the day zero samples by dividing the 18s

normalized value by the average of the day zero 18s normalization numbers for that gene.

23. If you did duplicates, average together the day 0 normalized values for each sample for each gene. Then average together the 4 day 0 normalized values for each condition and find the standard error of the mean. Plot the mean ± SEM. If there are order of magnitude differences between your conditions, plot on a log scale, otherwise do linear. Run stats.

A6. Mayer's Hematoxylin stain for Nuclear blebbing For Cartilage Tissue

Material:

Mayer's Hematoxylin (Sigma #MHS15-500ml)

Acid solution : 0.5% HCL in 80 % ETHOH (.5ml of conc. HCl in 100ml of 80%ETHOH)

Permonat (Fisher #SP15-100)

Procedure:

Deparaffinize:

Xylene	5 minutes
Xylene	5 minutes
100% ETHOH	3 minutes
100% ETHOH	3 minutes
80% ETHOH	2 minutes
80% ETHOH	2 minutes

Washing in Tap water for 5 minutes

Hematoxylin solution (Filter before use) for 5 minutes

Washing in tap water for 5 minutes

Dip few times in Acid alcohol (0.5% HCL in 80 % ETHOH)

Washing in Tap water for 5 minutes

Dehydration:

80% ETHOH	2 minutes
80% ETHOH	2 minutes
100% ETHOH	3 minutes
100% ETHOH	3 minutes
Xylene	5 minutes
Xylene	5 minutes

Put cover slip on (permount Fisher #SP15-100)